Understanding Environmental Change and Biodiversity in a Dryland Ecosystem through Quantification of Climate Variability and Land Modification: The Case of the Dhofar Cloud Forest, Oman

by

Christopher S. Galletti

A Dissertation Presented in Partial Fulfillment
of the Requirements for the Degree
Doctor of Philosophy

Approved August 2015 by the
Graduate Supervisory Committee:

B.L. Turner II, Chair
Patricia L. Fall
Soe W. Myint

ARIZONA STATE UNIVERSITY

December 2015

ABSTRACT

The Dhofar Cloud Forest is one of the most diverse ecosystems on the Arabian Peninsula. As part of the South Arabian Cloud Forest that extends from southern Oman to Yemen, the cloud forest is an important center of endemism and provides valuable ecosystem services to those living in the region. There have been various claims made about the health of the cloud forest and its surrounding region, the most prominent of which are: 1) variability of the Indian Summer Monsoon threatens long-term vegetation health, and 2) human encroachment is causing deforestation and land degradation. This dissertation uses three independent studies to test these claims and bring new insight about the biodiversity of the cloud forest.

Evidence is presented that shows that the vegetation dynamics of the cloud forest are resilient to most of the variability in the monsoon. Much of the biodiversity in the cloud forest is dominated by a few species with high abundance and a moderate number of species at low abundance. The characteristic tree species include *Anogeissus dhofarica* and *Commiphora* spp. These species tend to dominate the forested regions of the study area. Grasslands are dominated by species associated with overgrazing (*Calotropis procera* and *Solanum incanum*). Analysis from a land cover study conducted between 1988 and 2013 shows that deforestation has occurred to approximately 8% of the study area and decreased vegetation fractions are found throughout the region. Areas around the city of Salalah, located close to the cloud forest, show widespread degradation in the 21st century based on an NDVI time series analysis. It is concluded that humans are the primary driver of environmental change. Much of this change is tied to national policies and development priorities implemented after the Dhofar War in the 1970's.

DEDICATION

To Sanda and Lucy:

I love you

ACKNOWLEDGMENTS

I would like to first thank my advisor and committee chair, Professor B.L. Turner II, for all his hard work and support during the writing of this dissertation. Billie is always ready to assist and offer advice, and his wisdom and ability to think critically are traits I would like to emulate in my own career. He has been gracious with his time and patience, and always showed support during my graduate studies - even when my research ideas were somewhat eccentric. I would also like to thank my other advisors and members of my committee, Professors Pat Fall and Soe Myint. Pat has been immensely supportive throughout my graduate career and graciously assisted with fieldwork in Oman. Soe is my mentor in remote sensing and his comments and insight have been critical to my research and this dissertation.

There are several people to thank for my time in Oman. Dr. Said AlSaqri provided institutional backing through the Diwan for Economic Planning Affairs, and supported my time in Oman as well as helped arrange some of the most vital aspects of my fieldwork. Dr. Annette Patzelt provided support and encouragement for my research in Dhofar. Dr. Hassan Kashoob offered valuable advice and helped with support through Dhofar University.

During my time at Arizona State University, I was lucky to have the opportunity to interact with many great people. Karina Benessaiah, John Connors, and Jesse Sayles provided a great deal of encouragement, late night board-gaming, and stimulating conversations. Members of the Remote Sensing and Geoinformatics Lab - Xiaoxiao Li, Chao Fan, Baojuan Zheng, and Yujia Zhang - helped with research, intellectual discussions, and a positive work environment. Professor Anthony Brazel provided insight

and advice numerous times during my graduate studies. I had the great privilege to conduct research and publish with several other former and current geography students at ASU, including Shai Kaplan, Kelly Turner, Liz Ridder, Tracy Schirmang, Kevin Kane, and Winston Chow. Professor Steven Falconer assisted with my fieldwork, for which I am very grateful. Finally, I offer a special thanks to Dr. Jeffrey Rose for putting me on the path to my doctorate.

Funding for my dissertation research came from a Fulbright Grant to Oman (funded through the U.S. Department of State), and was sponsored in Oman by the Office of the Advisor to His Majesty The Sultan for Economic Planning Affairs. My early graduate studies and research were supported by the Gilbert F. White Fellowship for Environment and Society. I also received financial and institutional support from the School of Geographical Sciences and Urban Planning and Central Arizona Phoenix - Long Term Ecological Research (CAP-LTER; NSF grant number DEB-1026865).

Finally, I acknowledge some of the most important people in my life, without them I would not have made it to this point. To my mother, father, brothers, sister-in-law, niece, and nephews – thank you for your many years of support and love, I am lucky to call you my family. Lastly, to my wife Sanda – you are a constant source of inspiration in my life. You helped with fieldwork in Oman despite having to complete your own dissertation and you carried me through some of the most difficult periods of my research. We are expecting our first baby in November and I could not have picked a better partner to share this next adventure with – thank you and I love you.

TABLE OF CONTENTS

Page

CHAPTER Page

APPENDIX

LIST OF TABLES

LIST OF FIGURES

Figure Page

CHAPTER 1

DRYLANDS, ENVIRONMENTAL CHANGE, AND LAND CHANGE SCIENCE: INTRODUCTION AND BACKGROUND TO THE CASE OF DHOFAR, OMAN

1.1 Introduction

Sensitive dryland environments comprise 41% of the Earth's surface and 38% of the world's population (Reynolds et al. 2007). Human activity and climate variability are fundamental influences in these environments. Human activity has and is expected to amplify land changes in drylands, especially as the global population climbs to almost 10 billion by 2050 (PRB 2012) and is increasingly situated in urban areas, raising expectations in the material standards of living (Seto et al. 2010) and placing more demand on hinterlands (Defries and Pandey 2010, Seto et al. 2012). In addition to these direct changes on the land, human activity indirectly shapes terrestrial environments through its impacts on climate, regional to global in kind (Pielke 2005). These changes are and will affect dryland climate variability and the boundary conditions in social-environmental systems (Zhang et al 2007).

Climate and land changes are underway in the sensitive drylands of Dhofar, Oman. This region has a recent oral history of deforestation and intensified grazing, both of which appear to be amplified by the economic development and population growth in Salalah. This change takes places in the context of a climate regime dominated by the Indian Summer Monsoon (ISM), which provides valuable precipitation and cooling winds during the summer months, allowing a diverse ecosystem to thrive that contrasts to the drier desert environments that dominate the remainder of Oman. It is not yet clear

how climate warming is affecting this precipitation, but there has been a noted increase to temperature in the region (AlSarmi and Washington 2011) and speculation that variability in the monsoon is increasing.

The dual forces of human activity and climate variability are both identified as causes of a decline in a highly important ecosystem, the Dhofar cloud forest, which is part of a larger South Arabian Cloud Forest that spans Yemen and Oman. This open woodland has witnessed significant changes in land cover and is believed to be susceptible to climate changes through the variability of the monsoon. This dissertation investigates three aspects of the cloud forest in Oman: 1) its biodiversity and relationship to the environment, 2) monsoonal variability and its relationship to cloud forest phenology and vegetation dynamics, and 3) the role of human activities in changing land cover.

1.2 Research Background to the Problem

This research topically addresses dryland environmental change, a subset of the broader theme of land change science. These themes and approaches are treated in turn in the following sections.

1.2.1 Environmental Change in Dryland Environments

A major concern in climate change is how alteration of dominant climate regimes will affect global weather patterns. For example, the El Nino Southern Oscillation (ENSO) and the North Atlantic Oscillation (NAO) have been shown to alter weather patterns globally (Hurrel 1995, Cook et al. 1999, Anyamba et al. 2001, Sun et al. 2008),

primarily through teleconnections. The ENSO can affect ecosystems throughout Africa, North America, and the Indian Ocean (Cook et al. 1999, Anyamba et al. 2001, Kumar et al. 2006). In the deep past, monsoonal winds, as measured from Arabian Sea cores, have been shown to correlate with ice-rafted debris in the North Atlantic, as affected by the NAO (Anderson et al. 2002). In either case, the ENSO and NAO are measured by indices, and these indices can be compared to local climate data to predict how climate anomalies associated with these regimes will affect temperature and precipitation in local regions (e.g. Pozo-Vazquez et al. 2001).

Aridification or desertification is not only a product of climate oscillations, but of inappropriate human use of drylands (Reynolds and Stafford-Smith 2002). Understanding their relative roles is often a vexing issue. Several examples, illustrate this problem. The 1930s Dust Bowl in the southern Great Plains of the United States has long been identified as climatic drought affecting inadequate farming practices. Recent modeling work, however, indicates that such a large magnitude drought in the center of the U.S. involved feedbacks between large-scale land clearing and poor farming practices (Cook et al 2009). Decades (1960s-80s) of drought in the Sahel of Africa were attributed to land degradation from cropping and grazing (Fairhead and Leach 1986, Reynolds and Stafford-Smith 2002). Human-induced land degradation was called into question when a recovery of the Sahel was instigated by a change in sea surface temperature in the Atlantic Ocean during the 1990's (Hulme 2001). Local human-induced environmental impacts notwithstanding, the large aridification of the Sahel was largely climatic in origin (Nicholson 1993, Nicholson 2009) with localized impacts related to land uses. Finally, comparisons of human and environmental responses to drought cycles, stocking, land

management decisions, and institutional action in Australia demonstrates how land management decisions to continue high stocking rates, despite decreasing biomass, amplified land degradation in the outback in the face of drought (Stafford-Smith et al. 2007). These examples highlight the critical role of an integrated analysis of the coupled human environment system, but it also highlights how human actions and institutional policies can be just as formidable for land change as the climate.

1.2.2 Land Change Science

Land change or land system science (LCS) examines human-environment interactions on ecosystem and human wellbeing (Turner, Lambin, and Reenberg 2007). It does so through monitoring and observation, coupled human-environment analysis, modeling, and synthesis. Observations and monitoring of the human environment often use remote sensing to measure change. A variety of platforms and technologies have enabled multi-decadal monitoring of the Earth system. In general, there are three scales used for Earth observation: high, medium, and low resolution. High-resolution imagery can provide fine scale monitoring, between 1 and 15 m, and is often used for cross-sectional snapshots of the environment (e.g. Walsh and et al. 2008a,b). Perhaps the most common sensors employed for large-area studies of land change, however, are medium resolution imagery, such as Landsat, which has a 30 m resolution (e.g., Gutman et al. 2004). MODIS, another important platform, is a low resolution sensor (compared to Landsat) capable of capturing Earth observations between 250 m and 1 km in resolution, but it has the capability of generating snapshots of vegetation, surface temperature, and albedo every eight to sixteen days, making its temporal resolution nearly unmatched by

other sensors (Justice et al. 1998). It is increasingly common to combine data from multiple sensors to understand land change.

Regardless of the sensor, land-use/cover maps can be generated from classified images. Biophysical variables can also be quantified directly, for example: NDVI, temperature, albedo, emissivity, and evapotranspiration. Finally, the form of the land can be discerned as well, usually from configuration metrics derived from classified images (Turner 1989). Human and environmental subsystems are inherently complex, elevating the usefulness of modeling as a tool to combine observations from remote sensing with biophysical impacts/feedbacks and land-use change drivers (NRC 2014). Common modeling methods in LCS include, among many others, agent based models (ABM) and economic models. ABM's simulate a process using various software agents to mimic real world behavior. They can incorporate socioeconomic data, environmental data from remote sensing, and lab data (Manson and Evans 2007). Economic models of land change attempt to capture key characteristics of behavior that lead to certain land change outcomes. Regression models are common (e.g. Southgate et al. 2009) where conceptual models of a dependent land change outcome variable are tested for correlation with a variety of possible drivers (the independent variables). No matter the type of model used, the process of modeling in LCS is useful for linking the socioeconomic drivers with biophysical outcomes and feedbacks.

An ongoing problem has been to link the land change observed in remote sensing with the socioeconomic drivers of change, in part because these drivers are arrayed along a proximate to distal axis. The direct or immediate drivers are easy to identify and associate quantitatively to land change. Typically the more distal the driver, the more

difficult it is to demonstrate such associations. To this end, synthesis in LCS has focused on uncovering the socioeconomic drivers that may be complex and masked from direct observation (Lambin et al. 2001; Seto and Reenberg 2014). In Vietnam, for example, reforestation is prevalent despite a large internal demand for wood. In this case, wood is imported to serve demand, while regenerating local forests (Meyfroidt and Lambin 2009). Whether direct or indirect, globalization is a persistent force affecting land cover change around the world (Liu et al. 2013, Meyfroidt and Lambin 2009, Seto and Reenberg forthcoming). Access to markets creates complexity and price vulnerabilities, and along with economic fluctuations from globalization causes uncertainty (Defries et al. 2010). LCS and global change studies show that environmental change is a complex process. Distal influences can be attributed to changes in population, technology, urbanization, institutions, and globalization (Turner and Robbins 2008, Brannstrom and Vadjunec 2014, Seto and Reenberg 2014). These four aspects place pressure on human environment systems, which affects ecosystem services through the supply and demand of industrial goods and services. Globalization seems to be the common distal factor at the heart of land change (Lambin et al 2001), but population, technology, institutions, and urbanization play an important role as conduits for the demand of resources and ecosystem services, and seem to be at the heart of wider changes taking place in the global environment, including anthropogenic climate change (Liu et al. 2013).

1.2.3 Quantifying Environmental Change

Two common methods for analysis of remotely sensed images, and the methods that are used here, are the subpixel method and time series analysis. The subpixel

approach offers an understanding of how land covers fractionally occupy a pixel. Time series analysis is suitable for understanding the role that climate plays on environmental features, such as phenology and teleconnections.

1.2.4 Subpixel Approach

Ground covers that occupy varying proportions of the landscape can be extracted from the pixel by assuming that each pixel comprises a combination of all possible ground covers in the scene (Settle and Drake 1993). Generally, the classic approach to finding endmember combinations is known as the linear mixture model or as spectral mixture analysis (SMA; Settle and Drake 1993). To achieve understanding of what ground covers occupy a pixel each pixel is considered to be a linear combination of differing endmembers, which is denoted mathematically as,

$$x = \sum_{i=1}^{n} f_i P_{i\lambda} + \epsilon \qquad (1)$$

where x is the scene pixel, n is the number of endmembers, f_i is the fraction of the pixel occupied by that endmember, $P_{i\lambda}$ represents the reflectance values of the endmember at each band λ, and ϵ is an error term. One constraint is usually imposed on the model,

$$\sum_{i=1}^{n} f_i = 1 \qquad (2)$$

This constraint ensures that no combination of endmembers occupies more than 100% of the pixel. Modeling of the pixels requires training data taken within the image scene or some measured reflectance for each endmember n. Measured reflectance values can come from spectrometer readings or one of many published spectral libraries, and usually

are taken without atmospheric conditions or disturbance. Training data are usually preferred because even when an image is converted to reflectance, the atmospherically corrected scenes are usually not absolutely correct, which can obscure the results. Training data are therefore preferable because the pixel's reflectance values are adequately drawn from within the image along with any noise inherent within the image.

There are some limitations to using SMA. First, the number of endmembers cannot exceed the number of bands plus one (Settle and Drake 1993). In a Landsat 5 TM image with six visible and near infrared bands only seven endmembers can be modeled. This restriction of endmembers in the scene may not represent reality, especially for a heterogeneous image with a great number of different land covers. Second, endmembers and their training data must be chosen to be as close as possible to the reflectance values of the land cover or class being modeled, therefore the selection of training data is critical (e.g. Dawelbait and Morari 2012).

One improvement to the SMA that addresses some of the limitations with the classic approach is multiple endmember spectral mixture analysis (MESMA). MESMA was developed as a way to address the limitation in SMA that requires that all endmembers of interest be modeled at every pixel (Roberts et al. 1998). This approach allows the number and type of endmembers to vary from one pixel to the next. Endmembers can be selected from spectra measured in the field or laboratory, or selected from within the image. Models are selected by using the model with the minimum root mean square error (RMSE). RMSE is defined as,

$$RMSE = \sqrt{\frac{\sum_{i=1}^{\lambda}(\epsilon_i)^2}{N}} \qquad (3)$$

N is the number of reference endmembers. The RMSE measures the residual error of a subpixel estimator. Fractions are also allowed to vary between -0.01 and 1.01. The benefits of using this approach are that endmembers can be modeled as two or more endmember models. For example, MESMA has been used to model vegetation, soil, shade, and senesced grass in the Santa Ynez Mountains of California and other environments, and has been effective in mapping subpixel fractions (Dennison and Roberts 2003).

1.2.5 Time Series Analysis

Whether using a subpixel approach or a pixel based approach, imagery can be coupled with time series analysis to measure environmental change. Researchers have noted that high temporal resolution studies are most likely best for uncovering the effects of climate variability and anthropogenic changes. Lambin and Linderman (2006) point out that the most common data for studying land change are generally higher spatial, lower temporal resolution satellites. Land-cover conversions, like deforestation, can be ideally studied with these types of data because changes to the tree cover fluctuate less than the temporal coverage of the satellite. However, land-cover alterations, such as degradation of pastures on grasslands, might not be as easily detectable because they differ from one year to the next, and sometimes within the same year. Land-cover alteration is the absence of a conversion of one land-cover type to another. Alteration through degradation might result in a lower overall net primary production, but the land cover will still remain grass.

A variety of methods have been used to circumvent the problem in land-cover alteration. One way to measure these alterations (in this case, overgrazing) is to use a linear correction of NDVI values over a study period to compensate for rainfall variability (Archer 2004). Another important technique is time series analysis of remotely sensed images, particularly for phenology analysis, which is the study of the greening period of vegetation. Phenology analysis is associated with a peak in the growing season and then the senescence of the vegetation to an annual minimum during a yearly cycle (de Beurs and Henebry 2010). While phenology can be estimated with a number of different techniques, satellites can make the task of estimating phenology parameters easy by compiling a time series of NDVI rasters, preferably of high temporal resolution (such as monthly or every 16 days). Once a high temporal resolution of NDVI images is compiled, a trend can be estimated. Calculating trends can include a linear regression of the time series or some non-parametric calculation of the trend line. Non-parametric trends are often considered to be advantageous because they are not reliant on certain statistical assumptions. Panday and Ghamire (2012) used a seasonal trend analysis to assess NDVI time series over the Hindu-Kush region of the Himalayas between 1982 and 2006. The NDVI data were first processed using a harmonic regression, which fits a curve to the data (Eastman et al. 2009). Once the harmonic regression was applied, they analyzed three aspects of the data for trends: Amplitude 0, Amplitude 1, and Phase 1 (Eastman et al. 2009; 2013). Amplitude 0 is the average annual NDVI value. Amplitude 1 is the magnitude of the peak NDVI value over a year while considering the minimum as well. Phase 1 represents the timing of the maximum NDVI value at a pixel; an assessment of the Phase 1 signal gives the timing of the

greening cycle. A trend assessment algorithm can then be used to determine the slope of a trend and its significance for these three parameters (Eastman et al. 2009; Neeti and Eastman 2012). A common way to derive a trend slope is by using a Theil-Sen median slope, which is a non-parametric technique that performs a pair-wise comparison of time series observations in the NDVI images (Theil 1950; Sen 1968). Finally, the significance of the Theil-Sen median slope is assessed using a Man Kendall test to detect whether the trend is significantly increasing or decreasing monotonically (Mann 1945).

1.3. Research Problems and Questions

1.3.1 Study Area & Problem Specification

The study area for this dissertation is the Dhofar portion of the South Arabian Cloud Forest, also known as the Dhofar cloud forest (Figure 1.1). The South Arabian Cloud Forest is a deciduous, seasonal forest (Hildebrandt 2005) that exists in fragments along the southern coast of Oman and Yemen. Two mountains are the primary focus throughout this dissertation, Jabal Qara and Jabal Qamar, both of which are in Dhofar, Oman, and house the largest potions of the cloud forest. The cloud forest, thought to be the native home of frankincense (*Boswellia sacra)*, is comprised mainly of broadleaf tree species (Kurschner et al 2004) and grasslands. The Indian Summer Monsoon (ISM) provides the essential precipitation that supports the ecosystem and gives the region its unique, oasis-like landscape.

The start and end of the ISM (known locally in Arabic as *khareef*) as well as the intensity of the winds varies by year (Anderson et al. 2002, Goswami and Mohan 2001, Gupta et al. 2003, Kumar et al. 2006, Scholte et al. 2010). *Khareef* is generated when a

summer upwelling of cold water in the Indian Ocean creates cloud fog that pushes against the Dhofar Mountain range for about three months, from approximately the end of June to the beginning of September. Horizontal precipitation from the summer clouds provides light drizzle and substantial cloud moisture (Hildebrandt 2005, Hildebrandt and Eltahir 2006, Hildebrandt and Eltahir 2007). Dense vegetation grows in direct contrast to the more arid lands located to the north of the cloud forest. From what is known about the timing and intensity of the ISM in other parts of the Indian Ocean, the beginning and ending, as well as the intensity of the ISM can vary from one season to the next.

The cloud forest provides ecosystem services that are essential to local livelihoods, including ecotourism, biomass production for rangelands, amongst others (e.g. frankincense extraction, wood harvesting, water provisioning). Numerous factors have raised concerns regarding land-use and land-cover change in the forest. First, camel and bovine grazing on the cloud forest's rangelands are thought to have caused degradation of the grasslands as well as a reduction in tree density (Hildebrandt and Eltahir 2006). Second, modernization, supported by global demand for Oman's modest oil reserves have encouraged infrastructure development, such as roads and buildings for new settlements, as well as the growth of Salalah, the nearby city, that may indirectly affect the cloud forest.

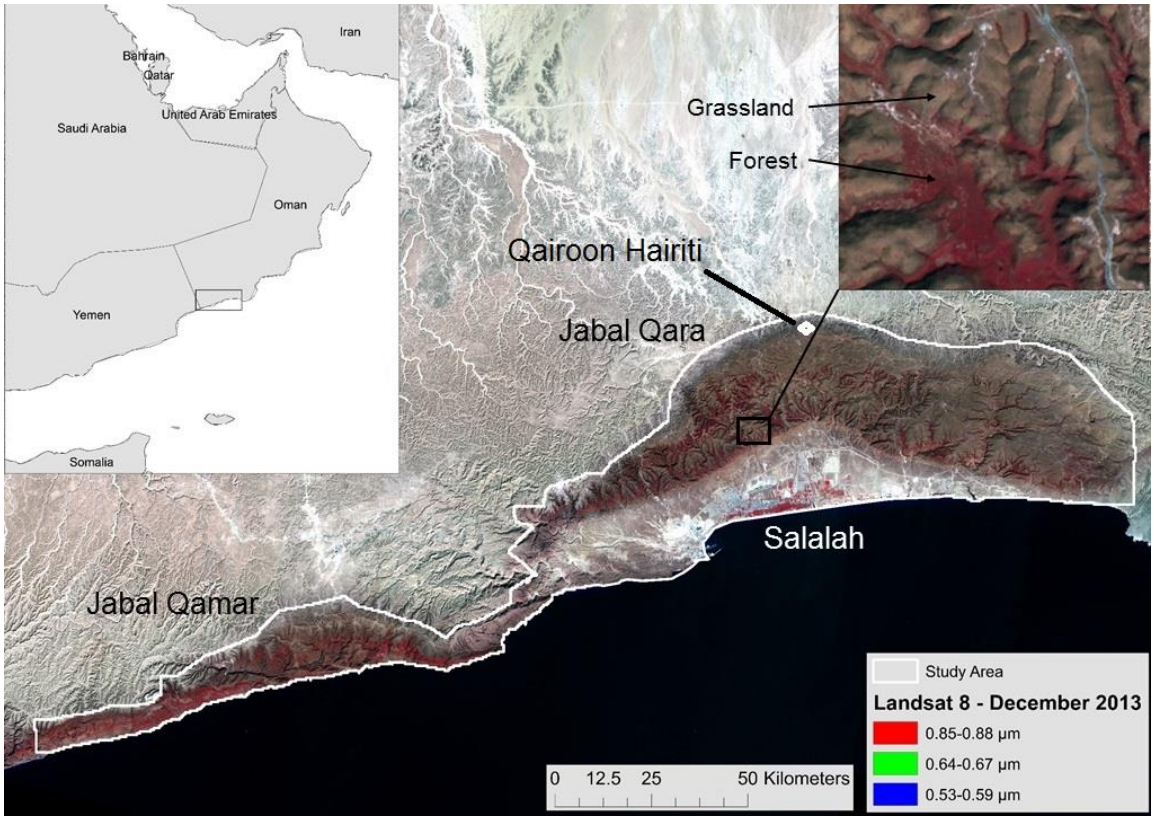

Figure 1.1: Landsat image of the study area in Dhofar, Oman. The cloud forest consists of grasslands and forests. Two primary mountains (Jabal Qara and Jabal Qamar), along with the coastal region around the city of Salalah are the boundaries of the study area. A climate station used in this dissertation is located at the town of Qairoon Hairiti.

1.3.2 Research questions

The land changes underway in the cloud forest of the Dhofar area remain undocumented and lack systematic assessments of their magnitude and cause. Climate variability may obscure the attribution of anthropogenic and other sources of land change, while inadequate understanding of climate dynamics impedes our understanding of the role of temperature and precipitation variability. This dissertation provides a systematic assessment of land changes in the Dhofar cloud forest, and synthesis links to causes. In addition, it seeks to demonstrate the role of climatic drivers in this forest,

focusing on the delineation of their relative roles and the consequences to phenology. These general queries are addressed through a specific set of questions asked about the study site.

1. What is the annual variability in monsoon conditions in the Dhofar cloud forest, and how can this variability be quantified using climate and remote sensing data?
2. How sensitive is the phenology of the Dhofar cloud forest to variability of the monsoon and oscillations in climate teleconnections?
3. What is the distribution of trees and shrubs across the Dhofar cloud forest?
4. What is the trend in NDVI over the last 13 years? How does this trend relate to deforestation, overgrazing, and the built environment?
5. What land changes have occurred between 1970 and today? What are the causes?

1.4 Organization of Dissertation

This dissertation incorporates three types of analyses organized in three studies (research papers) to investigate the relative roles of climate and anthropogenic influences in shaping the environment in Dhofar, Oman. Each paper, the data (see also Table 1.1), and analyses are noted below.

Table 1.1: Datasets used in this dissertation

Data Category	Data Set	Description	Time Frame
Climate	Temperature	Daily and monthly averages. Time series. Stations: Qairoon Hairiti	2001-2013 (QH)
	Precipitation	Daily and monthly averages. Time series. Stations: Qairoon Hairiti	2001-2013 (QH)
	Reanalysis II	Forecasted climate variables used to understand the timing of the monsoon	1979-2013
Environment	NDVI	16 day MODIS time series	2001-2013
	Slope	Derived from elevation	1999
	Aspect	Derived from elevation	1999
	Hydrology	Derived from elevation	1999
	Elevation	Meters above sea level; from Shuttle Radar Topography Mission	1999
	Tree and shrub survey data	Primary data collected during survey. Includes the density, frequency, and cover of dominant species	2013
Land cover/use	Built environment	Derived from Landsat 5-8	1988 and 2013
	Forest (trees)	Derived from Landsat 5-8	1988 and 2013
	Grassland	Derived from Landsat 5-8	1988 and 2013
	Shrubs	Derived from Landsat 5-8	1988 and 2013
	Agriculture	Derived from Landsat 5-8	1988 and 2013
	Coastal alluvium	Derived from Landsat 5-8	1988 and 2013
	Desert gravel plains	Derived from Landsat 5-8	1988 and 2013
	Water	Derived from Landsat 5-8	1988 and 2013
	Impervious surfaces	Derived from Landsat 5-8	1988 and 2013

1.4.1 Indian Ocean Monsoon Dynamics in Southern Arabia and Effects on the Vegetation Phenology of a Seasonal Cloud Forest

Chapter 2 identifies correlations between the climate dynamics of the southern Arabian Peninsula and the Dhofar cloud forest. Comparisons are drawn between yearly monsoonal precipitation, monsoon timing, and temperature with seasonal parameters of cloud forest vegetation.

Precipitation data were collected at Qairoon Hairiti (in the Dhofar cloud forest, see Figure 1.1), while temperature data came from Reanalysis II (NOAA; Kanamitsu et al. 2002). Time series of climate regimes were constructed from data addressing three

climate phenomena: the Indian Ocean Dipole (IOD), ENSO, and sea surface temperatures (SST). These three phenomena have been shown to influence weather and climate near the Arabian Peninsula. To measure the impact of these three climate phenomena, correlations are drawn between their index series and seasonal parameters for the cloud forest. Mean annual NDVI (Amplitude 0), magnitude of the peak NDVI signal (Amplitude 1), and timing of peak greenness (Phase 1) were extracted for the Dhofar Cloud forest using the Earth Trends Modeler in Idrisi.

Correlation between time series and the relationship between phenology and climate are derived using linear models from the Earth Trends Modeler in Idrisi. Linear models in time series analysis are analogous to those from linear regression. Common metrics for evaluating the model, such as the slope, intercept, coefficients, R^2, and residuals, are used to assess the correlation between climate indices (SST, IOD and ENSO). The purpose of this analysis is to measure how much influence the various climate regimes have on local Dhofar climate and cloud forest phenology, which is important for understanding the vulnerability from global climate change and tipping elements in the Earth system (Lenton et al. 2008).

The start and end of the Indian Ocean Monsoon is developed in two models. The first model is based on maximum daily temperature data from Reanalysis II (Kanamitsu et al. 2002) for the period 1979 to 2013. The second model constructs the start and end of the monsoon using cloud cover data from 2001 to 2013 using MODIS daily images. Average values of the MODIS band-4 reflectance are used to measure cloud cover over the study area. The timing and length of the monsoon are compared with MODIS NDVI

time series and sum NDVI values for October to December (Wessels and colleagues 2012).

A Theil-Sen median trend was used to estimate changes in NDVI between 2001 and 2013 (Theil 1950, Sen 1968). The identification of trends provides insight into conditions for increased or decreased biomass production. These climate trends are compared to cloud forest NDVI trends at 12 random sites.

1.4.2 Drivers of Plant Diversity in the South Arabian Cloud Forest

The primary goal of Chapter 3 is to understand mechanisms that drive biodiversity in the Dhofar cloud forest. A floral survey is conducted to measure biodiversity and to understand the mechanisms of biodiversity patterns.

Three measurements—density, cover, and frequency (Mitchell 2007)—were taken for 102 randomly selected surveyed plots. The importance value of a species was calculated and mapped for all plots, providing a geographic distribution of the principal species and to help define the various ecological communities.

In addition to importance value, biodiversity indices were calculated from the vegetation data. The diversity measurements were used to determine biodiversity patterns.

Finally, assessment of the distribution of species and biodiversity hotspots of the tree and shrub species surveyed constitute two distinct sub-analyses: those within the cloud forest proper and those within the plateau grasslands. Chapter 2 tests several hypotheses about biodiversity patterns and uses a cluster analysis to define the vegetation communities. The floral analysis includes many environmental variables (e.g., slope,

elevation, hydrology, aspect), climate variables (precipitation and temperature), as well as anthropogenic variables (e.g., distance to roads, and distance to buildings).

1.4.3 Land Changes and their Drivers in the Dhofar, Oman Cloud Forest and Coastal Zone between 1988 and 2013

Chapter 2 and 3 improve understanding of how the climate has affected the overall ecosystem of the cloud forest, biogeography of the cloud forest, and crucial areas of biodiversity that are susceptible to human impacts and variable climate. Chapter 4 quantifies the changes in land covers and uses in Dhofar's cloud forest and the adjacent coastal zone and associates these changes to various drivers of change.

Land change is quantified between 1988 and 2013. The first year captures the beginning of major socioeconomic changes in Oman, registered by the growth of Salalah. The land-cover categories addressed are trees, grasses, shrubs, agriculture, coastal alluvium, desert gravel plains, water, roads, and built environment. These categories included the major land-covers observed in the cloud forest zone and the lands surrounding the forest. Special attention is given to the identification of overgrazing and deforestation (i.e., forest thinning). Change analysis is conducted with Idrisi Land Change Modeler (LCM). LCM analyzes land-cover images to determine areas of change and provide transition areas and prediction of change. Additionally, a sub-pixel analysis measures the shifts in forest fractions (i.e., thinning) between 1988 and 2013.

CHAPTER 2

AN ASSESSMENT OF MONSOON TIMING, CLIMATE REGIMES, AND MONSOON VARIABILITY ON VEGETATION DYNAMICS IN SOUTHERN ARABIA

2.1 Abstract

The Indian Summer Monsoon (ISM) is critical for vegetation in southern Arabia, particularly for the drought deciduous cloud forest in the Dhofar region of Oman. This paper investigates two potential influences of variance or changes in the ISM on the vegetation dynamics in the cloud forest. The first involves the relationship between monsoon variability and timing, and seasonal vegetation. The second addresses the correlation between normalized difference vegetation index (NDVI) time series, acquired from MODIS satellite imagery, and climate systems, such as El Niño Southern Oscillation (ENSO), Indian Ocean Dipole (IOD), and sea surface temperatures (SST) in the Arabian Sea. Additionally, timing of the monsoon was modeled using Reanalysis II data and daily satellite images from MODIS.

The findings reveal that the seasonal vegetation parameters are resistant to variability in measureable precipitation, monsoon length, and temperature. The strongest correlations were found with June precipitation and temperature, but these were generally weak to moderate explanations of the variance. Even broader climate regimes, such as ENSO and IOD, show weak to no correlation with NDVI time series. Cloud forest phenology shows a stronger correlation to SST in the Arabian Sea, with SST about six to

nine months out of phase with NDVI time series (SST leading). The evidence, therefore, suggests that the cloud forest is resilient in the face of climate change.

2.2 Introduction

The Indian Summer Monsoon (ISM; henceforth, monsoon) is foundational for the vegetation of the Southern Arabian Peninsula. Known locally as *khareef,* the monsoon is responsible for most of the precipitation in the southern region of Oman, or Dhofar, as well as parts of Yemen. Monsoon precipitation supports the ecosystem of the Dhofar Mountains, where a drought deciduous cloud forest thrives in those parts of the mountains near the coast (Hildebrandt and Eltahir 2006). This cloud forest, part of the South Arabian Cloud Forest, is one of the most diverse ecosystems in the peninsula (Miller and Morris 1988; Ghazanfar and Fisher 1998).

The ISM reliably develops over the Arabian Sea in late May and early June of each year (Fieux and Stommel 1977; Joseph et al. 1994; Fasullo and Webster 2003; Joseph et al. 2006). In general, warmer terrestrial air masses meet cooler ocean air masses caused by upwelling off the coast of the Arabian Peninsula. As these two air masses meet, clouds form along southern part of the peninsula. The clouds arrive several weeks after the ISM winds develop out of the southwest and are responsible for the highest period of precipitation.

Several studies demonstrate that the monsoon delivered more rainfall in past pluvial periods over the southern Arabian Peninsula (Fleitmann et al. 2003; Fleitmann et al. 2004; Blechschmidt et al. 2009; Cremaschi and Negrino 2005; Fleitmann and Matter 2009; Fleitmann et al. 2011). These studies link increased rainfall to warming during

peak interglacial periods, such as the Early Holocene and the Last Interglacial, and were driven by changes in the Intertropical Convergence Zone (ITCZ) and minimal Arctic sea ice extent (Overpeck et al. 1996; Fleitmann and Matter 2009). The effects of current anthropogenic climate change on monsoon rainfall are largely unknown. There is some indication that monsoon rainfall in India changed in the latter part of the 20th century, leading to a significant reduction in moderate and heavy rainfall days owing to a weakening monsoon circulation pattern (Krishnan et al., 2013). Climate model simulations suggest that global warming has the potential to destabilize the monsoon even further (Krishnan et al. 2013). Recent warming across the Arabian Peninsula (AlSarmi and Washington 2011), perhaps linked to anthropogenic climate change (IPCC 2014), has sparked interest in the study of the monsoon, with attention to vulnerabilities to its stability and impacts on vegetation. Some evidence points to a decreasing trend in rainfall, but results are not necessarily significant statistically (Kwarteng et al. 2009; AlSarmi and Washington 2011). At least one study did find significant results indicating decreasing July and August precipitation trends over Salalah in Dhofar, Oman (AlSarmi and Washington 2011). The consequences of this decrease for the cloud forest vegetation are not well understood, mainly because time series analyses of vegetation dynamics and climate variability have not been worked out.

Broader climate factors and their effects on the cloud forest are another area of emerging interest. The Indian Ocean Dipole (IOD), an oscillation of sea surface temperatures in the eastern and western parts of the Indian Ocean, is one such factor (Saji et al. 1999). Positive and negative modes of the IOD have been correlated to droughts and floods in Africa, Australia, and Indonesia, and they may affect the ISM (Ashok et al.

2001, 2004). The El Niño Southern Oscillation (ENSO) may also affect the ISM, though the relationship is thought to be indirect (Charabi 2009).

This paper provides new evidence and analysis directed to the question of ISM variability and vegetation consequences for the Dhofar cloud forest of Oman. It explores the timing of the monsoon using satellite imagery and climate data from ground stations and Reanalysis 2. In addition, it explores how monsoon variability and other climate factors may influence vegetation dynamics in the cloud forest using a time series of satellite images. In the process, this study

- models the timing of the monsoon in southeast Arabia;
- describes the characteristics of the cloud forest's phenology;
- determines the sensitivity of vegetation dynamics to climate variability; and,
- determines the relationship between broader climate factors and cloud forest dynamics.

2.3 Study Area

The study area includes the southern portions of the Arabian Peninsula and the South Arabian Cloud Forest in Dhofar, Oman. Also addressed are the broader climate patterns for the monsoon across southeastern Arabia and the Arabian Sea. Vegetation patterns and phenology are restricted to the cloud forest in Dhofar, Oman.

The cloud forest occupies the mountain range in Dhofar (Figure 1.1). Three primary mountains comprise the range: Jabal Qara, Jabal Qamar, and Jabal Samhan. The cloud forest is primarily situated in Jabal Qara and Jabal Qamar, but a small section runs along the cliffs of Jabal Samhan.

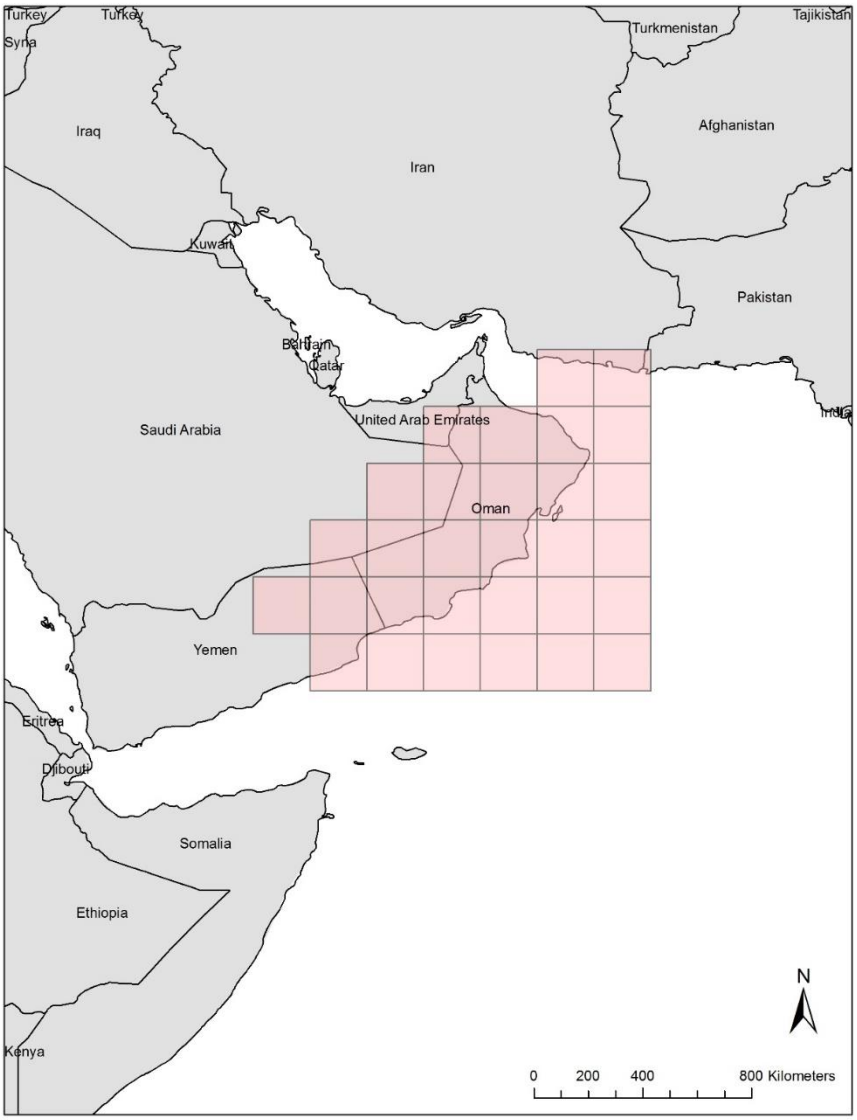

Figure 2.1: 30 Reanalysis 2 grids were used to study the start and end of the monsoon season. The grids were selected for their coverage of southeastern Arabia and adjoining portions of the Arabian Sea. Each grid has a spatial resolution of approximately 210 km.

The landscape of the cloud forest is comprised of grasslands, shrublands, and forest (Miller and Morris 1988; Pickering and Patzelt 2008; Patzelt 2011). There is also a large coastal plain just south of Jabal Qara that benefits from the monsoon. The mountains and coastal plain are partitioned by foothills covered with vegetation similar to

that found in the cloud forest. Approximately 29% of the cloud forest and coastal plain has tree cover, the rest is a mix of grasslands and shrublands. Because this region is one of the few areas on the Arabian Peninsula to have dense vegetation, grazing is heavy and animal husbandry is widespread. Cattle, camels, and goats are the primary livestock and are important sources of subsistence for the people living in the Dhofar Mountains (Janzen 1986; 2000).

The vegetation reaches peak biomass during the monsoon and senesces several months after the monsoon fog subsides (Hildebrandt and Eltahir 2006). Forested areas are descended from an ancient forest that once stretched from India to Africa during the Tertiary period (Kürschner et al. 2004). Current vegetation is associated with the Saharo-Sindian and Saharo-Arabian phytogeographic zones (Ghazanfar and Fisher 1998; Parker and Rose 2008).

The yearly temperature range for the cloud forest can vary from mean minimum temperatures of 19° C in January to mean maximum temperatures around 32.5° C in June (Galletti forthcoming). Daily average temperatures are less than 25° C during monsoon months. Mean annual precipitation normally measures around 200 mm. Monsoon precipitation on average accounts for more than 100 mm a year. The driest months are usually November, December, and January, when precipitation is less than 10 mm on average.

Table 2.1: Variables and parameters used in this study

Description	Name	Data Source	Time Frame
Normalized Difference Vegetation Index	NDVI	MODIS 16-day (250 m)	2001-2013
Cloud cover	Cloud cover	MODIS daily	2001-2013
Maximum daily temperature at 2 m	Tmax_daily	Reanalysis II (NOAA)	1979-2013
Mean yearly NDVI	Amplitude 0	MODIS 16-day NDVI	2001-2013
Difference between peak and minimum NDVI	Amplitude 1	MODIS 16-day NDVI	2001-2013
Timing of growth season	Phase 1	MODIS 16-day NDVI	2001-2013
Sum of October to December NDVI	ΣOND	MODIS 16-day NDVI	2001-2013
Day of year of peak temperature	First apex	Tmax_daily (Reanalysis II)	1979-2013
Day of year of second thermal peak	Second apex	Tmax (Reanalysis II)	1979-2013
Height of monsoon intensity-day of year	Tmin	Tmax (Reanalysis II)	1979-2013
Area under the curve between first apex and second apex	AUC	Tmax (Reanalysis II)	1979-2013
Total yearly precipitation	Total Prc.	Climate Station Data	2001-2013
June precipitation	June	Climate Station Data	2001-2013
July precipitation	July	Climate Station Data	2001-2013
August precipitation	Aug	Climate Station Data	2001-2013
September precipitation	Sept	Climate Station Data	2001-2013
Total precipitation for June, July, August, September	JJAS	Climate Station Data	2001-2013
Total precipitation for July and August	JA	Climate Station Data	2001-2013
Length of monsoon based on cloud cover	Length	Cloud cover	2001-2013
Length of monsoon season based on Tmax_daily	Apex to apex	Tmax_daily	1979-2013
Sea surface temps in Arabian Sea	SST	NOAA (via Clark Labs)	2001-2009
Intensity of the Indian Ocean dipole – Dipole Mode Index	DMI	JAMSTEC	2001-2009
El Niño Cycle, Niño 3.4 Index	Nino34	NOAA	2001-2009
El Niño Cycle, Southern Oscillation Index	SOI	NOAA	2001-2009

2.4 Data and Methods

2.4.1 Climate, Monsoon Timing, and Analysis

Table 2.1 lists the variables used in this study, a combination of observed and modeled data, as well as measures derived from them. Two separate models were developed to study the onset and withdrawal of the monsoon. The first model is based on temperature data, and the second, on observations of cloud cover.

The first model of the monsoon was developed using Reanalysis 2 data (Kanamitsu et al. 2002) for the period 1979-2013 over 30 grids covering southeast Arabia and the Arabian Sea (Figure 2.1). Two meter maximum daily temperature was used to define the monsoon season by fitting a curve to the daily temperature observations using a polynomial regression (based on a 15^{th} order polynomial). The polynomial curve was fitted to each year between 1979 and 2013. Temperature maxima and minima were extracted for each year and provide the monsoon seasonal parameters used to estimate the timing of the monsoon.

Moderate Resolution Imaging Spectroradiometer (MODIS; Justice et al. 1998) imagery was used to observe daily cloud cover and estimate the temporal dynamics of the monsoon. MODIS daily images from 2001 to 2013 were visually analyzed to measure the timing of consistent cloud cover over the study area. Three days of continuous cloud cover observed in June or July with no breaks in cloud cover for more than two days was used to establish the onset of the monsoon as experienced on the ground. The end of the monsoon was registered by three consecutive cloud-free days after the end of August.

In addition to the monsoon models, several climate variables were estimated using climate station data from Qairoon Hairiti, located within the cloud forest. Table 1 lists

these variables, which are mostly combinations of precipitation accumulation for the monsoon months or precipitation for an individual month.

2.4.2 Vegetation Data and Analysis

MODIS was used to obtain time series data of NDVI for the study area. MODIS creates a composite NDVI image every 16-days based on the highest NDVI value observed for a pixel at resolution is 250 m (Justice et al. 1998), which results in 23 composite images per year. MODIS images were collected for the period 2001-2013.

Analysis of vegetation data includes the creation of bivariate linear models to explore relationships between vegetation patterns and broader climate regimes. These models use the MODIS NDVI data as a dependent variable; climate indices and SST monthly data are used as explanatory variables. Sixteen-day MODIS data were transformed to monthly averages (to fit the data measurements of the climate indices). The four climate indices were: Niño 3.4 index (an index of the El Niño Southern Oscillation [ENSO] based on SST models [Rayner et al. 2003]); the Southern Oscillation Index (SOI; another index of ENSO [Trenberth 1984]); the Dipole Mode Index (DMI; an index of the IOD based on SST differentials between the east and west Indian Ocean [Saji et al. 1999]); and SST in the Arabian Sea. The Niño 3.4 and SOI datasets were obtained from NOAA NCDC. The SST data were obtained for the years of 1982 to 2009 from Clark Labs, which was based on a NOAA AVHRR dataset (Reynolds et al. 2002). These bivariate analyses are based on the period 2001-2009 when all climate, SST, and NDVI observations are aligned.

2.4.3 Seasonal Parameters of Vegetation

Seasonal vegetation variables were estimated using methods from Eastman and associates (2009; 2013). Mean annual NDVI (Amplitude 0), NDVI annual cycle (Amplitude 1), timing of the peak annual NDVI cycle (Phase 1), and sum of the NDVI for October to December (ΣOND) were derived from MODIS 16-day NDVI composite images. Amplitude 1 is calculated by taking the difference between the maximum and minimum values of a modeled NDVI curve (Eastman et al. 2013). Amplitude 0 is the mean annual NDVI. Phase 1 is the timing of the peak of the annual cycle. ΣOND is derived by summing all 16-day composite images for October to December of each year. ΣOND is a useful parameter because it measures the sum NDVI of the study area right before senescence and during months that have very low cloud cover. Phase 1, Amplitude 0, and Amplitude 1 are derived from curves that are fitted to the yearly NDVI observations using a harmonic regression model (Eastman 2009).

A trend analysis of the seasonal parameters measures systematic changes in phenology between 2001 and 2013 (Eastman et al. 2009; 2013). A Theil-Sen median slope is used to estimate the trend slope, reliably estimating the trend despite noise and outliers (Theil 1950, Sen 1968). Z-values are used to determine statistical significance. Additionally, a trend analysis was also conducted on the monsoon seasonal parameters modeled by the Reanalysis II data, as well as SST over the Arabian Sea.

Twelve random sites were selected to estimate the relationship between Phase 1, Amplitude 0, Amplitude 1, ΣOND, and climate variables. Of these 12 sites, three are dominated by shrub cover, three by grass covers, and five by forest covers. A linear model is used to measure the strength of the relationship between precipitation variables

(total yearly precipitation, June/July/August/September precipitation, JJAS precipitation, and JA precipitation), the monsoon season (AUC and Apex to Apex), and the length of the monsoon period as estimated from cloud cover. The fitted curves also provide estimates of green-up and green-down for 2001 and 2013. For each of the 12 sites, the green-up and green-down was measured to estimate the timing of the growing season. The green-up period is the approximate day of year (DOY) when seasonal growth has reached 40% of the maximum. The green-down period is the approximate DOY when senescence is estimated to begin, which is indicated by 40% of the maximum but on the declining side of the curve rather than the inclining side.

2.5 Results

2.5.1 Monsoon Timing

Figure 2.2 shows the maximum daily temperature progression for 2013 along with a fitted curved derived from a 15^{th} order polynomial regression. Two apices and a local minimum distinctly occur during the late spring, summer, and fall season (Figure 2.2). These three model parameters are part of a U-shaped curve that defines the progression of the monsoon season. These model parameters are labeled: first apex (season start or onset), Tmin (peak intensity or the bottom of the U-shaped curve), and second apex (season end or withdrawal).

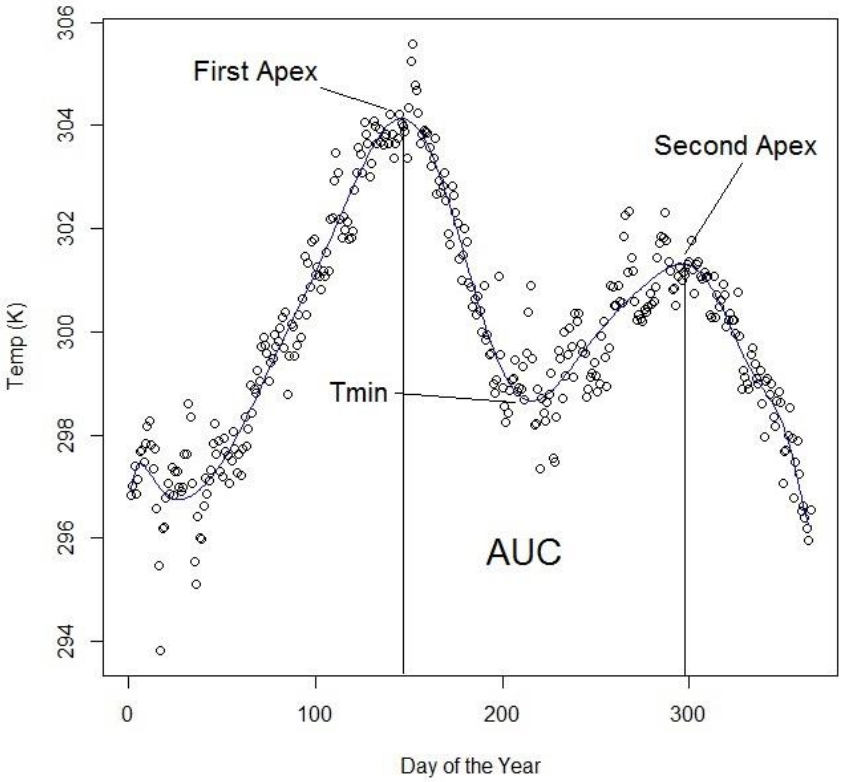

Figure 2.2: Daily maximum temperatures from Reanalysis 2 data for 2013. The monsoon season starts around the first apex and ends around the second apex. The height of the monsoon season occurs around Tmin. The area under the curve (AUC) helps measure the thermal intensity of the monsoon season.

Table 2.2: The start (onset) and end (withdrawal) of the monsoon estimated from Reanalysis II temperature data, and daily MODIS images of cloud cover. Values indicate day of year (DOY), or number of days for 'Length'

	Reanalysis II Temperature Model				**MODIS Cloud Cover Observations**		
Year	**Onset**	**Height**	**Withdrawal**	**Length**	**Onset**	**Withdrawal**	**Length**
1979	153	230	328	175			
1980	141	234	303	163			
1981	146	227	298	152			
1982	155	232	296	142			
1983	150	249	294	143			
1984	147	257	327	180			
1985	141	229	341	200			
1986	143	228	324	181			
1987	150	230	316	166			
1988	145	238	327	182			
1989	145	221	304	159			
1990	141	237	298	157			
1991	145	241	303	159			
1992	156	240	303	147			
1993	155	248	302	147			
1994	145	253	300	155			
1995	152	247	337	185			
1996	154	242	356	202			
1997	154	233	338	184			
1998	149	250	320	171			
1999	136	238	324	189			
2000	143	241	301	158			
2001	146	227	316	170	176	252	76
2002	140	236	332	192	179	259	80
2003	152	239	304	152	167	256	89
2004	141	239	313	171	186	256	70
2005	154	243	307	153	174	269	95
2006	150	237	311	161	182	256	74
2007	154	243	298	144	168	256	88
2008	150	236	290	140	182	247	65
2009	149	251	332	183	171	252	81
2010	141	237	331	190	169	258	89
2011	149	259	312	163	186	255	69
2012	149	249	326	177	164	248	84
2013	144	221	317	172	174	247	73
Mean	**148**	**239**	**315**	**167.56**	**175**	**255**	**79.46**
S.D.	**5.18**	**9.35**	**15.73**	**16.98**	**7.04**	**5.7**	**8.82**

Based on Reanalysis data from 1979 to 2013, maximum air temperatures reach the first apex on average around the 144th day of the year over the Arabian Sea (standard deviation = 6.1 days; Table 2.2), and on average around the 155th day of the year (DOY)

over land (S.D. = 7.7 days). After temperatures reach their peak, a steady decline follows until they reach a minimum (Tmin), on average around the 240th DOY over the Arabian Sea (S.D. = 13.2 days) and around the 233rd DOY over land (S.D. = 15.3 days). Once the minimum is obtained, temperatures steadily incline until they reach a second maximum temperature apex, which occurs on average around the 317th DOY over the Arabian Sea (S.D. = 24.1 days) and around the 307th DOY over land (S.D. = 36.5 days). These three temperature parameters and the U-shaped curve were also present in climate station data from both Salalah and Qairoon Hairiti.

In Dhofar, the monsoon is generally defined by the presence of clouds and light drizzle, not the temperature apices or Tmin as defined above. Estimates for the start and end of the monsoon, as defined by cloud cover, were reconstructed for the period between 2001 and 2013 using MODIS daily images of cloud cover over the Dhofar Mountains (Table 2). According to these data, the mean start of the monsoon is the 175th DOY (S.D. 7.04), which is about 20 days after the first temperature apex. The mean end of the monsoon is approximately the 255th DOY (S.D. 5.7), or approximately 52 days before the second apex. The mean length of the monsoon is about 80 days (S.D. 8.82 days).

The trend analysis of the timing of the monsoon season shows few significant trends for each of the 30 grids where the Reanalysis II data were collected (Figure 2). The parameter with the most significant trends was the second apex. Six of thirty grids showed a significant increase in the DOY of the second apex. On average the second apex increased by about 16.7 seven days between 1979 and 2013 for these six grids. Other parameters had three or fewer grids with a significant trend.

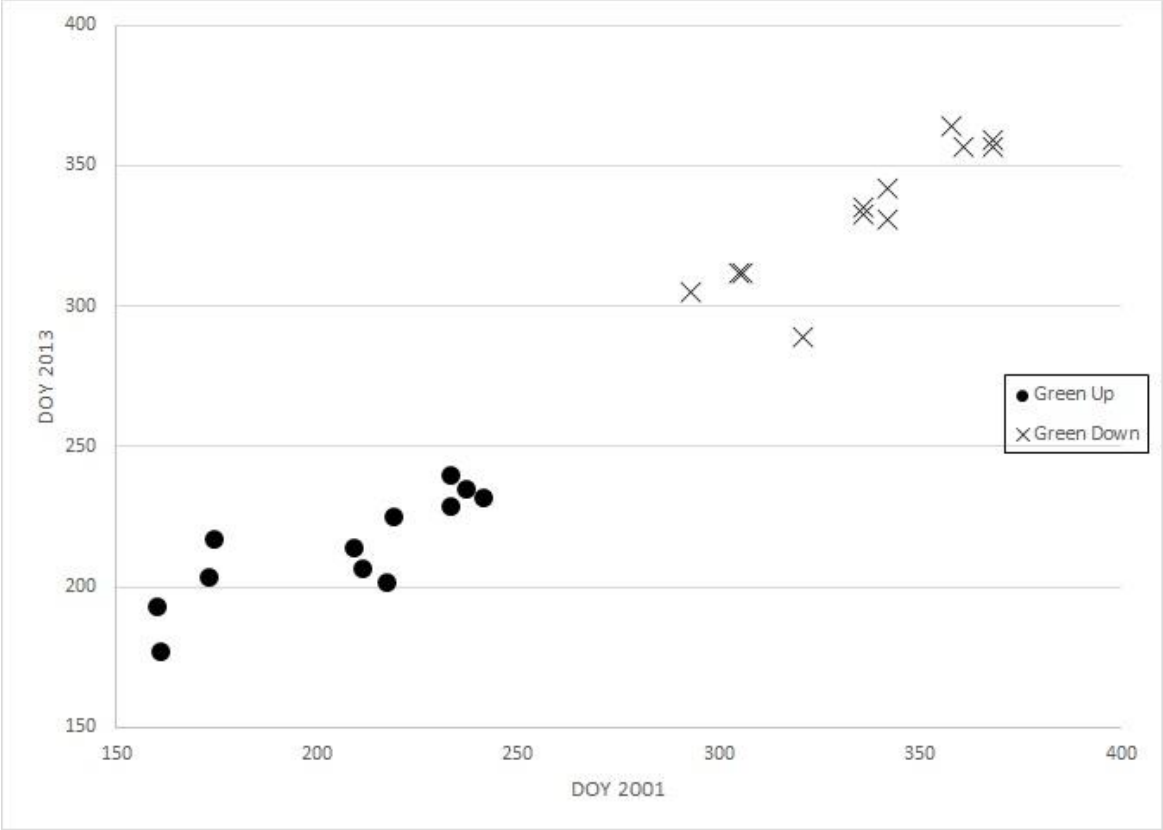

Figure 2.3: The green-up and green-down periods for 12 sites across the study area based on MODIS NDVI data for 2001 and 2013.

2.5.2 Cloud Forest Phenology

A comparison of green-up and green-down based on MODIS NDVI images at 12 sites (chosen because they are representative of various areas of the cloud forest) showed that growing seasons are fairly consistent between the two years examined, 2001 and 2013 (Figure 2.3). For 2001, the mean DOY the cloud forest reached 40% green-up is about the 205th DOY (S.D. 29.18 days), while green-down occurred around 336th DOY (S.D. = 24.43 days). For 2013, the results were similar with 40% green-up occurring on average around the 214th DOY (S.D. 18.01 days), and the 40% green-down occurring around the 333rd DOY (S.D. = 23.23 days). The mean length of the prime growing season

was about 130 days (S.D. = 9.71 days) in 2001, and 118 days (S.D. = 9.98 days) in 2013. With regards to land cover, grass covers generally began their prime growing season earlier than tree covers (mean = 199th DOY, S.D. 18.66 days) and ended earlier (mean = 323rd DOY, S.D. 17.88 days) than tree covers (green-up: mean = 217th DOY, S.D. 24.04 days; mean green-down = 344th DOY, S.D. 21.42 days). For shrub covers, the start and end of prime growing was between the grass and forest covers (mean green-up = 206th DOY, S.D. 26.25 days; the mean green-down = 327th DOY, S.D. 26.08 days).

The results of the seasonal trend analyses are shown in Figures 2.4, 2.5, 2.6, and 2.7. Amplitude 0 and Amplitude 1 trends (Figures 2.5 and 2.6) are negative mainly around the city of Salalah (see details in Galletti et al. forthcoming). The ΣOND (Figure 2.7) trends also show significant negative trends along the coast near the city of Salalah, which may indicate declining vegetation due to human activity near the city. The timing of the peak growing season (Phase 1; Figure 2.4) appears to be significant at only two primary clusters: one around the western edge of the cloud forest, and another on the eastern edge. Both of these clusters show significant negative trends, indicating that the growing season starts earlier (approximately 3-4 days earlier in the west and 2-14 days earlier in the east). The rest of the image, with the exception of small pockets here and there, shows mainly no significant Phase 1 trends.

Correlations between the key seasonal parameters (Amplitude 0, Amplitude 1, Phase 1, and ΣOND) and climate variables showed mainly weak to moderate correlation and no systematic correlation across the 12 sites (Tables 2.3, 2.4, 2.5, and 2.6). Phase 1 revealed weak to moderate correlation with June precipitation, but there were inconsistencies between negative and positive correlations. Amplitude 0 showed weak to

moderate positive correlation to AUC, while Amplitude 1 showed weak to moderate negative correlation with June and July precipitation across several sites. ΣOND showed mainly weak correlation to all climate variables.

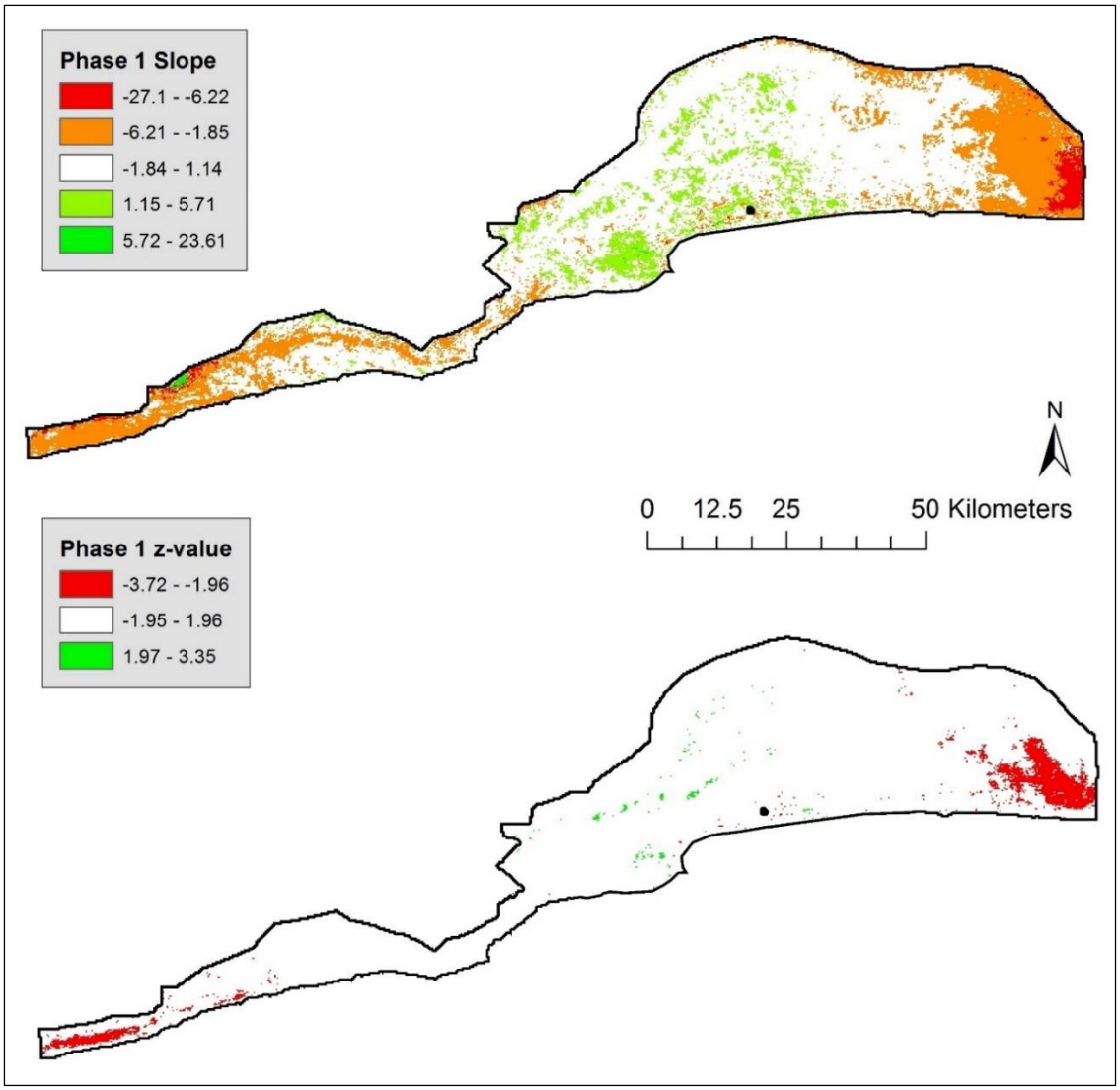

Figure 2.4: Trend analysis of Phase 1 (timing of the peak of the cycle). Top map shows the slope of the trend (change in NDVI/year). Bottom map shows z-values, which are used to measure significance.

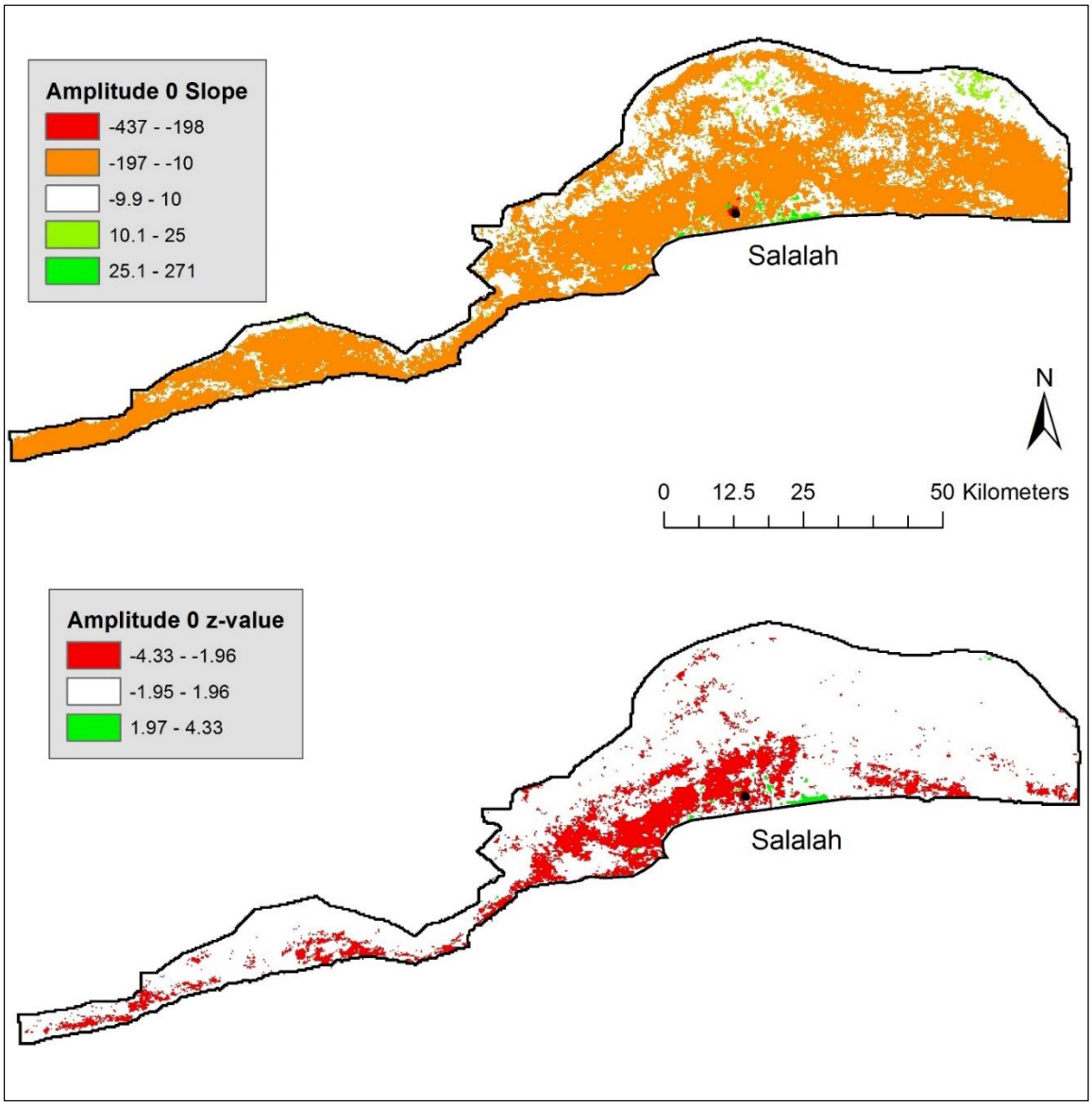

Figure 2.5: Trend analysis of Amplitude 0 (mean yearly NDVI). Top map shows the slope of the trend. Bottom map shows z-values, which are used to measure significance.

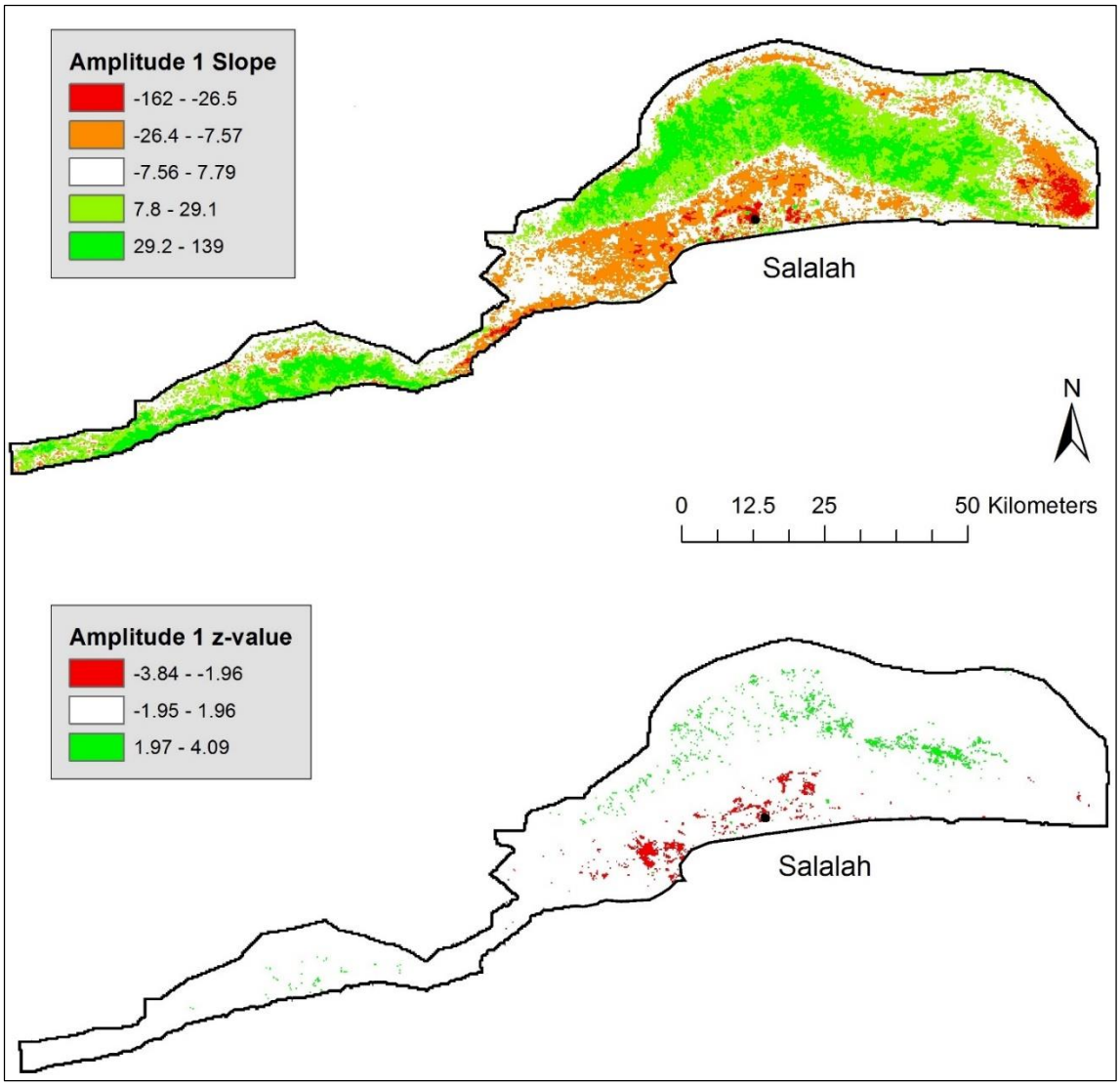

Figure 2.6: Trend analysis of Amplitude 1 (difference between peak and minimum NDVI). Top map shows the slope of the trend. Bottom map shows z-values, which are used to measure significance.

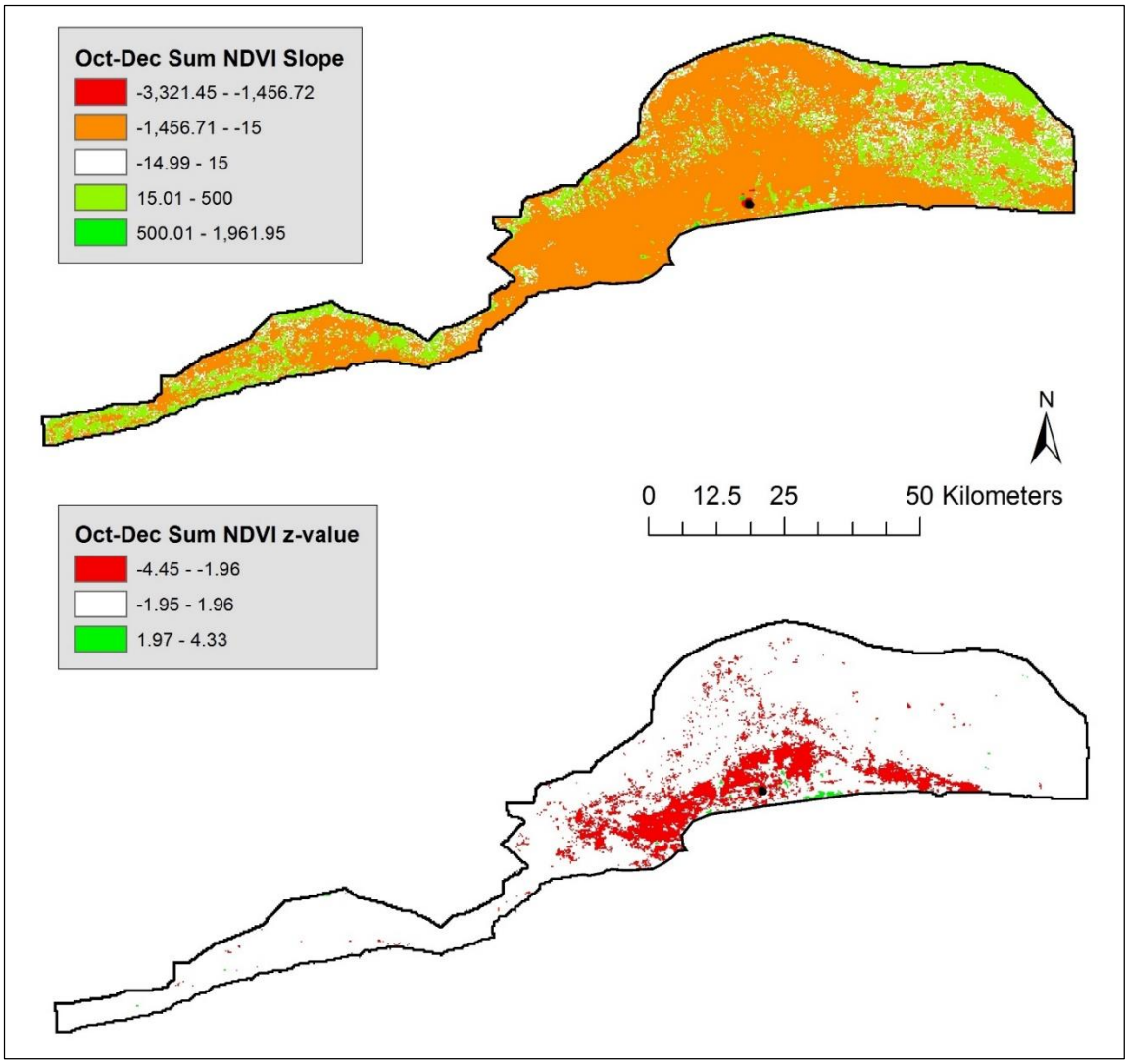

Figure 2.7: Trend analysis of ΣOND (Sum of NDVI for October, November, and December). Top map shows the slope of the trend. Bottom map shows z-values, which are used to measure significance.

Table 2.3: R^2 values for the relationship between yearly Phase 1 values (2001-2013) and 10 monsoon parameters at 12 cloud forest sites. Values in bold are $R^2 > 0.1$. (+) = positive correlation, (-) is negative. * = $p < 0.05$

Site	AUC	Total Prc.	June	July	Aug	Sept	JJAS	JA	Length	Apex to Apex	P1 Mean	P1 Std.
1	0.035	0.060	0.086	0.002	0.002	0.004	0.000	0.000	0.091	0.064	132.5	13.0
2	0.007	0.069	**0.392 (+)***	0.001	0.009	0.008	0.018	0.003	**0.171 (+)**	0.007	173.3	14.0
3	0.090	0.038	**0.388 (-)***	0.001	0.091	0.003	0.043	0.021	0.088	0.026	140.6	15.4
4	**0.179 (+)**	0.017	0.006	0.007	0.000	0.016	0.001	0.003	0.016	0.001	178.7	41.0
5	0.021	0.069	**0.327 (-)***	0.001	0.084	0.057	0.047	0.020	0.046	0.055	139.6	19.0
6	0.019	0.039	**0.210 (+)**	0.012	0.006	0.044	0.002	0.001	**0.101 (+)**	0.002	174.9	14.5
7	0.014	0.031	**0.189 (+)**	0.012	0.002	0.041	0.001	0.002	0.046	0.004	174.9	28.9
8	**0.138 (+)**	0.093	**0.160 (+)**	0.002	0.007	0.013	0.013	0.004	0.007	0.000	194.9	27.1
9	0.071	**0.125 (+)**	**0.194 (+)**	0.006	0.040	**0.145 (+)**	0.044	0.017	0.064	0.011	172.3	23.6
10	**0.144 (+)**	0.061	0.072	0.003	0.005	0.030	0.012	0.004	0.008	0.001	193.2	36.5
11	0.033	**0.148 (+)**	**0.123 (-)**	0.011	0.053	0.030	0.041	0.026	0.058	0.093	149.7	13.1
12	**0.417 (+)***	0.098	0.072	**0.134 (-)**	**0.375 (-)***	**0.181 (-)**	**0.260 (-)**	**0.231 (-)**	0.004	**0.171 (+)**	142.3	15.6

Table 2.4: R^2 values for the relationship between yearly Amplitude 0 values (2001-2013) and 10 monsoon parameters at 12 cloud forest sites. Values in bold are $R^2 > 0.1$. (+) = positive correlation, (-) is negative. * = $p < 0.05$

Site	AUC	Total Prc	June	July	Aug	Sept	JJAS	JA	Length	Apex to Apex	A0 Mean	A0 Std.
1	**0.190 (+)**	**0.127 (-)**	0.012	**0.404 (+)***	**0.369 (-)***	**0.164 (-)**	**0.375 (-)***	**0.416 (-)***	**0.105 (+)**	0.050	4284.1	275.8
2	0.044	0.007	**0.238 (+)**	0.005	0.021	0.081	0.005	0.011	0.052	0.020	2708.6	170.6
3	0.021	0.059	0.077	**0.194 (-)**	**0.138 (-)**	0.098	**0.149 (-)**	**0.182 (-)**	0.056	0.000	3806.2	305.8
4	0.017	0.002	0.084	0.038	0.001	0.014	0.009	0.017	0.000	0.031	2409.4	252.0
5	0.000	0.069	0.062	**0.179 (-)**	**0.115 (-)**	0.082	**0.133 (-)**	**0.162 (-)**	0.035	0.027	3601.4	211.9
6	**0.116 (+)**	0.093	0.077	0.009	0.013	0.026	0.021	0.011	0.067	0.015	2776.4	147.2
7	**0.157 (+)**	0.020	0.097	0.028	0.017	0.000	0.011	0.025	0.019	0.000	3992.3	342.5
8	**0.203 (+)**	0.020	0.083	0.005	0.003	0.009	0.002	0.005	0.004	0.000	2804.5	261.4
9	**0.161 (+)**	0.026	0.016	0.010	0.004	0.020	0.002	0.008	0.005	0.020	4336.1	266.1
10	**0.333 (+)***	0.006	0.005	0.004	0.033	0.019	0.012	0.013	0.002	0.009	2810.3	301.2
11	0.000	0.026	0.066	0.016	0.078	**0.207 (-)**	0.038	0.038	0.055	0.028	2568.4	132.0
12	**0.215 (+)**	0.033	0.014	**0.173 (-)**	**0.189 (-)**	**0.130 (-)**	**0.176 (-)**	**0.191 (-)**	0.025	0.031	2849.1	226.4

Table 2.5: R^2 values for the relationship between yearly Amplitude 1 values (2001-2013) and 10 monsoon parameters at 12 cloud forest sites. Values in bold are $R^2 > 0.1$. (+) = positive correlation, (-) is negative. * = $p < 0.05$

Site	AUC	Total Prc.	June	July	Aug	Sept	JJAS	JA	Length	Apex to Apex	A1 Mean	A1 Std.
1	**0.122 (-)**	0.017	**0.240 (-)**	0.066	0.028	0.020	0.027	0.052	0.017	0.000	2022.2	417.4
2	0.014	0.070	0.041	**0.255 (-)**	**0.124 (+)**	0.048	**0.211 (+)**	**0.210 (+)**	0.086	0.000	1026.3	182.5
3	0.031	0.014	**0.140 (-)**	0.061	0.001	0.006	0.009	0.027	0.002	0.003	1685.2	519.9
4	0.021	0.011	0.004	0.004	0.000	0.014	0.001	0.002	0.031	0.076	470.3	257.0
5	**0.155 (-)**	0.042	**0.128 (-)**	0.047	0.002	0.005	0.008	0.024	0.004	0.002	1525.8	544.4
6	0.001	0.104	0.000	**0.232 (-)**	**0.211 (+)**	**0.158 (+)**	**0.232 (+)**	**0.239 (+)**	0.099	**0.116 (+)**	1005.2	225.7
7	0.095	0.000	**0.110 (-)**	**0.130 (-)**	0.074	0.008	0.075	**0.113 (+)**	0.029	0.000	1580.1	493.7
8	0.057	0.001	0.002	0.011	0.003	0.020	0.005	0.008	0.000	0.021	916.5	325.9
9	0.093	0.005	0.038	0.065	0.020	0.016	0.025	0.047	0.005	0.000	1670.9	496.3
10	**0.110 (+)**	0.025	0.026	0.003	0.029	0.066	0.020	0.011	0.011	0.031	850.1	349.9
11	0.000	0.007	0.064	**0.136 (-)**	0.024	0.000	0.054	0.085	0.000	0.000	1085.0	204.1
12	0.002	0.023	0.006	**0.191 (-)**	0.039	0.000	0.094	**0.123 (+)**	0.033	0.024	924.6	272.4

Table 2.6: R^2 values for the relationship between yearly ΣOND values (2001-2013) and 10 monsoon parameters at 12 cloud forest sites. Values in bold are $R^2 > 0.1$. (+) = positive correlation, (-) is negative. * = $p < 0.05$

Site	AUC	Total Prc.	June	July	Aug	Sept	JJAS	JA	Length	Apex to Apex	ΣOND Mean	ΣOND Std.
1	0.085	0.010	0.035	0.002	0.000	0.000	0.000	0.001	0.000	0.019	37469.6	1881.6
2	0.002	0.000	0.029	0.000	0.001	0.019	0.000	0.000	0.020	0.057	17913.2	1203.4
3	0.000	0.002	**0.205 (+)**	0.002	0.001	0.027	0.005	0.002	**0.284 (+)**	0.000	32345.9	2762.3
4	0.024	0.027	**0.217 (+)**	0.011	0.010	0.025	0.017	0.011	0.001	**0.252 (-)**	14876.2	1569.9
5	0.079	0.009	0.091	0.000	0.003	0.001	0.002	0.000	**0.142 (+)**	0.040	30286.7	1889.9
6	0.071	0.005	0.015	0.011	0.013	0.011	0.010	0.013	0.023	0.076	18067.0	899.3
7	0.034	0.017	0.045	0.001	0.024	**0.153 (-)**	0.019	0.006	0.012	0.011	30001.3	3192.9
8	0.001	0.023	0.017	0.007	0.013	0.088	0.019	0.010	0.013	0.009	17033.3	1565.1
9	0.014	0.059	0.031	0.021	0.094	**0.366 (-)***	0.079	0.047	0.008	0.007	32573.8	3461.2
10	0.018	0.038	0.072	0.011	0.051	**0.189 (-)**	0.048	0.025	0.067	0.000	17167.1	1773.8
11	0.021	0.095	**0.154 (+)**	0.040	0.046	0.000	0.056	0.045	0.003	0.096	19710.1	2265.4
12	0.016	0.054	**0.376 (+)***	0.011	0.022	0.001	0.032	0.015	**0.233 (+)**	0.001	20552.8	1552.2

2.5.3 Climate Regimes and Vegetation Dynamics

In the analysis of the relationship between monthly NDVI and broader climate factors, two indices showed moderate correlation to monthly NDVI time series: DMI and SST (Figures 2.8 and 2.9). Generally, only weak correlations ($R^2 < 0.1$) were found between monthly NDVI and SOI/Nino34 indices for the time period of 2001 to 2009.

The relationship between monthly NDVI values and the Indian Ocean Dipole is strongest when the two times series are concurrent (Figure 2.8B) and when the DMI is shifted one month earlier (Figure 2.8C). This relationship, though, is not widespread throughout the cloud forest. The highest correlations are concentrated in the northern and eastern portions of Jabal Qara and some parts of Jabal Qamar.

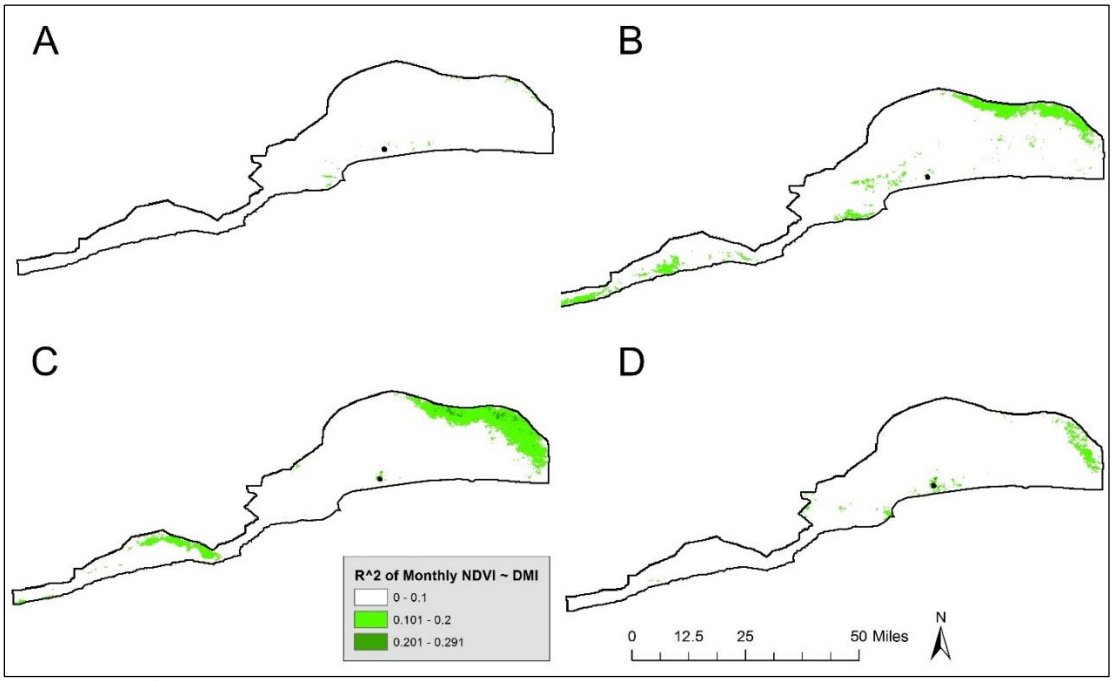

Figure 2.8: R^2 of the linear relationship between monthly NDVI and DMI for 2001 to 2009. The individual maps show the relationship at different monthly lags: A) lag 1, B) lag 0, C) lag -1, D) lag -2. Positive lags shift the index to a later time period, negative lags shift the DMI to an earlier time (e.g. lag of -2 shifts the DMI to two months earlier than the corresponding NDVI monthly value).

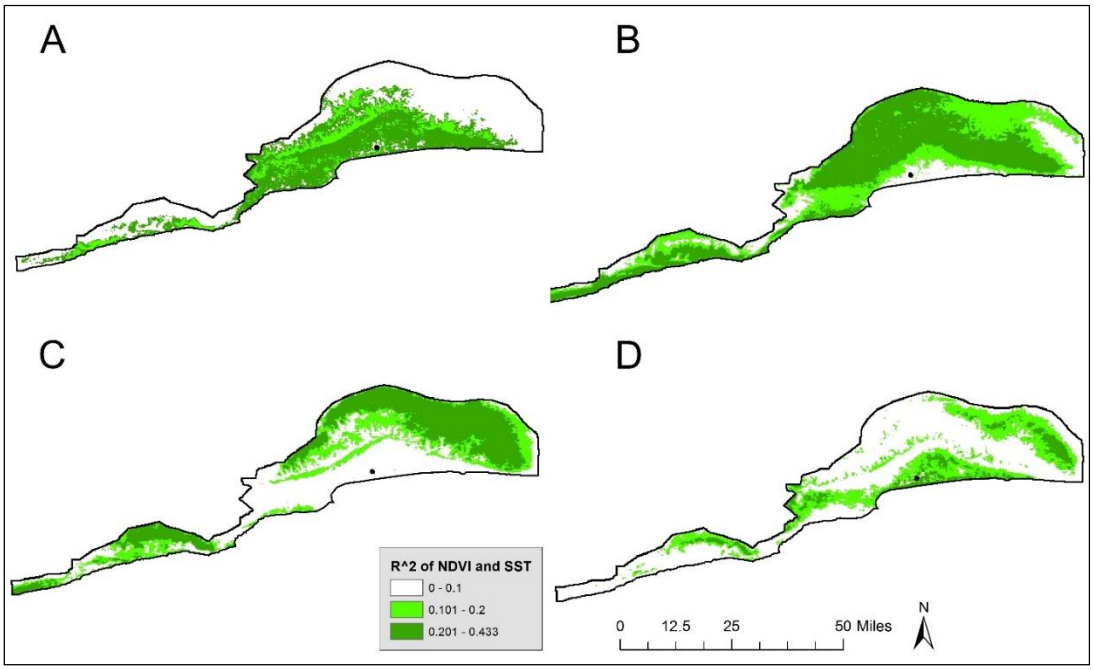

Figure 2.9: R^2 of the linear relationship between monthly NDVI and SST in Arabian Sea for 2001 to 2009. The individual maps show the relationship when SST are shifted to earlier time lags: A) lag -6, B) lag -7, C) lag -8, D) lag -9. (e.g. -6 shifts the SST to 6 months earlier than the corresponding NDVI values).

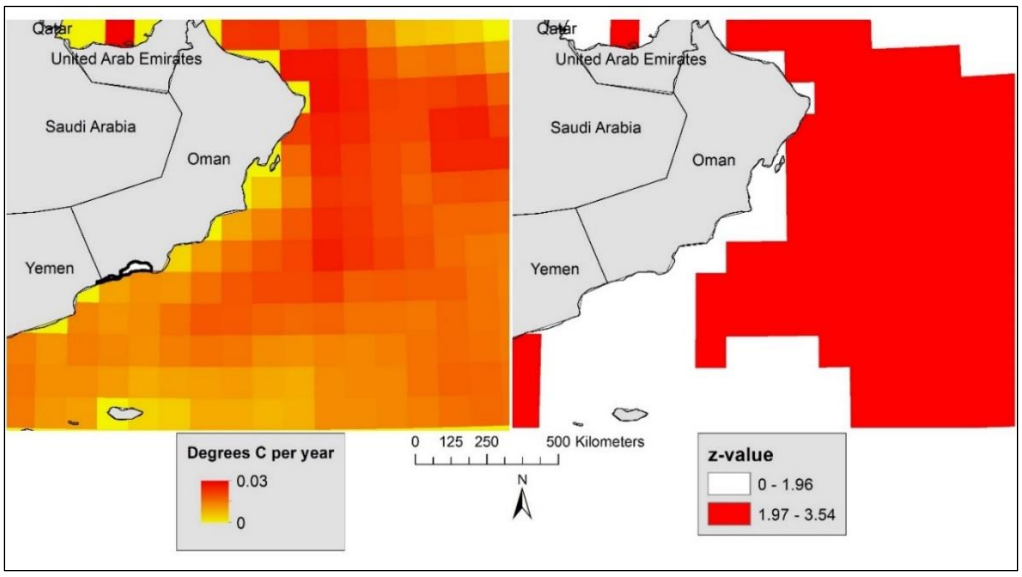

Figure 2.10: Trend analysis of the mean yearly sea surface temperatures in the Arabian Sea. The left image shows the slope of the trend (in degrees C) per year between 1982 and 2009. The right image shows the z-values for each grid.

It should come as no surprise that the strongest relationship is between monthly NDVI and SST in the Arabian Sea. The strongest correlation occurs when SST is shifted six to nine months earlier (Figure 2.9), suggesting that the processes that affect biomass growth and senescence are out of phase by about six to nine months with the development of SST in the Arabian Sea. Further analysis reveals that the average yearly surface temperature is significantly increasing in a large part of the Arabian Sea, but not significantly increasing along the coast of Oman (Figure 2.10). A trend analysis of average SST during the months of June, July, August, and September show no significant trends except in one or two pixels.

2.6 Discussion

2.6.1 Monsoon Timing

The monsoon season was defined using two different datasets: maximum daily temperatures from Reanalysis 2 data, and cloud cover data from MODIS daily imagery. These datasets gave two different pictures of the timing of the monsoon.

The seasonal parameters as described by the Reanalysis 2 temperature data (Tmax_daily) show that the onset of the monsoon season typically begins right after temperatures reach a peak (the first apex). After these temperatures reach their peak, a gradual decline begins until a local minimum (Tmin) is reached. Tmin is characterized by a significant drop in air temperature compared to the first apex, and most likely signals the height of the monsoon season (Figure 2.2). The monsoon begins to dissipate after Tmin is reached and daily temperatures start to incline until they reach the second apex.

Once temperatures have reached this second apex, it is likely that the influence of monsoon winds and colder SSTs off the coast of Arabia has completely subsided.

The onset and withdrawal of the monsoon is difficult to time precisely. Previous studies have attempted to reconstruct the onset over the Indian Subcontinent (e.g. Fieux and Stommel 1977; Joseph et al. 1994; Fasullo and Webster 2003; Joseph et al. 2006). These studies have used a wide variety of indices to recreate the onset of the monsoon, ranging from historical ship records (Fieux and Stommel 1977), to rain gauge data (Joseph et al. 1994), to hydrological indices (Fasullo and Webster 2003). The biggest discrepancy is that that neither of the two models developed in this study perfectly aligns with the timing of the monsoon in these other studies. The mean onset of the monsoon season, as modeled by the first apex in this paper, is very close to the dates of monsoon onset reported in the other studies (e.g. Fieux and Stommel 1977; Joseph et al. 1994; Fasullo and Webster 2003; Joseph et al. 2006).

Only one other study known to this author attempts to date the withdrawal of the monsoon (Fasullo and Webster 2003), Based on the Hydrologic Onset and Withdrawal index (HOWI) between 1948 and 2000, it concludes that the monsoon consistently ends in August or September, and 48 of the 53 years reported in their study show the withdrawal date between August 20th and September 27th. The model of monsoon timing based on Reanalysis 2 results reported here indicates an end to the monsoon season occurring much later in the year, but the model using the cloud cover data indicate monsoon withdrawal around the same time as reported by Fasullo and Webster (2003), between September 4th and September 26th for the period 2001 to 2013. The much later dates reported by the second apex are likely a temperature progression influenced by

post-monsoon conditions. After the monsoon season, winds become weaker and shift to an eastward source over the equator accompanied by warmer ocean water displacing upwelling (Schott and McCreary 2001).

Addressing the monsoon season by temperature data from Reanalysis 2 provides a set of conditions that are easily modeled using curve fitting; measuring the timing of the monsoon becomes a simple task of extracting maxima, minima, and, if a general measurement of intensity is desired, calculating the AUC for the season. For this reason, it is a useful tool for understanding monsoon progression. But the model developed from cloud cover data is more appropriate to measuring the actual onset and withdrawal of the monsoon as it is experienced in southern Arabia (Hildebrandt and Eltahir 2007). This model is assumed to be more accurate because it captures the conditions most associated with the monsoon in southern Arabia: cloud fog driving an increase in ground moisture (Hildebrandt 2005; Hildebrandt et al. 2006; Abdul-Wahab et al. 2007; Hildebrandt and Eltahir 2007; Scholte and De Geest 2010). Indeed, most people living in Dhofar would describe the start of the monsoon by consistent cloud cover and fog moisture, as well as a general decrease in temperatures.

The limitation to using cloud cover data from sources like MODIS is that the imagery can only capture a single snapshot at one point in time (during the morning). While persistence of cloud cover is a defining characteristic of the monsoon in Dhofar, there is a possibility that a morning snapshot could miss the formation of monsoon clouds; during the visual analysis it was noted that some breaks in cloud cover, where several images showed no cloud cover over the study area, occurred well into the monsoon season. Another limitation is that cloud cover data alone does not predict

precipitation. The amount of fog moisture is critical for tree growth (Hildebrandt et al. 2007a,b). MODIS provides a two-dimensional snapshot of the Earth's surface, but not vertical measurements of cloud height or moisture content. Despite these limitations, satellite imagery remains one of the best ways for determining the onset and withdrawal of the monsoon season in southern Arabia.

The trend analyses show little evidence for widespread changes to the monsoon timing. The model developed with Reanalysis 2 data had the longest time series and was the primary focus for this analysis. The second apex showed some indication that it was occurring later in the year, but only in a handful of the 30 grids. The trend of the timing of the first apex and Tmin also gave little indication of significant change.

2.6.2 Phenology

The mean 40% green-up (start of the peak growing season) for 2001 and 2013 occurred about 30 to 40 days after the onset of the monsoon in Arabia, while the mean 40% green-down (senescence onset) occurred about 85 days after the monsoon ended. Trees required about 2.5 more weeks than grasses to reach the 40% green-up mark, but were able to stave off senescence for 3 weeks longer than grass covers. The rooting depth is critical for water uptake in the cloud forest trees (Hildebrandt 2005), allowing them to delay leaf fall until water stress reaches a critical juncture (Reich and Borchert 1984). Horizontal precipitation is another factor in delaying tree senescence. Additional moisture over tree canopy occurs because of turbulent redistribution and edge effects (Hildebrandt 2005; Hildebrandt and Eltahir 2006; Hildebrandt and Eltahir 2007), and has

been shown to be critical in maintaining tree cover in Dhofar and promoting sapling growth. Shrub phenology tended to be in the middle of these two covers.

2.6.3 Vegetation Dynamics and Climate Variability

The relationship between the seasonal vegetation parameters (Phase 1, Amplitude 0, Amplitude 1, and ΣOND) and climate variables showed some weak to moderate correlation, but the lack of consistency suggests that the vegetation dynamics are mostly resistant to the inter-annual variability of the ten climate variables used in this study (Table 2.3, 2.4, 2.5, and 2.6). The timing of the peak NDVI (Phase 1) shows weak to moderate correlation with June precipitation at 8 of the 12 sites (Table 2.3). This correlation is likely related to the start of the monsoon. High amounts of precipitation in June can signal an early start to the growing season. But, the positive and negative correlation suggests that there is an inconsistency in the relationship between Phase 1 and June precipitation. Amplitude 0 showed the most consistent correlations with AUC (6 of 12 sites with $R^2 > 0.1$), and July and August precipitation. Amplitude 1 showed mainly weak, but some moderate correlation with June, July, August, and September precipitation. ΣOND showed little widespread correlation to any single variable.

These results suggest that precipitation and the AUC have some influence on seasonal vegetation parameters, but they are not dominant in the cloud forest's phenology. There are two likely reasons for this. First, the cloud cover is a critical climatic component in the success of the ecosystem's ability to maintain high vegetation density, despite the arid conditions of southern Arabia (Hildebrandt 2005; Hildebrandt et al. 2007). Cloud cover reduces the effects of incoming shortwave solar radiation and

tempers evapotranspiration. Second, the moisture in the cloud fog is distributed through horizontal precipitation (Hildebrandt 2005; Hildebrandt and Eltahir 2006; Hildebrandt and Eltahir 2007) and wind speed (Abdul-Wahab 2007). Precipitation as measured by climate stations may underestimate the amount of moisture transferred to the ground during the monsoon because fog moisture redistributes through turbulence and edge effects (Hildebrandt 2005; Hildebrandt and Eltahir 2007). Ideally, the relationship between the seasonal vegetation parameters and climate should also include spatially and temporally explicit fog moisture data. Despite the limitations in measuring precipitation, the phenology of the cloud forest is remarkably resilient to the variability of measurable precipitation, as well as the length of the monsoon and the AUC, apparently because of the dichotomous and orographic nature of cloud cover during the monsoon season.

The trend analyses bolster the argument that the cloud forest is resilient in the face of climate variability. The significant ΣOND, Amplitude 0, and Amplitude 1 trends are primarily associated with the coastal plain, and likely linked to human impacts (Galletti et al. forthcoming). The Phase 1 trends do show some changes in the seasonality of the NDVI peak, mainly at two prominent clusters at the east and west margins that are associated with a shift to earlier dates for Phase 1. A longer time series is required to determine if this trend is indicative of climate changes or human impacts. Since these two clusters sit on the margins, a climate explanation is possible if cloud cover, and thus moisture potential, is changing over these areas. Another possible factor could be the IOD. The relationship between NDVI time series and the DMI showed weak positive correlations at the margins of the cloud forest (Figure 2.8). While these weak DMI correlations are close in proximity, they did not overlap completely.

2.6.4 Vegetation Dynamics, Teleconnections, and Climate Regimes

Vegetation phenology has a week relationship with the DMI and a stronger relationship with SST in the Arabian Sea. Correlations to ENSO were weak ($R^2 < 0.1$), which is perhaps not surprising since recent observations have shown a weakening in the relationship between ENSO and ISM in the latter part of the 20th century (Kumar et al. 1999). The IOD is thought to directly influence monsoon conditions (Ashok et al. 2001; Ashok et al. 2004). In addition, research shows that the ENSO might have connections with the IOD (Allen et al. 2001), perhaps indicating that the ENSO indirectly affects monsoon conditions, an issue of ongoing debate (Ihara et al. 2008). The strongest correlation between the NDVI time series and DMI were at the margins of the cloud forest, which suggests that most of the forest may be shielded from IOD events. The 13 years of NDVI observations used in this study may not be long enough to assess any low frequency connections between the IOD and cloud forest vegetation. Previous research on a connection between the IOD and rainfall in southern Arabia found no significant relationship (Charabi 2009).

The connection between the SST in the Arabian Sea and vegetation dynamics in the cloud forest shows the strongest correlation between any two variables tested in this study. This correlation is positive and seems to be about six to nine months out of phase. Thus, the SST acts as a leading indicator of NDVI values in the cloud forest. The strength of this relationship is tied to the development of the monsoon. During the monsoon season, SST becomes cooler because of upwelling by the Somali Current. The Somali Current passes through the strait between the island of Socatra and the Horn of Africa in late spring or early summer (Schott and McCreary 2001). The cooler SST and a shift in

wind direction (southwest) cause clouds to form when air masses over the ocean meet the warmer air-flow over land.

The findings presented above suggest that the Dhofar cloud forest is resistant to various climate variability, with the likely exception of shifts in SST. If this is the case, then the biodiversity of the cloud forest may be protected from climate changes unless the monsoon destabilizes over southern Arabia. Two hypothetical ways the monsoon can destabilize are by 1) temperatures cooling over the Arabian land mass, and 2) the upwelling off the Arabian coast being undermined by warming ocean temperatures. Empirical observations and trend analyses of temperatures over the Arabian Peninsula show significant warming (AlSarmi and Washington 2011), which eliminates cooling land surface temperatures as a long-term threat. This leaves warming of SST off the coast of Arabia as the likeliest threat to cloud forest flora. In the analysis from this paper, there was no significant SST trend detected directly off the coast of southern Arabia; waters in the central and eastern portions of the Arabian Sea are significantly warming though (Figure 2.10). In the long term, changes to SST off the coast of Arabia require alterations to upwelling, which would require heating of deeper ocean layers and the Somali Current. Nieves and colleagues (2015) found that warming was occurring in the 100 to 300 meter layer of the Indian Ocean, but this seems to be isolated mainly to the eastern Indian Ocean. If heating occurs to the subsurface waters of the Somali basin - where the Somali Current forms - this could potentially change upwelling off the coast of Arabia and thus impact cloud formation over Dhofar. As of now, a trend analysis (reported earlier) on SST during the monsoon (June, July, August, and September) revealed no

significant warming trend for any of these months, but models should explore the likelihood of this happening under future climate change scenarios.

2.7 Conclusion

The model of the monsoon season over the southern Arabian Peninsula based on cloud cover data captures the onset and withdrawal more closely to that experienced by those living in in the Dhofar area. While further confirmation is required, the model appears to offer a promising way to determine empirically the timing of the monsoon. The Dhofar cloud forest reaches its peak growing period about a month after the monsoon's onset and continues until several months after the monsoon's withdrawal. Weak to moderate correlations between certain monsoon variables and vegetation seasonality parameters suggests that the cloud forest vegetation is resistant to fluctuations in precipitation, monsoon length, and temperature. The precipitation connection is masked by the source of water for the cloud forest, fog moisture, which is not measured accurately in rain gauges. The cloud cover, which reduces evapotranspiration, is linked closely to upwelling off the Arabian coast. Any warming to the Somali Current that drives upwelling could alter monsoon conditions and cause changes to the cloud forest.

2.8 Acknowledgements

Support for this research was provided in part by a Fulbright grant to Oman funded by the U.S. Department of State and sponsored by the Office of the Advisor to His Majesty The Sultan for Economic Planning Affairs. Special thanks to Sanda Heinz, Said Al-Saqri, Annette Patzelt, B. L. Turner II, Patricia Fall, and Soe Myint - all of whom

provided support and encouragement at various times during the research and writing of this paper.

2.9 References

Abdul-Wahab, S. A., H. Al-Hinai, K. A. Al-Najar, and M. S. Al-Kalbani (2007), Fog Water Harvesting: Quality of Fog Water Collected for Domestic and Agricultural Use, *Environ. Eng. Sci.*, *24*(4), 446–456, doi:10.1089/ees.2006.06-0066.

Allan, R., D. Chambers, W. Drosdowsky, H. Hendon, M. Latif, N. Nicholls, I. Smith, R. Stone, and Y. Tourre (2001), Is there an Indian Ocean dipole, and is it independent of the El Niño - Southern Oscillation?, *Clivar Exch.*, *6*(3), 18–22.

AlSarmi, S., and R. Washington (2011), Recent observed climate change over the Arabian Peninsula, *J. Geophys. Res.*, *116*(D11), D11109, doi:10.1029/2010JD015459.

Anderson, D. M., J. T. Overpeck, and A. K. Gupta (2002), Increase in the Asian southwest monsoon during the past four centuries., *Science*, *297*(5581), 596–9, doi:10.1126/science.1072881.

Ashok, K., Z. Guan, and T. Yamagata (2001), Impact of the Indian Ocean Dipole on the Relationship between the Indian Monsoon Rainfall and ENSO, *Geophys. Res. Lett.*, *28*(23), 4499–4502, doi:10.1029/2001GL013294.

Ashok, K., Z. Guan, N. H. Sagi, and T. Yagamata (2004), Individual and Combined influences of ENSO and the\rIndian Ocean Dipole on the Indian Summer Monsoon, *J. Clim.*, *17*(16), 3141–3155, doi:10.1175/1520-0442(2004)017<3141:IACIOE>2.0.CO;2.

Blechschmidt, I., A. Matter, F. Preusser, and D. Rieke-Zapp (2009), Monsoon triggered formation of Quaternary alluvial megafans in the interior of Oman, *Geomorphology*, *110*(3-4), 128–139, doi:10.1016/j.geomorph.2009.04.002.

Charabi, Y. (2009), Arabian summer monsoon variability: Teleconexion to ENSO and IOD, *Atmos. Res.*, *91*(1), 105–117, doi:10.1016/j.atmosres.2008.07.006.

Charabi, Y., and S. A. Abdul-Wahab (2009), Synoptic aspects of the summer monsoon of southern Oman and its global teleconnections, *J. Geophys. Res. Atmos.*, *114*(7), 1–9, doi:10.1029/2008JD010234.

Cremaschi, M., and F. Negrino (2005), Evidence for an abrupt climatic change at 8700 14C yr B.P. in rockshelters and caves of Gebel Qara (Dhofar-Oman): Palaeoenvironmental implications, *Geoarchaeology*, *20*(6), 559–579, doi:10.1002/gea.20068.

Eastman, J. R., F. Sangermano, B. Ghimire, H. Zhu, H. Chen, N. Neeti, Y. Cai, E. a. Machado, and S. C. Crema (2009), Seasonal trend analysis of image time series, *Int. J. Remote Sens.*, *30*(10), 2721–2726, doi:10.1080/01431160902755338.

Eastman, J. R., F. Sangermano, E. a. Machado, J. Rogan, and A. Anyamba (2013), Global trends in seasonality of Normalized Difference Vegetation Index (NDVI), 1982-2011, *Remote Sens.*, *5*(10), 4799–4818, doi:10.3390/rs5104799.

Fasullo, J., and P. J. Webster (2003), A hydrological definition of Indian Monsoon onset and withdrawal, *J. Clim.*, *16*(19), 3200–3211, doi:10.1175/1520-0442(2003)016<3200a:AHDOIM>2.0.CO;2.

Fieux, M., and H. Stommel (1977), Onset of the Southwest Monsoon over the Arabian Sea from Marine Reports of Surface Winds: Structure and Variability, *Mon. Weather Rev.*, *105*(2), 231–236.

Flagg, C. N., and H. S. Kim (1998), Upper ocean currents in the northern Arabian Sea from shipboard ADCP measurements collected during the 1994-1996 U.S. JGOFS and ONR programs, *Deep. Res. Part II Top. Stud. Oceanogr.*, *45*(10-11), 1917–1959, doi:10.1016/S0967-0645(98)00059-9.

Fleitmann, D., and A. Matter (2009), The speleothem record of climate variability in Southern Arabia, *Comptes Rendus Geosci.*, *341*(8-9), 633–642, doi:10.1016/j.crte.2009.01.006.

Fleitmann, D., S. J. Burns, M. Mudelsee, U. Neff, J. Kramers, A. Mangini, and A. Matter (2003), Holocene forcing of the Indian monsoon recorded in a stalagmite from southern Oman, *Science (80-.).*, *300*(5626), 1737–1739, doi:10.1126/science.1083130.

Fleitmann, D., S. J. Burns, U. Neff, M. Mudelsee, A. Mangini, and A. Matter (2004), Palaeoclimatic interpretation of high-resolution oxygen isotope profiles derived from annually laminated speleothems from Southern Oman, *Quat. Sci. Rev.*, *23*(7-8), 935–945, doi:10.1016/j.quascirev.2003.06.019.

Fleitmann, D., S. J. Burns, M. Pekala, A. Mangini, A. Al-Subbary, M. Al-Aowah, J. Kramers, and A. Matter (2011), Holocene and Pleistocene pluvial periods in Yemen, southern Arabia, *Quat. Sci. Rev.*, *30*(7-8), 783–787, doi:10.1016/j.quascirev.2011.01.004.

Ghazanfar, S. (1998), Status of the flora and plant conservation in the sultanate of Oman, *Biol. Conserv.*, *85*(5), 1167–1179.

Ghazanfar, S. A., and M. Fisher (eds) (1998), *Vegetation of the Arabian Peninsula*, edited by S. A. Ghazanfar and M. Fisher, Kluwer Academic Publishers, Dordrecht.

Gupta, A. K., D. M. Anderson, and J. T. Overpeck (2003), Abrupt changes in the Asian southwest monsoon during the Holocene and their links to the North Atlantic Ocean, *Nature*, *421*(6921), 354–7, doi:10.1038/nature01340.

Hildebrandt, A. (2005), Ecohydrology of a Seasonal Cloud Forest in Dhofar, PhD. Dissertation, Massachusetts Institute of Technology.

Hildebrandt, A., and E. A. B. Eltahir (2006), Forest on the edge: Seasonal cloud forest in Oman creates its own ecological niche, *Geophys. Res. Lett.*, *33*(11), 2–5, doi:10.1029/2006GL026022.

Hildebrandt, A., and E. a. B. Eltahir (2007), Ecohydrology of a seasonal cloud forest in Dhofar: 2. Role of clouds, soil type, and rooting depth in tree-grass competition, *Water Resour. Res.*, *43*(11), n/a–n/a, doi:10.1029/2006WR005262.

Hildebrandt, A., M. Al Aufi, M. Amerjeed, M. Shammas, and E. A. B. Eltahir (2007), Ecohydrology of a seasonal cloud forest in Dhofar: 1. Field experiment, *Water Resour. Res.*, *43*(10), 1–13, doi:10.1029/2006WR005261.

Ihara, C., Y. Kushnir, and M. a. Cane (2008), Warming trend of the Indian Ocean SST and Indian Ocean dipole from 1880 to 2004, *J. Clim.*, *21*(10), 2035–2046, doi:10.1175/2007JCLI1945.1.

IPCC (2014), *Synthesis Report. Contribution of Working Groups I, II and III to the Fifth Assessment Report of the Intergovernmental Panel on Climate Change*, edited by C. W. Team, R. K. Pachauri, and L. A. Meyer, IPCC, Geneva, Switzerland.

Janzen, J. (1986), *Nomads in the sultanate of Oman: tradition and development in Dhofar*, Westview Press, Boulder.

Janzen, J. (2000), The destruction of resources among the mountain nomads of Dhofar, in *The Transformation of Nomadic Society in the Arab East*, edited by M. Mundy and B. Musallam, pp. 160–175, Cambridge University Press, Cambridge, UK.

Joseph, P. V., J. K. Eischeid, and R. J. Pyle (1994), Interannual Variability of the Onset of the Indian Summer Monsoon and Its Association with Atmospheric Features, El Niño, and Sea Surface Temperature Anomalies, *J. Clim.*, *7*(1), 81–105, doi:10.1175/1520-0442(1994)007<0081:IVOTOO>2.0.CO;2.

Joseph, P. V., K. P. Sooraj, and C. K. Rajan (2006), The Summer Monsoon Onset Process Over South Asia and an Objective Method for the Date of Monsoon Onset over Kerala, *Int. J. Climatol.*, *26*, 1871–1893, doi:10.1002/joc.1340.

Justice, C. O. et al. (1998), The Moderate Resolution Imaging Spectroradiometer (MODIS): land remote sensing for global change research, *IEEE Trans. Geosci. Remote Sens.*, *36*(4), 1228–1249, doi:10.1109/36.701075.

Kanamitsu, M., W. Ebisuzaki, J. Woollen, S.-K. Yang, J. J. Hnilo, M. Fiorino, and G. L. Potter (2002), NCEP–DOE AMIP-II Reanalysis (R-2), *Bull. Am. Meteorol. Soc.*, *83*(11), 1631–1643, doi:10.1175/BAMS-83-11-1631.

Krishnan, R., T. P. Sabin, D. C. Ayantika, a. Kitoh, M. Sugi, H. Murakami, a. G. Turner, J. M. Slingo, and K. Rajendran (2013), Will the South Asian monsoon overturning circulation stabilize any further?, *Clim. Dyn.*, *40*(1-2), 187–211, doi:10.1007/s00382-012-1317-0.

Krishnaswamy, J., S. Vaidyanathan, B. Rajagopalan, M. Bonell, M. Sankaran, R. S. Bhalla, and S. Badiger (2014), Non-stationary and non-linear influence of ENSO and Indian Ocean Dipole on the variability of Indian monsoon rainfall and extreme rain events, *Clim. Dyn.*, doi:10.1007/s00382-014-2288-0.

Kumar, K. K., B. Rajagopalan, and M. A. Cane (1999), On the Weakening Relationship Between the Indian Monsoon and ENSO, *Science*, *284*(5423), 2156–2159, doi:10.1126/science.284.5423.2156.

Kumar, K. K., B. Rajagopalan, M. Hoerling, G. Bates, and M. Cane (2006), Unraveling the mystery of Indian monsoon failure during El Niño, *Science*, *314*(5796), 115–119.

Kürschner, H., P. Hein, N. Kilian, and M. A. Hubaishan (2004), The Hybantho durae-Anogeissetum dhofaricae ass. nova - phytosociology, structure and ecology of an endemic South Arabian forest community, *Phytocoenologia*, *34*, 569–612.

Kwarteng, A. Y., S. Dorvlo, and G. T. V. Kumar (2009), Analysis of a 27-year rainfall data (1977 – 2003) in the Sultanate of Oman, *Int. J. Climatol.*, *617*(July 2008), 605–617, doi:10.1002/joc.

Miller, A. G., and M. Morris (1988), *Plants of Dhofar, the southern region of Oman, traditional, economic and medicinal uses*, Office of the Adviser for Conservation of the Environment, Diwan of Royal Court, Sultanate of Oman.

Nieves, V., J. K. Willis, and W. C. Patzert (2015), Recent hiatus caused by decadal shift in Indo-Pacific heating, *Science*, *349*(6247), 532–535.

Overpeck, J. T., D. Anderson, S. Trumbore, and W. Prell (1996), The southwest Indian Monsoon over the last 18,000 years, *Clim. Dyn.*, *12*, 213–225.

Parker, A. G., and J. I. Rose (2008), Climate change and human origins in southern Arabia, *Proc. Semin. Arab. Stud.*, *38*, 25–42.

Patzelt, A. (2011), The Themeda Quadrivalvis Tall-Grass Savannah of Oman At the Crossroad Between Africa and Asia, *Edinburgh J. Bot.*, *68*(02), 301–319, doi:10.1017/S0960428611000217.

Pickering, H. A., and A. Patzelt (2008), *Field Guide to the Wild Plants of Oman*, Kew Publishing, Richmond, UK.

Rayner, N. A., D. E. Parker, E. B. Horton, C. K. Folland, L. V. Alexander, D. P. Rowell, E. C. Kent, and A. Kaplan (2003), Global analyses of sea surface temperature, sea ice, and night marine air temperature since the late Nineteenth Century, *J. Geophys. Res.*, *108*, doi:10.1029/2002JD002670.

Reich, P. B., and R. Borchert (1984), Water Stress and Tree Phenology in a Tropical Dry Forest in the Lowlands of Costa Rica, *J. Ecol.*, *72*(1), 61–74.

Reynolds, R. W., N. a. Rayner, T. M. Smith, D. C. Stokes, and W. Wang (2002), An improved in situ and satellite SST analysis for climate, *J. Clim.*, *15*(13), 1609–1625, doi:10.1175/1520-0442(2002)015<1609:AIISAS>2.0.CO;2.

Saji, N. H., B. N. Goswami, P. N. Vinayachandran, and T. Yamagata (1999), A dipole mode in the tropical Indian Ocean, *Nature*, *401*, 360–363.

Scholte, P., and P. De Geest (2010), The climate of Socotra Island (Yemen): A first-time assessment of the timing of the monsoon wind reversal and its influence on precipitation and vegetation patterns, *J. Arid Environ.*, *74*(11), 1507–1515, doi:10.1016/j.jaridenv.2010.05.017.

Schott, F. A., and J. P. McCreary (2001), The monsoon circulation of the Indian Ocean, *Prog. Oceanogr.*, *51*(1), 1–123, doi:10.1016/S0079-6611(01)00083-0.

Sen, P. K. (1968), Estimates of the regression coefficient based on Kendall's tau, *J. Am. Stat. Assoc.*, *63*, 1379–1389.

Shi, W., J. M. Morrison, E. Böhm, and V. Manghnani (2000), The Oman upwelling zone during 1993, 1994 and 1995, *Deep. Res. Part II Top. Stud. Oceanogr.*, *47*(7-8), 1227–1247, doi:10.1016/S0967-0645(99)00142-3.

Theil, H. (1950), A rank-invariant method of linear and polynomial regression analysis, I, II, III, *Proc. K. Ned. Acad. van Wet.*, *53*(386), 386–392, 512–525, 1397–1412.

Trenberth, K. E. (1984), Signal Versus Noise in the Southern Oscillation, *Mon. Weather Rev.*, *112*(2), 326–332, doi:10.1175/1520-0493(1984)112<0326:SVNITS>2.0.CO;2.

CHAPTER 3

DRIVERS OF PLANT DIVERSITY IN THE SOUTH ARABIAN CLOUD FOREST[1]

"No amount of book learning will make a man a scientific man: nothing but patient observation, and quiet and fair thought over what he has observed. He must go out for himself, see for himself, compare and judge for himself, in the field, the quarry, the cutting. He must study rocks, ores, fossils, in the nearest museum; and thus store in his head, not with words, but with facts. He must verify – as far as he can – what he reads in books, by his own observation; and be slow to believe anything, even on the highest scientific authority, till he has either seen it, or something like enough to it to make it seem to him probable, or at least possible." (Charles Kingsley, 1873, x)

3.1 Abstract

The South Arabian Cloud Forest is a drought deciduous semi-arid forest on the southern coast of the Arabian Peninsula. We describe the vegetation diversity of the South Arabian Cloud Forest and test three hypotheses to explain biodiversity patterns of woody plant species: (H1) neutral processes, (H2) biological interactions, and (H3) environmental gradients. We collected plant density, cover, and frequency at 102 sample points and estimated relative species abundances across two biomes: grasslands and forests. Cluster analysis, Mantel correlograms, and canonical correspondence analysis (CCA) are used to test our hypotheses.

The cluster analysis identified five vegetation groups. The two largest groups are dominated by a small number of species. *Anogeissus dhofarica* and *Commiphora* spp. account for 49% of the relative species abundance in forest plots, while *Calotropis procera, Commiphora* spp., and *Solanum incanum* account for 42% of the relative abundance in grassland plots. Based on our analyses, the (H2) biological interaction

[1] Co-authored with Patricia L. Fall

hypothesis offers the best explanation for biodiversity patterns in the cloud forest. However, the reason for this differs between the forest and grasslands. In forests, the diversity patterns are dominated by a few species of trees and shrubs (*A. dhofarica* and *Commiphora* spp.), most likely as a result of the region's biogeographical history. In grassland areas, however, diversity patterns are best explained as products of human activity. Conservation efforts should focus on rarer species, which drive diversity gradients across the region and are at risk of endangerment.

3.2 Introduction

The South Arabian Cloud Forest extends from the arid, southern reaches of Yemen east to the Dhofar Mountains of southern Oman. Plant surveys and biogeographical studies reveal a rich flora (Radcliffe Smith 1980; Miller and Morris 1988; Pickering and Patzelt 2008; Patzelt 2011) thought to be a remnant of a xerotropical forest with paleo-African origins that stretched from Africa to Asia during the Tertiary (Kürschner et al. 2004). Expanding populations and encroaching human influences threaten the biodiversity of the cloud forest, making it critical to understand the ecological structure of this unique ecosystem (Schlect et al. 2014).

Table 3.1: Three hypotheses and three tests of the drivers of plant diversity in the South Arabian Cloud Forest. Under each test, the expected outcome and variables used in the test are listed.

Hypothesis	Test		
	Cluster Analysis	Canonical Correspondence Analysis	Mantel Correlogram
H1: Neutral processes	No clear pattern of dominance in species abundances by a few species *Variable: number of dominant species per cluster group*	CCA explains less than 30% of the variance in the species abundances *Variable: species abundance as measured by importance value (IV). Environmental variables include climatic and physiographic*	Significant spatial autocorrelation shown with distance decay in the correlation *Variable: beta diversity measured using Brey-Curtis and based on species abundances using importance value (IV)*
H2: Biological interactions	Few species with high abundances *Variable: number of dominant species per cluster group*	CCA explains less than 30% of the variance in the species abundances *Variable: species abundance as measured by importance value (IV). Environmental variables include climatic and physiographic*	No spatial autocorrelation, or varying positive and negative spatial correlation *Variable: beta diversity measured using Brey-Curtis and based on species abundances using importance value (IV))*
H3: Environmental gradients	No clear pattern of dominance in species abundances by a few species *Variable: number of dominant species per cluster group*	CCA explains more than 30% of the variance in the species abundances *Variable: species abundance as measured by importance value (IV). Environmental variables include climatic and physiographic*	Significant spatial autocorrelation shown with distance decay in the correlation *Variable: beta diversity measured using Brey-Curtis and based on species abundances using importance value (IV)*

The cloud forest is a drought deciduous forest (Hildebrandt and Eltahir 2006; Hildebrandt and Eltahir 2007; Hildebrandt et al. 2007), supported by ample summer rain and cloud cover that compensate for limited precipitation through the rest of the year. While most of the Arabian Peninsula has low vegetation density indicative of arid regions, grasslands and forests flourish along the south facing slopes of the southern mountains of Yemen and Oman, giving the cloud forest a semi-arid, and sometimes

tropical, demeanor. During the summer months, temperature differentials between the Arabian Peninsula and the Arabian Sea cause clouds to form along the south-facing slopes of the mountains. The temperature differential between the land and sea cause the formation of the Indian Ocean Monsoon (also known locally as *khareef*), which provides the precipitation and cloud cover that allow flora to thrive in an otherwise arid region. Much of the vegetation senesces by December, where weather patterns return to the more dryland conditions that dominate most of Arabia. Beyond the coastal mountains, the characteristic desert ecosystem of the Arabian Peninsula prevails, and some floral species that thrive deep in the desert can be found in parts of the cloud forest.

Despite the uniqueness of the cloud forest, few studies assess its floral distribution, and understanding of its biodiversity remains limited. Understanding the drivers of biodiversity of the cloud forest will be crucial for its conservation. Neutral processes, defined by the limited dispersal capabilities of many species, help explain patterns of biodiversity in a wide range of biogeographical studies (e.g., Rosindell et al. 2011). Alternatively, biodiversity patterns may be dominated by the wide distribution of a few key taxa (e.g., Condit et al. 2002), particularly certain endemic species (*Anogeissus dhofarica* and *Maytenus dhofarensis*), as well as plant species common across South Arabia (*Calotropis procera*, *Commiphora* spp. and *Ficus* spp.). Finally, environmental filtering could lead to certain species populating specific niche environments (Shmida and Wilson 1985; Dauby et al. 2014). The cloud forest ecosystem features two distinct vegetation types (forests and grasslands) and a high level of topographic variability over short distances that separate forested regions from grasslands. We test three hypotheses to explain the biodiversity of the South Arabian Cloud Forest (Table 3.1).

Neutral Processes (H1). The neutral processes hypothesis explains biodiversity as the outcome of random processes and the limited dispersal capabilities of species (Hubbell 2006; Chisolm and Pacala 2010; Rosindell et al. 2011). According to this hypothesis, plant species are competitively equivalent, and through time biotic and stochastic processes can lead to certain taxa becoming more prevalent than others, resulting in spatially autocorrelated beta diversity patterns. Neutral processes would result in plant survey sites being more similar when they are closer spatially and progressively become less similar with distance; but no clear environmental gradient would explain diversity patterns.

Biological Interactions (H2). Studies of tropical forests, particularly in the Amazon, reveal that tree species diversity patterns are characterized by a small number of dominant species and low beta diversity (Pitman et al. 1999, 2001; Legendre et al. 2005; Tuomisto and Ruokolainen 2006). Biological interactions hypotheses (as part of dispersal theory) are thus used to explain patterns of community structure based on relatively homogeneous taxonomic composition and the wide distribution of a few dominant species. The spatial structure of beta diversity has no clear spatial autocorrelation, nor does it suggest that environmental factors explain patterns of diversity.

Environmental Gradients (H3). Niche environments that favor certain species can explain variation in species diversity. Diversity patterns that are influenced by environmental factors lead to various species flourishing in niches and, thus, diversity patterns between similar environmental contexts would match more closely than those that are in different environmental contexts. An analysis of the spatial patterning would reveal similarity amongst closely situated sites, and a strong correlation between

environmental factors and diversity patterns would exist. This hypothesis would predict spatial autocorrelation in beta diversity, and environmental variables would largely account for the variance in species abundances.

Conservation approaches related to (H1) neutral processes and (H2) biological interactions could be more regional in scope (e.g. Mac Nally 2007), where landscape-wide decisions about conservation would need to be made. Alternatively, conservation related to (H3) environmental gradients may entail a sampling of niches or targeting of certain environmental conditions (Rickbeil et al. 2014).

3.3 Study Area

The South Arabian Cloud Forest is wedged between the Arabian Sea and the desert gravel plains of the Nejd Plateau. Mountains run along the southern reaches of the Dhofar region in Oman to Al Mahra in Yemen. Research has shown that Arabia was more pluvial in the deep past, particularly during the last interglacial and the early Holocene (e.g., Fleitmann and Matter 2009). Today, the climate is dry most of the year except during the summer months when monsoon clouds blanket the region in mist (Kwarteng et al. 2007; AlSarmi and Washington 2011). During the monsoon, temperatures cool and precipitation increases dramatically, which allows vegetation in the cloud forest to flourish, and supports broadleaf trees, which are rare on the Arabian Peninsula.

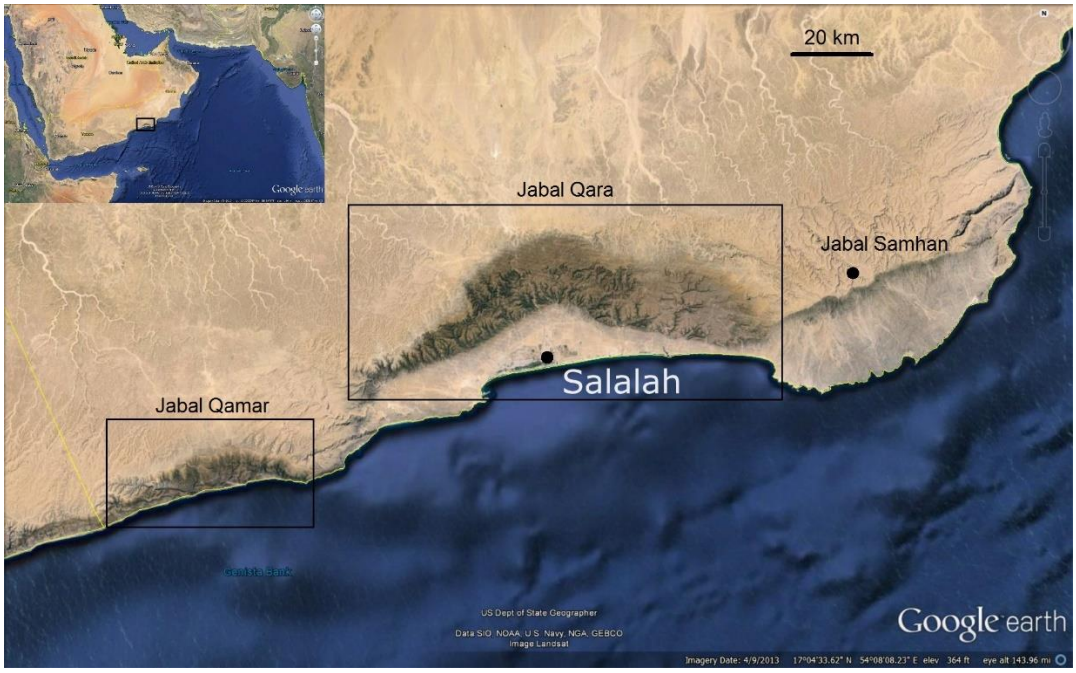

Figure 3.1: The study region in Dhofar, Oman, viewed through Google Earth. Shown are the two largest areas of the South Arabian Cloud Forest. The large box surrounds Jabal Qara and the smaller box to the southwest is Jabal Qamar. Jabal Samhan is just to the east of Jabal Qara. Salalah, the largest city in the region, is situated just to the south of Jabal Qara.

Stretches of desert and coastal plain separate the cloud forest into fragments. Our study looked at two of these fragments: Jabal Qamar to the west and Jabal Qara to the east (Figure 3.1). Jabal Qara, the larger fragment of the cloud forest, forms a crescent shape around the port city of Salalah on Oman's southernmost coastal plain. This coastal plain runs from the eastern portion of Jabal Qamar, across the southern span of Jabal Qara, to the southern portions of the region's largest mountain, Jabal Samhan. Jabal Qamar runs directly along the coast of the Arabian Sea.

The density of vegetation ranges from that seen in tropical-like conditions to those seen in arid zones. The cloud forest ecosystem is partitioned into two primary biomes: forests and grasslands; but a secondary biome, shrublands, also exists, usually in

association with the parts of the cloud forest that are more arid. Foothills leading up to the mountains of Dhofar are vegetated with a mixture of forests, shrublands and grasslands, usually with decreasing plant density as one approaches the sea. The vegetation in the cloud forest is associated with the Saharo-Sindian and Saharo-Arabian phytogeographic zones (Ghazanfar and Fisher 1998; Parker and Rose 2008), and it is thought that the forests are a remnant of a much bigger ancient forest that once stretched from Africa to India and possibly beyond (Kürschner et al. 2004).

3.4 Materials and Methods

3.4.1 Fieldwork and Floral Survey

Data on tree and shrub distributions were collected during fieldwork conducted between January and April 2013. Random points were generated using ArcGIS across the cloud forest, and each of these points was used to identify a survey sample point (89 random points). The study area was isolated for selection of these random points using a mask of high NDVI pixels (>.1 in an October 2000 Landsat 7 image) plus a 1000 m buffer. Thirteen additional non-random points were selected to provide coverage of areas or terrains that were underrepresented in the distribution of the random points, making a total of 102 sample points. Data on trees and shrubs were measured using the point-centered quarter method (PCQM; Mitchell 2007). Absolute plant density (no./m^2), cover (basal area/hectare), and frequency (%/sample point) were measured for all woody species along a westerly transect from each sample point.

For each sample point we determined the mean distance *r*, which is the sum of the distances to the measured trees divided by the number of quarters (*j*) at a subsample point

(*i*). Subsample points are points at each of our sample points where observations were made. For each sample point, we used about five subsample points, and each subsample point is divided into four quarters. R_{ij} is the total distance between the species and our random sample points in meters, n_i is the number of subsample sample points (following Mitchell 2007):

$$\bar{r} = \frac{\sum_{i=1}^{n} \sum_{j=1}^{n} R_{ij}}{4n_i}$$

Absolute density may be estimated as:

$$d = \frac{1}{\bar{r}^2}$$

Absolute cover is first calculated by estimating the planar area of each species' trunk.

$$A = \frac{c^2}{4\pi}$$

in which c is the circumference of the species trunk, and *A* (the planar area) is divided by the number of species (n_s) per sample point to arrive at the mean basal area (*MBA*):

$$MBA = \frac{A}{n_s}$$

The absolute coverage of a species (measured as total basal area per hectare) at a sample point is calculated as:

$$c = MBA * d * \frac{1\ m^2}{10{,}000\ cm^2}$$

Finally, absolute species frequency is calculated as:

$$f = \frac{number\ of\ subsample\ points\ where\ a\ species\ is\ observed}{total\ number\ of\ subsample\ points} * 100$$

f is measured as a percentage.

Relative density, cover, and frequency were calculated by dividing each of these three metrics by the sum total of each metric for all species per sample point. We also calculated importance values (IV) (relative cover + relative density + relative frequency = IV) (*sensu* Mitchell 2007), which estimate the relative abundance of each species per sample point. Our cluster analysis, Mantel correlograms, and canonical correspondence analysis (CCA) use importance values as measures of species abundances.

3.4.2 Environmental and Climate Data

Temperature and precipitation data were obtained from the Bioclim dataset (Hijmans et al. 2005). Rasters were used to represent precipitation and temperature variables (see Appendix A, Table A.1). Physiographic variables (elevation, slope, aspect, and hydrology) were derived from the SRTM 90m digital elevation model. The hydrology raster shows the distance of any pixel to the nearest "stream" pixel, which estimates proximity to locations where precipitation aggregates, such as wadis. Aspect is split into two different raster variables: northness (cosine of aspect) and eastness (sine of the aspect). In total, the analyses used 18 variables (see Appendix A).

3.4.3 Cluster Analysis

Cluster analysis was used to group the 102 sample points according to species similarity and dissimilarity based on relative species importance values. A Bray-Curtis index was used to measure ecological differences between sample points. The resulting dendrograms are generated using Ward linkage. A classification tree indicates how clusters are separated according to environmental variables. Misclassification rates and a

confusion matrix were used to assess the classification tree. Once the clusters were identified, we summed the importance values for each species across the cluster groups. Silhouette widths were used to evaluate how well the cluster groups were partitioned based on the composition of species in each group (Rousseeuw 1987), and are interpreted similarly to a correlation coefficient (see Appendix B).

3.4.4 Mantel Correlogram

Mantel correlograms were used to measure the spatial autocorrelation of beta diversity of species between sample points (Borcard and Legendre 2012). Beta diversity was measured using distance matrices. Importance values (IV) measure species abundance at each site. Dissimilarity between sites was measured using the Bray-Curtis index. Before the correlogram was computed, the dissimilarity matrix was spatially detrended. The significance of groups in the correlograms was computed based on 999 permutations of the data. We used progressive correction and p-value adjustments for multiple testing, as suggested by Legendre and Legendre (2012) and Borcard et al. (2011).

3.4.5 Canonical Correspondence Analysis

We used canonical correspondence analysis (CCA; ter Braak 1986) to analyze relationships between species abundances (as measured using IV) and environmental gradients, based on 20 environmental variables (see discussion above) and a stepwise variable selection function. An F test was used to determine a parsimonious number of explanatory variables. Once this subset of variables was isolated using the method

above, a variance inflation test was run using the variance inflation factor (VIF) as a metric. Any variable with a VIF score greater than 5 was removed before the model was retested. In some cases – based on trial and error – a variable with a low VIF was removed to lower the overall probability of variance inflation if variables with high VIF could not reduce variance inflation when they were removed. Three CCA model classes were created for forest, grassland, and combined forest and grassland (i.e., the whole study area). A separate CCA model was run on latitude and longitude to measure the amount of variance in species abundances explained by geographical location and distance between sites.

Table 3.2: Relative abundance of the eight most common species across the cloud forest. All other species are found at less than 5% of the total relative abundance. The sum total abundance of the eight species are shown in the third to last column.

	A. dhofarica	B. hirtum	C. procera	Commiphora spp.	F. vasta	J. dhofarica	M. dhofarensis	S. incanum	Z. spina-christi	Sum Total Relative Abund-ance	Total Number of Species Observed	Median Species Abund-ance
All 102 sample points											52	0.50%
> 5% abundance	16.02		7.31	19.23	5.03	5.27	6.31	7.90	5.33	72.40%		
>10% abundance	16.02			19.23						35.25%		
Forest (n=36)											36	0.90%
> 5% abundance	27.15	5.42		22.16		6.40	5.17			66.29%		
>10% abundance	27.15			22.16						49.31%		
Grassland (n=59)											40	0.60%
> 5% abundance	9.32		12.53	17.18	7.14		7.73	12.19	7.94	74.04%		
>10% abundance			12.53	17.18				12.19		41.90%		

3.5 Results

Our survey results record 52 woody plant species at 102 sample points. Eight species are found in relative abundances above 5% across the entire the study area (Table 3.2). These eight species comprise 72.4% of the overall plant abundance across the study area. Two species, *Anogeissus dhofarica* and *Commiphora* spp., are found in abundances greater than 10% and comprise 35.2% of the plant species counts in the study area. At forest sample points, five species have relative frequencies higher than 5% and account for 66.3% of the total relative abundance. Among grassland samples, seven species are found in relative abundances greater than 5% and account for 74.0% of grassland plant species abundances. Cluster analysis identified five vegetation groups in the cloud forest (Figure 3.2). The first cluster includes *Solanum incanum, Calotropis procera, Maytenus dhofarensis*, and *Ziziphus spina-christi* (Figure 3.3). The second cluster, generally comprised of forest samples (Appendix B, Table B.1), is dominated by *A. dhofarica* and *Commiphora* spp. The third cluster, characterized by a variety of forest and shrubland species, includes *A. dhofarica, B. hirtum, Commiphora* spp., *Acacia senegal*, and *Croton confertus*. The fourth cluster includes a dominant taxon, *Commiphora* sp., in conjunction with the less frequent species *F. vasta, S. incanum, A. senegal, E. balsamifera*, and *M. dhofarensis*. The dominant species in the fifth cluster are *A. nilotica, A. senegal, Boscia arabica, Boswellia sacra, Commiphora* spp., and *J. dhofarica*. Cluster 5 represents a mix of environments, including shrublands and grasslands, as well as the foothills along the southern reaches of the Dhofar Mountains. The third, fourth and fifth clusters have low silhouette widths (see Appendix B), are more likely to include outliers, and are more variable in their species compositions.

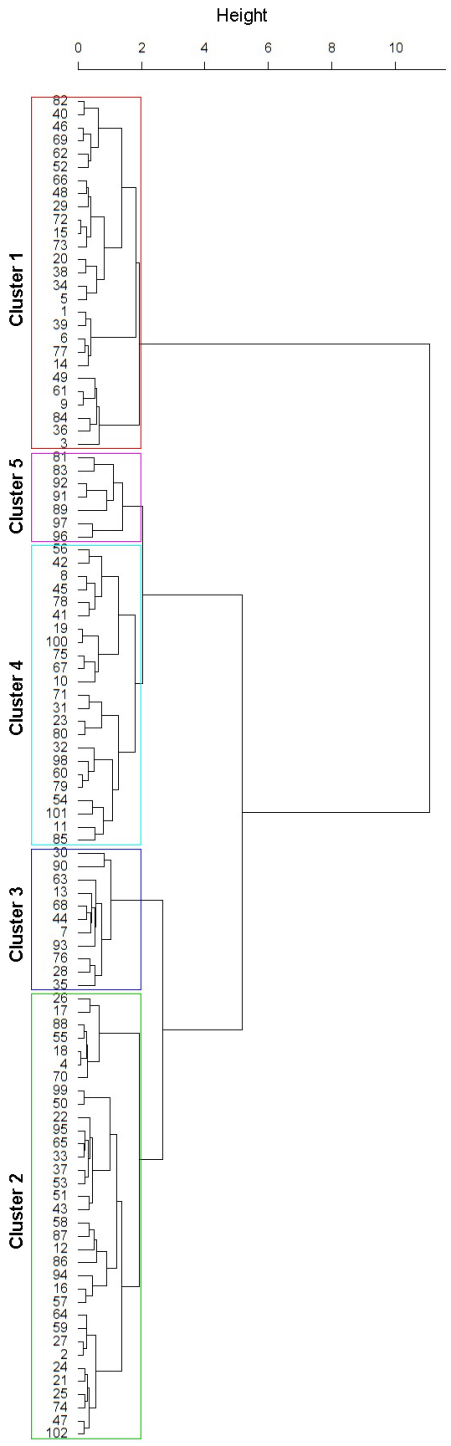

Figure 3.2: Cluster dendrogram showing five clusters based on Ward linkage. Species abundance values (importance values; IV) for each sample point were used to create the dendrogram. The cluster groups were selected using the Mantel statistic (see Appendix A). The numbers in the figure refer to sample points.

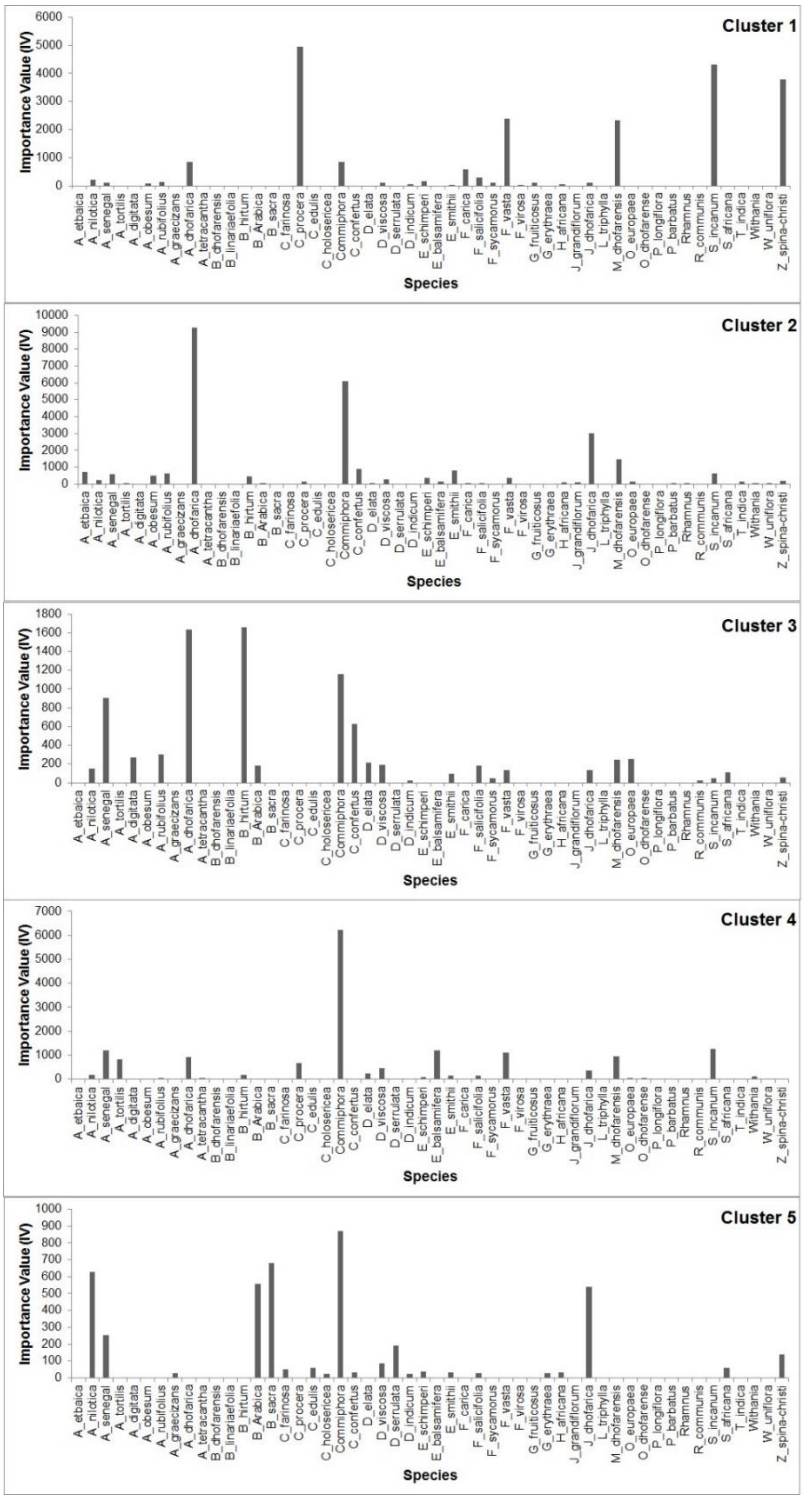

Figure 3.3: Species abundances in each of the five cluster groups based on importance values (IV).

We produced three Mantel correlograms to assess possible spatial autocorrelation of beta diversity (Figure 3.4) over all sample points in the entire study area (Figure 3.4A), in forested areas (Figure 3.4B) and in grasslands (Figure 3.4C). For grassland areas the first, third, and fourth distance bins showed positive correlations, while the second, fifth and sixth bins were negatively correlated. The levels of autocorrelation for the first two distance bins were statistically significant, while the remaining distance bins did not reveal significant autocorrelation. The sharp drop from positive to negative correlation between the first two distance bins, suggests that a level of autocorrelation exists, which becomes more ambiguous and switches between positive and negative correlations in the more distant bins. The lack of significance at the third through last distance bins most likely indicates a near equal division of shared and differing species between sample points. For forested regions, the first four distance bins were correlated negatively, the fifth bin was positively correlated, and the correlation shown by the last bin was approximately zero. However, these distance bins show no significant correlation in beta diversity measurements. In the combined grassland and forested areas the first and fourth bins were positively correlated, while the rest were negatively correlated.

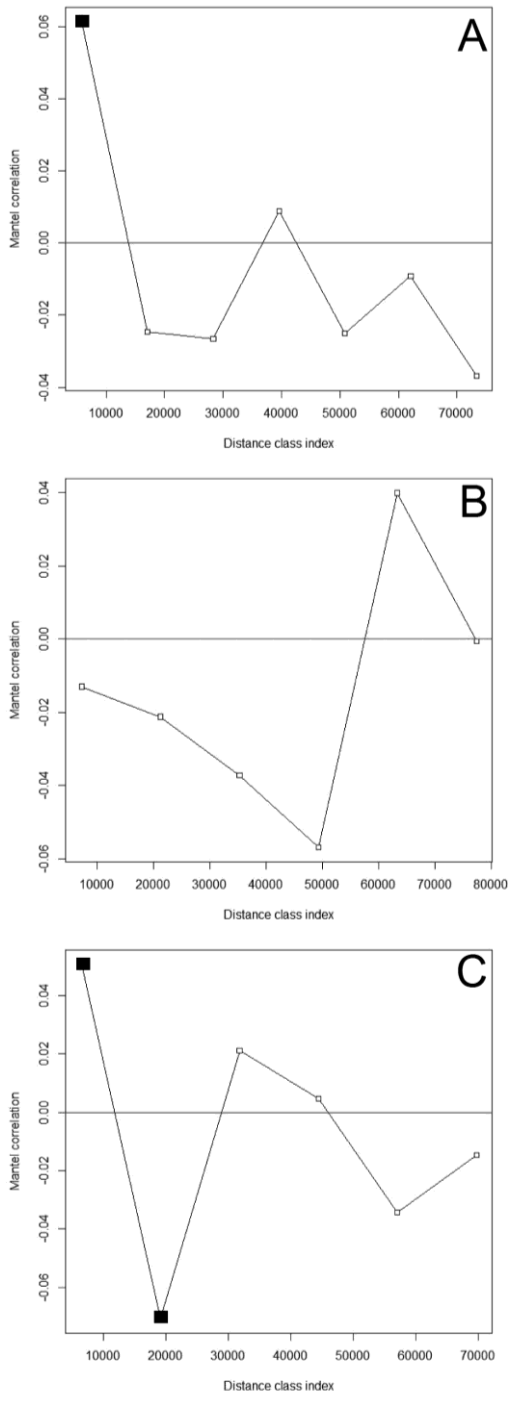

Figure 3.4: Mantel correlograms showing distance bins along the x-axis and the Mantel correlation along the y-axis for: (A) all points in the study area, (B) forest sample points, and (C) grassland sample points. Values above the line show positive correlation and values below show negative correlation. Significant values are shown as solid boxes, insignificant values as open boxes.

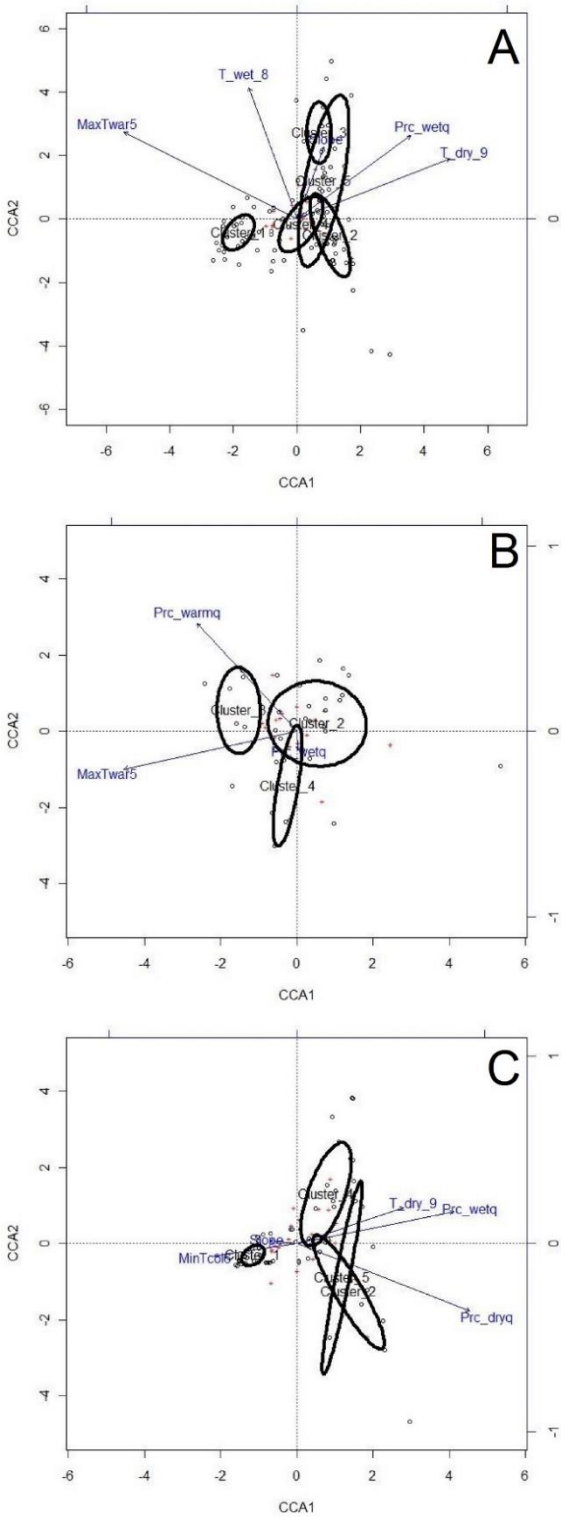

Figure 3.5: Ordination diagrams showing the relationship between the first two axes (CCA1 and CCA2) along with variable scores, sites, and clusters for: (A) all samples points in the study area, (B) forest sample points, and (C) grassland sample points.

Table 3.3 shows the explained variance for three CCA models for 1) the entire study area (all 102 sample points; Figure 3.5A), 2) the forested areas (Figure 3.5B), and 3) the grassland areas (Figure 3.5C). For the entire study area, five variables were used to build the CCA model (see Appendix A, Table A.2). Two variables, maximum temperature of the warmest month and mean temperature of the wettest month, had the highest scores for the first and second CCA axes, respectively. Our CCA model of the forest sample points was based on three variables (Appendix A, Table A.3). The highest scores on the first and second axes of the forest CCA model pertained to maximum temperature of the warmest month and precipitation of the warmest quarter.

Table 3.3: Variance explained and unexplained by the CCA analysis for the entire study area, for forests, and for grassland areas. ***All three CCA model results were significant at the 0.001 level or better based on 9999 permutations of an ANOVA test. See Appendix B for more details.

	Explained	Unexplained	Significance
Study Area	0.165	0.835	***
Forest	0.1876	0.8124	***
Grassland	0.2194	0.7806	***

In the grassland model, five variables were used to construct the CCA model (Appendix A, Table A.4). Precipitation of the driest quarter had the leading score for the CCA1 and CCA2 axes. The grassland model explained the highest level of variance (0.2194). All three models were found significant based on 9999 permutations of an ANOVA test (see Table 3.3). We also ran another three models for each of same three zones that used only spatial variables (latitude and longitude; Table 3.3). While each of these models was statistically significant based on an ANOVA test, they all explained

low levels of variance (the highest = 0.1078 for forest sample plots), suggesting that latitude and longitude tend to be weaker than environmental variables in explaining species abundance in the cloud forest.

3.6 Discussion and Conclusions

Our results reveal that the diversity and distribution of woody plants differ between the biomes of the cloud forest. If we consider the entire study area (all 102 sample points), the biological interactions hypothesis (H2) is affirmed most strongly, based on three major results. First, eight species account for over 70% of the relative species abundances, and just two species (*A. dhofarica* and *Commiphora* sp.) comprise over 35% of the relative species abundances - while the median among all species is less than 1%. The near ubiquitous distribution of *A. dhofarica* and *Commiphora* spp. defines the phytosociological structure of the cloud forest (Kürschner et al. 2004), which also lends support to our acceptance of this hypothesis. Second, our results show a lack of spatial autocorrelation structure in our beta diversity measurements. While the first distance bin (see Fig. 4A) shows significant correlation, the subsequent bins show mostly negative (but not significant) spatial correlation. Both the lack of significance and only a single positive correlation value at the fourth bin indicates that there is no clear spatial correlation in the beta diversity over the entire study area. Third, the CCA model explains less than 17% of the variance across the entire study area according to our environmental variables. We would expect a higher level of explained variance if environmental gradients (H3) best explained our patterns of biodiversity. But one other factor to consider for why environmental gradients are not as strong of an explanation is that cloud

cover is the single most important environmental factor, to such an extent that its mere presence is the one factor needed to sustain the environment (see Chapter 2). The clouds are present at the start of the monsoon and persist throughout the monsoon season. There seems to be little spatial variability. Thus the benefits of the cloud cover (reduced evapotranspiration and fog moisture) are ubiquitous.

For forest sample plots, the biological interactions hypothesis (H2) again provides the best explanation of diversity patterns. Only two taxa, *A. dhofarica* and *Commiphora* spp., comprise the most prevalent species in forested areas, as seen in the cluster analysis and relative taxonomic abundances. Cluster 2 is defined strongly by *A. dhofarica* and *Commiphora* spp., and to a lesser extent by *J. dhofarica*. While Cluster 3 includes more species, only five stand out: *A. dhofarica*, *B. hirtum*, *Commiphora* sp., *A. Senegal*, and *C. confertus*. The success of *A. dhofarica* and *Commiphora* spp., both in terms of the cluster analysis and their common occurrence at both forest and overall sample points, is perhaps the strongest evidence that the biodiversity patterns in the cloud forest are rooted in the dispersal success of these two species. The lack of spatial autocorrelation structure and the low explained variance of the CCA analysis (less than 19%) are used to refute the environmental gradients hypothesis (H3) and the neutral processes hypothesis (H1). The biological interaction hypothesis (H2), which was developed from observations of tropical forests (Pitman et al. 1999, 2001; Condit et al. 2002), similarly explains biodiversity patterns best in the South Arabian Cloud Forest, which lies just outside of the tropical zone. The cloud forest is derived from an ancient tropical forest (Kürschner et al. 2004) and, accordingly, the species that populate the cloud forest today have evolved from these tropical sources. As a contributing factor in this evolution, interglacials

between the Tertiary and present have included periods of much greater precipitation (Burns et al. 2001; Fleitmann et al. 2004; Fleitmann and Matter 2009). This increased precipitation may have expanded the cloud forest in conditions closer to those found in modern tropical forests. Today, despite dry conditions during most of the year, the modern monsoon season provides enough moisture for tropical conditions, and near constant cloud cover, for a substantial part of the year.

In grassland areas, the biological interactions hypothesis (H2) also explains diversity patterns most effectively, but most likely due to land-use decisions. Grazing indicators (e.g., *S. incanum* and *C. procera*), as well as trees and shrubs found typically in rangelands (e.g., *Ficus* sp., *Z. spina-christi*, and *M. dhofarensis*), prevail in Cluster 1 (Appendix A), to an extent that strongly supports the biological interactions hypothesis (H2). The environmental gradients hypothesis is not supported in light of the low level of overall explained variance (less than 22%), despite showing stronger explained variance than in forested areas or the study area as a whole. The Mantel correlograms show stronger evidence for spatial autocorrelation structure than in forested areas. The lack of clear distance decay in Mantel correlograms and significance in the farthest distance bins refute the neutral processes hypothesis (H1). The biological interactions hypothesis (H2) explains diversity patterns in the grasslands based, in part, on the influences of human activity, especially animal husbandry. Herds of camel, cattle, and goats are common throughout the cloud forest. Among the plant species common to the grassland areas, *S. incanum* and *C. procera* are poisonous to livestock (Miller and Morris 1988; Mekonnen 1994), giving these species a competitive advantage over other taxa that are more

palatable to livestock. Grassland areas also are flatter and more suitable for grazing large herds.

Because the forested areas are dominated by a limited number of species with wide dispersal capabilities, preservation of the cloud forest's biodiversity will depend on widespread adoption of conservation measures that protect rare species. Conservation has been a priority in Dhofar for some time (Ghazanfar 1998) and its success will depend on a comprehensive approach that focuses more on tree and shrub species that occur in relatively low abundances. Regional conservation practices (i.e. conservation practices aimed at the entire cloud forest, and not just certain parts) have been deemed important in other cloud forests (Williams-Linera 2002) based on the heterogeneity of species composition across short distances. A similar strategy might be needed in Dhofar, but for different reasons. Pastoralism is a longstanding component of traditional society in Dhofar (Janzen 1986), and vegetation across the region is increasingly impacted by encroaching herds of camels, cattle and goats, as well as infrastructure development. Restoration of biodiversity in grasslands is notoriously difficult without abandonment of the range, or long-term relief from grazing activities (e.g. Vuorio et al. 2014), and recent studies have shown that grasslands are often neglected in conservation efforts (Grau et al. 2014). Foothills areas, which are in close proximity to the city of Salalah, are vulnerable to rapidly increasing urban expansion and other human activity. Forested areas are still populated by a diverse array of floral species, but will require large intact protected forests to reliably safeguard biodiversity (Berhane et al. 2015). Any conservation effort will need to account for the variety of human activity, and, because the biodiversity patterns are defined by the dominance of a small subset of species, priority should be

given to those species found in low abundance, mainly because they will have a greater likelihood of becoming endangered. Conservation efforts in the grassland and shrubland areas will most likely prove even more difficult without a significant restoration effort that incorporates the range of socio-economic activities that are dependent on these environments.

3.7 Acknowledgements

Much of the research was supported by work conducted through a Fulbright Grant to Oman (awarded to Galletti) from the U.S. State Department and sponsored by The Office of the Advisor to His Majesty The Sultan for Economic Planning Affairs. We offer special thanks to Said Al-Saqri and Annette Patzelt for support during the Fulbright grant period. Finally, we would like to thank Steven Falconer and Sanda Heinz for assistance with data collection.

3.8 References

AlSarmi, S., and R. Washington (2011), Recent observed climate change over the Arabian Peninsula, *J. Geophys. Res.*, *116*(D11), D11109, doi:10.1029/2010JD015459.

Berhane, A., Ø. Totland, M. Haile, and S. R. Moe (2015), Intense use of woody plants in a semiarid environment of Northern Ethiopia: Effects on species composition, richness and diversity, *J. Arid Environ.*, *114*, 14–21, doi:10.1016/j.jaridenv.2014.11.001.

Borcard, D., and P. Legendre (2012), Is the Mantel correlogram powerful enough to be useful in ecological analysis? A simulation study, *Ecology*, *93*(6), 1473–1481, doi:10.1890/11-1737.1.

Borcard, D., F. Gillet, and P. Legendre (2011), *Numerical Ecology with R*, Springer, New York.

Burns, S. J., D. Fleitmann, A. Matter, U. Neff, and A. Mangini (2001), Speleothem evidence from Oman for continental pluvial events during interglacial periods, *Geology*, *29*(7), 623, doi:10.1130/0091-7613(2001)029<0623:SEFOFC>2.0.CO;2.

Chisholm, R. A., and S. W. Pacala (2010), Niche and neutral models predict asymptotically equivalent species abundance distributions in high-diversity ecological communities., *Proc. Natl. Acad. Sci. U. S. A.*, *107*(36), 15821–5, doi:10.1073/pnas.1009387107.

Condit, R. et al. (2002), Beta-diversity in tropical forest trees, *Science*, *295*(5555), 666–9, doi:10.1126/science.1066854.

Dauby, G., O. J. Hardy, M. Leal, F. Breteler, and T. Stévart (2014), Drivers of tree diversity in tropical rain forests: new insights from a comparison between littoral and hilly landscapes of Central Africa, edited by P. Linder, *J. Biogeogr.*, *41*(3), 574–586, doi:10.1111/jbi.12233.

Fleitmann, D., and A. Matter (2009), The speleothem record of climate variability in Southern Arabia, *Comptes Rendus Geosci.*, *341*(8-9), 633–642, doi:10.1016/j.crte.2009.01.006.

Fleitmann, D., S. J. Burns, U. Neff, M. Mudelsee, A. Mangini, and A. Matter (2004), Palaeoclimatic interpretation of high-resolution oxygen isotope profiles derived from annually laminated speleothems from Southern Oman, *Quat. Sci. Rev.*, *23*(7-8), 935–945, doi:10.1016/j.quascirev.2003.06.019.

Ghazanfar, S. (1998), Status of the flora and plant conservation in the sultanate of Oman, *Biol. Conserv.*, *85*(3), 287–295, doi:10.1016/S0006-3207(97)00162-6.

Ghazanfar, S. A., and M. Fisher (eds) (1998), *Vegetation of the Arabian Peninsula*, edited by S. A. Ghazanfar and M. Fisher, Kluwer Academic Publishers, Dordrecht.

Grau, H. R., R. Torres, N. I. Gasparri, P. G. Blendinger, S. Marinaro, and L. Macchi (2014), Natural grasslands in the Chaco. A neglected ecosystem under threat by agriculture expansion and forest-oriented conservation policies, *J. Arid Environ.*, *(in press)*, doi:10.1016/j.jaridenv.2014.12.006.

Hijmans, R. J., S. E. Cameron, J. L. Parra, P. G. Jones, and A. Jarvis (2005), Very high resolution interpolated climate surfaces for global land areas, *Int. J. Climatol.*, *25*(15), 1965–1978, doi:10.1002/joc.1276.

Hildebrandt, A., and E. A. B. Eltahir (2006), Forest on the edge: Seasonal cloud forest in Oman creates its own ecological niche, *Geophys. Res. Lett.*, *33*(11), 2–5, doi:10.1029/2006GL026022.

Hildebrandt, A., and E. A. B. Eltahir (2007), Ecohydrology of a seasonal cloud forest in Dhofar: 2. Role of clouds, soil type, and rooting depth in tree-grass competition, *Water Resour. Res.*, *43*(11), 1–13, doi:10.1029/2006WR005262.

Hildebrandt, A., M. Al Aufi, M. Amerjeed, M. Shammas, and E. A. B. Eltahir (2007), Ecohydrology of a seasonal cloud forest in Dhofar: 1. Field experiment, *Water Resour. Res.*, *43*(10), 1–13, doi:10.1029/2006WR005261.

Hubbell, S. P. (2006), Neutral theory and the evolution of ecological equivalence, *Ecology*, *87*(6), 1387–1398.

Janzen, J. (1986), *Nomads in the sultanate of Oman: tradition and development in Dhofar*, Westview Press, Boulder.

Kürschner, H., P. Hein, N. Kilian, and M. A. Hubaishan (2004), The Hybantho durae-Anogeissetum dhofaricae ass. nova - phytosociology, structure and ecology of an endemic South Arabian forest community, *Phytocoenologia*, *34*, 569–612.

Kwarteng, A. Y., S. Dorvlo, and G. T. V. Kumar (2009), Analysis of a 27-year rainfall data (1977 – 2003) in the Sultanate of Oman, *Int. J. Climatol.*, *617*(July 2008), 605–617, doi:10.1002/joc.

Legendre, P., and L. Legendre (1998), *Numerical ecology*, Developments in evironmental modelling, edited by S. E. Edition, Elsevier.

Legendre, P., D. Borcard, and P. R. Peres-Neto (2005), Analyzing beta diversity: Partitioning the spatial variation of community composition data, *Ecol. Monogr.*, *75*(4), 435–450.

Mekonnen, Y. (1994), A survey of plants (potentially) toxic to livestock in the Ethiopian flora, *Sinet, an Ethiop. J. Sci.*, *17*(1), 9–32.

Miller, A. G., and M. Morris (1988), *Plants of Dhofar, The Southern Region of Oman: Traditional, Economic, and Medicinal Uses*, Office of the Adviser for Conservation of the Environment, Diwan of Royal Court, Sultanate of Oman.

Mitchell, K. (2007), *Quantitative analysis by the point-centered quarter method*, Geneva, NY.

Mac Nally, R. (2007), Use of the abundance spectrum and relative-abundance distributions to analyze assemblage change in massively altered landscapes, *Am. Nat.*, *170*(3), 319–30, doi:10.1086/519859.

Parker, A. G., and J. I. Rose (2008), Climate change and human origins in southern Arabia, *Proc. Semin. Arab. Stud.*, *38*, 25–42.

Patzelt, A. (2011), The Themeda Quadrivalvis Tall-Grass Savannah of Oman At the Crossroad Between Africa and Asia, *Edinburgh J. Bot.*, *68*(02), 301–319, doi:10.1017/S0960428611000217.

Pickering, H., and A. Patzelt (2008), *Field Guide to the Wild Plants of Oman*, Royal Botanical Gardens, Kew, Kew, United Kingdom.

Pitman, N. C. A., J. Terborgh, M. R. Silman, and P. Nunez V. (1999), Tree Species Distributions in an Upper Amazonian Forest, *Ecology*, *80*(8), 2651–2661.

Pitman, N. C. A., J. W. Terborgh, M. R. Silman, P. N. V, A. David, C. E. Cerón, W. A. Palacios, and M. Aulestia (2001), Dominance and Distribution of Tree Species in Upper Amazonian Terra Firme Forests, *Ecology*, *82*(8), 2101–2117.

Radcliffe Smith A (1980), The vegetation of Dhofar, in *The scientific results of the Oman Flora and Fauna Survey, 1977, (Dhofar)*, edited by N. Shaw-Reade, S, B. Sale, J, D. Gallagher, M, and H. Daly, R, pp. 59–86.

Rickbeil, G. J. M., N. C. Coops, M. E. Andrew, D. K. Bolton, N. Mahony, and T. A. Nelson (2014), Assessing conservation regionalization schemes: employing a beta diversity metric to test the environmental surrogacy approach, edited by S. Ferrier, *Divers. Distrib.*, *20*(5), 503–514, doi:10.1111/ddi.12146.

Rosindell, J., S. P. Hubbell, and R. S. Etienne (2011), The unified neutral theory of biodiversity and biogeography at age ten., *Trends Ecol. Evol.*, *26*(7), 340–8, doi:10.1016/j.tree.2011.03.024.

Rousseeuw, P. J. (1987), Silhouettes: A graphical aid to the interpretation and validation of cluster analysis, *J. Comput. Appl. Math.*, *20*, 53–65, doi:10.1016/0377-0427(87)90125-7.

Schlecht, E., L. G. H. Zaballos, D. Quiroz, P. Scholte, and A. Buerkert (2014), Traditional land use and reconsideration of environmental zoning in the Hawf Protected Area, south-eastern Yemen, *J. Arid Environ.*, *109*, 92–102, doi:10.1016/j.jaridenv.2014.05.016.

Shmida, A., and M. V. Wilson (1985), Biological determinants of species diversity, *J. Biogeogr.*, *12*(1), 1–20.

Tuomisto, H., and K. Ruokolainen (2006), Analyzing or explaining beta diversity? Understanding the targets of different methods of analysis, *Ecology*, *87*(11), 2697–2708.

Vuorio, V., A. Muchiru, R. S. Reid, and J. O. Ogutu (2014), How pastoralism changes savanna vegetation : impact of old pastoral settlements on plant diversity and abundance in south-western Kenya, *Biodivers. Conserv.*, *23*, 3219–3240, doi:10.1007/s10531-014-0777-4.

Williams-Linera, G. (2002), Tree species richness complementarity , disturbance and fragmentation in a Mexican tropical montane cloud forest, *Biodivers. Conserv.*, *11*, 1825–1943.

CHAPTER 4

LAND CHANGES AND THEIR DRIVERS IN THE CLOUD FOREST AND COASTAL ZONE OF DHOFAR, OMAN, BETWEEN 1988 AND 2013[2]

4.1 Abstract

Several analyses are used to measure environmental changes in the cloud forest and coastal plain in Dhofar, southern Oman, including a land change analysis, multiple endmember spectral mixture analysis (MESMA), cluster analysis using local indicators of spatial association (LISA), and trend analysis of NDVI time series. The results demonstrate systematic degradation and loss of vegetation types in the cloud forest, and loss of native land covers to impervious surfaces on the coastal plain; decreases in woody plant vegetation in almost half of the cloud forest in distinctive hotspots of loss; and significant decreases in NDVI trends around the city of Salalah, along the coastal plain, and in parts of the cloud forest.

The proximate drivers of these changes in the cloud forest appear to be changes in grazing activities, while the growth of Salalah, especially its peri-urban area, altered the coastal plain. These drivers, in turn, are linked to distal ones, foremost changes in Omani policies and investments in the Dhofar area, traced to government responses to the Dhofar War (1970-1975), which have resulted in increased livestock populations and urban growth.

[2] Co-authored with B.L. Turner II and Soe W. Myint

4.2 Introduction

Deforestation and land degradation are recognized problems in dryland environments that cover about 41% of the terrestrial surface of the Earth (Reynolds et al. 2007). Worldwide net primary production of grass- and rangelands has declined due to intensified land uses (e.g., Bai et al. 2008; Li et al. 2012), and the loss of ecosystem services to dryland degradation affects some 250 million people (Reynolds et al. 2007). As a result, dryland deforestation and land degradation have drawn international attention through such programs as the U.N.'s 1992 Convention to Combat Desertification (UNEP 1994) and the 2006 International Year of the Desert and Desertification.

The causes of this degradation, both climatic and anthropogenic in kind, have drawn substantial research attention. Anthropogenic causes have been arrayed along a continuum between proximate and distal causes, depending on the immediacy of human activities and processes to the actual land change and consequences in question (Serneels & Lambin 2001; Geist and Lambin 2002; Lambin et al. 2003; Turner et al. 2007). Proximate causes, such as agricultural expansion or land-use intensification, are relatively easy to correlate strongly with land changes, whereas distal causes (aka underlying or root causes and teleconnections), such as international policies and markets, prove to be a challenge, commonly linked to actual land changes conceptually or through interpretations of case studies (Brannstrom & Vadjunec 2014; Lambin et al. 2001; Liu et al. 2013; Vayda & Walters 1999). It is also recognized that distal and proximate causes interact in ways that amplify or attenuate land change (Defries et al. 2010; Seto & Reenberg 2014).

Dryland degradation, linked variously to proximate and distal causes, is apparent in the southern Arabian Peninsula, including within the South Arabian Cloud Forest, near Salalah, Dhofar, Oman. Cloud forest ecosystems generally occupy only a small portion of the world's forests, but are usually rich in ecosystem services and biodiversity (Higuera et al. 2013). Dhofar's portion of the South Arabian Cloud Forest consists of forest, shrub, and grasslands that have been decreasing in biomass and tree species during the lifetime of satellite observations of the region. The causes of this change—climatic, owing to changes in the Indian Ocean monsoon (Kumar et al. 2011) or anthropogenic—are contested, but the most immediate human activities altering the cloud forest ecosystem are not. These activities involve increasing camel, goat, and bovine grazing (Miller and Morris 1988; Ghazanfar 1998; Hildebrandt and Eltahir 2006; Patzelt 2011; El-Sheikh 2013). The reasons for grazing intensification, as provided by local land managers and observers, may be grouped into two, possibly interlinked, causes. One hypothesis holds that increases in livelihood standards, owing to expanding household income portfolios and improved access to water wells and animal support services, has increased herd size (Janzen 2000). Another perspecitve focuses on broader infrastructure development, foremost road construction, which has spurred peri-urban development and market access, amplifying herd densities.

These more proximate causes, in turn, are clearly linked to changes in the national policies of Oman. Begun in the 1970's as a response to internal revolts against the government, attention was given to livelihood improvements, including in the mountains of Dhofar where the cloud forest resides (Janzen 2000; Petersen 2004a; Petersen 2011). Investments were made specifically to increase water wells, subsidize cattle feed (Janzen

1986: 195-196), employ adult males (e.g., to fight against Omani dissidents), and increase commercial investments in the nearby city of Salalah (Janzen 1986: 173-175). Complementing this policy change was one directed toward infrastructure modernization, especially emerging in the 1980s (O'Reilly 1998; Allen and Rigsbee 2000; Peterson 2004a,b), focusing on large infrastructure, such as roads, schools, and airports.

The changes to the cloud forest land cover and land uses, foremost grazing practices linked to herd size, constitute common wisdom in southern Oman. Actual documentation, however, has been lacking. This research seeks to rectify this lacuna. First, it seeks to identify systematically the land-cover changes in the cloud forest and coastal plain of Dhofar from 1988 to 2013 through the use of satellite data, determining the kind and amount land-cover changes during that period. Second, it qualitatively probes the roles of two specific development paths—infrastructure development and livelihood improvements—in terms of generating the changes observed. Data limitations impeded quantitative assessments of the causes.

4.3 Study Area

The study area is the Dhofar portion of the South Arabian Cloud Forest and the immediate surrounding area within the Governate of Dhofar, Oman. The cloud forest is a drought-deciduous, seasonal cloud forest (Hildebrandt 2005) that lies along the southern coasts of Oman and Yemen. Three dominant natural land covers (forest, grass, and shrubs) occupy two primary biomes: forest and grassland. The forests consist of broadleaf and evergreen species of trees and shrubs (Miller and Morris 1988), usually found in southerly draining *wadis*. The grasslands have trees and shrubs, but usually in

much lower density than the forest (Patzelt 2011). There is also a third subsidiary, hybrid biome, the foothills of the mountains, which has a mix of grasses, shrubs, and trees. The foothills run along the southern portion of the cloud forest and act as a partition between the coastal area and the Dhofar Mountains.

Three mountains comprise the Dhofar range: Jabal Qara, Jabal Qamar, and Jabal Samhan. Transects running from Jabal Qara and Jabal Qamar to the coastal planes are used as the study area because they capture substantial portions of the cloud forest as well as the urban development of Salalah (Figure 1.1). The total area examined covered 3,069 km^2, of which about 28.6% is forest. Sloping plateaus that are incised by wadis define the topography. Despite the usual desert conditions of southern Arabia, precipitation in the study area is reliable during the summer months (June to September) when the Indian Ocean Monsoon (IOM) forms. While the IOM can be variable from one year to the next (Anderson et al. 2002; Goswami and Mohan 2001; Gupta et al. 2003; Kumar et al. 2006; Charabi and Abdul-Wahab 2009; Scholte et al. 2010), cloud cover and fog moisture are abundant enough to allow dense vegetation to grow. The precipitation during the monsoon is usually fog moisture, rather than heavy rainfall. Trees act as a comb when the fog forms, allowing moisture to collect on the leaves and branches and then fall to the ground (Hildebrandt 2005; Hildebrandt and Eltahir 2006; Hildebrandt and Eltahir 2007). Because of this, direct measurements of precipitation can be inaccurate, but estimates range to 250 mm annually. Heavy bursts of rainfall are possible all year round, but most of the year is usually dry outside of monsoon season.

The grasslands and forests are heavily grazed by goats, camels, and cattle, which belong to several groups of people living in the Dhofar Mountains (Janzen 1986). Herds

are kept in the mountains for most of the year and are usually brought down to the coastal regions at the start of the monsoon. While herding is still the primary occupation for many groups living in the mountains, the growing economy in Salalah has begun to attract a diverse range of activities. Salalah, which lies along the coast just south of Jabal Qara, has grown considerably in the last few decades. The income generated from oil revenues, shipping, livestock, frankincense trade, and agriculture has begun to shift livelihoods away from traditional lifestyles to urban professional ones, with a greater portion of the population attending college and working in the city. This remains a process in transition; many individuals still practice traditional herding, part time in some cases, while working in Salalah.

4.4 Methods

Landscape change is addressed in three ways. First is a land change analysis, which identifies key transitions from one land cover to another between 1988 and 2013. A total of nine land cover types were identified, but our focus is on the transition between six of these land covers: coastal alluvium, grass, shrubs, trees, roads, and the built environment. Second is a subpixel analysis that is used to measure changes in woody plant coverage. Finally, a trend analysis identifies changes in the vegetation index, in this case NDVI, signaling vegetation health. The time period for the trend analysis is 2001 to 2013, a 13 year period that roughly coincides with renewed efforts to develop infrastructure across Oman and Dhofar.

Table 4.1: The nine land covers and their description used in the land change analysis

Class	Description
Desert gravel plains (DGP)	Desert region surrounding the northern portions of the cloud forest
Water (W)	Primarily ocean and inlets
Coastal alluvium (CA)	The arid land cover occupying the coastal area south of the foothills and around the city of Salalah
Agriculture (Ag)	Agriculture plots, mainly in and around the city of Salalah
Grass (Gr)	Grassland areas where trees are sparse
Trees (Tr)	Forested areas where trees form a coherent canopy
Shrubs (Shr)	Areas where shrubs tend to dominate, primarily around eastern portions of Jabal Qara, foothills, and Northern portions of Jabal Qamar – can include a moderate density of trees that are too sparse to form a coherent canopy
Roads (Rd)	This category includes asphalt tarmac and hard packed dirt roads.
Built environment (BE)	Generally buildings, structures, or high density urban areas, and may include surrounding roads or pavement

4.4.1 Land Change Analysis

Two sets of Landsat images were classified; one set each for 1988 and 2013 (4 images total - for 1988, the scenes ID's are LT41590481988340XXX02 and LT41600481988347AAA04; for 2013, LC81600482013343LGN00 and LC81590482013336LGN00). These images were collected in the early part of December, when the distinction between grass, trees, and shrubs is fairly stark. Digital numbers were converted to reflectance values using metadata coefficients, a dark object subtraction, and

climate data records (Masek et al. 2006; USGS 2015). Principle component bands were calculated and added to the image stack to facilitate classification. An object-based image analysis method (OBIA; Blaschke 2010) was employed for land cover classification. Nine land covers were classified (Table 1): desert gravel plains (DGP), water (W), coastal alluvium (CA), agriculture (Ag), grass (Gr), trees (Tr), Shrubs (Shr), Roads (Rd), and built environment (BE) (Table 1). The land covers were selected based on field observations and environmental descriptions in Miller and Morris (1988).

Transition matrices were used to identify *systematic* land-cover transformation, which is a conversion from one land cover to another, while accounting for *expected* land-cover changes (Pontius et al. 2004). *Expected* land changes are due to possible random chance, small changes in large land-cover categories, errors in land-cover maps, and so on. The transition matrix was developed using the methods outlined in Pontius et al. (2004) and Alo and Pontius (2008). *Observed* versus *expected* land-cover transitions can be found by analyzing the tradeoffs between land covers as shown in rows and columns of a transition matrix. Rows of the transition matrix are the land covers as they stand in 1988 and columns represent the land covers in 2013. Diagonal values show persistence of land-cover types, while off-diagonal values show the transition from the land cover for that row (1988) to the land cover for that column (2013). At the end of each row, a sum shows the total land-cover *loss* plus persistence as well as the total loss for that row's land-cover category. At the end of each column, a sum shows the total land-cover *gain* plus the persistence as well as the total gain for that column's land-cover category. *Expected* transitions are calculated by analyzing the *observed* land-cover gains and losses and using the formulae in Alo and Pontius (2008; page 288, equations 1 and

2). If the observed loss minus the expected loss is positive for a matrix cell, then that row's land cover is systematically losing to the land cover in the column; if it is negative, it is resisting systematic loss. If the observed gain minus the expected gain is positive for the matrix cell, then that column's land cover is systematically gaining from the land cover in the row; if it is negative, it rebuffs systematic gain from the land cover for that row (Alo and Pontius 2008).

4.4.2 Vegetation Fraction and Subpixel Analysis

Ground covers that occupy varying proportions of a pixel in a satellite image can be extracted using methods collectively known as subpixel analysis. The basis of this method lies in the assumption that surface materials may be smaller than the resolution of the image's pixel. The surface material proportions within a pixel can be estimated by using a linear combination of reflectance values of known ground targets, called endmembers. This approach has been generally termed spectral mixture analysis (SMA; Settle and Drake 1993), and is often used to model three primary components: vegetation, impervious surfaces, and soil (V-I-S). It is used here to extract vegetation fraction, a useful indicator of degradation and deforestation (e.g. Dawelbait and Morari 2012).

Our subpixel approach uses an extension of the SMA method known as multiple endmember spectral mixture analysis (MESMA; Roberts et al. 1998). MESMA has an advantage over SMA in that a subset of the total number of endmembers can be modeled for each pixel, rather than using a linear combination of all endmembers. Three steps are used to arrive at the endmember proportions (Powell and Roberts 2010). The first step constructs a library of endmembers. For each endmember, the reflectance values from

satellite images are recorded for each band. Finding representative endmembers can be accomplished using reflectance values from a known spectral library or gathered from within the image by selecting 'pure' pixels (i.e., pixels that are made up almost entirely of a single endmember). The second step is to construct possible models of endmember combinations that best fit the known reflectance values at each pixel. To do this, the endmember proportions must equal 1, each endmember fraction must be constrained between 0 and 1, and the root mean square error (RMSE) cannot exceed a certain value (Powell and Roberts 2010). The final step is model selection.

A pixel purity index (PPI; Boardman et al. 1995) finds meaningful endmembers and was used to construct an endmember library for this study. Over one hundred possible endmembers were reduced to three primary V-I-S categories, using methods developed by Dennison and Roberts (2003). Vegetation endmembers were selected mainly from areas of tree canopy (1988 n=5, 2013 n=23). Impervious surface endmembers were selected from roads, hard packed dirt tracks, buildings, and desert hard scrabble (1988 n=7, 2013 n=16). Finally, soil was selected from exposed organic soils in the cloud forest and coastal alluvium (1988 n=4, 2013 n=4). To arrive at our final models, we used a four endmember model (V-I-S + shade) and set the RMSE to 0.25. Any pixels that could not meet the RMSE criteria were masked from our analysis, along with water pixels and shaded regions.

Since there is no test to determine the statistical significance for the vegetation fraction, we identified systematic areas of increase and decrease in this fraction by searching for statistically significant spatial clusters. We determined significant spatial clusters by using local indicators of spatial association (LISA; Anselin 1995), which

organizes pixels of high vegetation fraction (vegetation fraction gains) and pixels of low vegetation fraction (vegetation fraction losses) into clusters. LISA statistics help breakdown the global Moran's *I* test for spatial autocorrelation into local components. These local components can be interpreted as spatial clusters or hot spots. The clusters are tested for significance by using a conditional permutation framework.

4.4.3 Time Series Analysis

One advantage of regularly collected NDVI observations is that these data can be analyzed using the dynamics of the system over time. The dynamics can be associated with the mean value observed throughout the year, or the highest value observed, and so on. Trend analysis was used to determine if key NDVI time series were increasing or decreasing with time, providing a proxy of ecosystem health (Bai et al. 2008; Hilker 2014). An increase in the trend (positive slope) indicates an NDVI value is getting stronger with time and implies that net primary production may be increasing. A decreasing trend (negative slope) indicates and implies the opposite.

Before the trend can be estimated, the yearly observations need to be modeled so that key parameters can be extracted. We used the seasonal trend analysis methods outlined in Eastman and others (2009; 2013) to model the mean annual NDVI (referred to as Amplitude 0) and the NDVI annual cycle (referred to as Amplitude 1). The Amplitude 1 signal is the difference between the minimum and maximum NDVI observations (Eastman et al. 2013), whereas Amplitude 0 is an average of the annual NDVI signal. These two observations are extracted by using a harmonic regression to model the yearly NDVI cycle. A Theil-Sen median slope is then calculated on the Amplitude 0 and 1

values for each year. This median slope calculation is robust and can reliably estimate the trend slope even in the presence of noise and outliers (Theil 1950, Sen 1968). Up to 29% of the observations can be outliers. Once the slope is calculated, a Mann-Kendal test for trend significance is created along with z-values, of which we used the z-values to help determine statistical significance. The NDVI observations were obtained from the MODIS 16-day NDVI product at 250 m resolution for the years 2001 to 2013 (MODIS tile 23 horizontal, 7 vertical).

4.5 Results

4.5.1 Transition Matrix

Considerable change in the environment of the cloud forest is revealed (Figure 2.1). Trees had a net loss of about 23,165 ha, and coastal alluvium about 13,469 ha. In contrast, roads gained about 12,535 ha, the built environment increased by about 9,157 ha, and grass and shrub covers had a net gain of 15,147 ha and 59 ha, respectively. But, the net gains in shrubs and grasses mask a more complex exchange between land covers.

Tables 4.2 and 4.3 show the transition matrix and a matrix of systematic gains and losses. According to these matrices, a few land covers systematically transitioned to other land covers. Despite the large net loss in cover, trees are systematically losing coverage to only one other land-cover category, shrubs. About 4% of the landscape transitioned this way (Table 4.2), barely above what was expected from random chance (Table 4.3). Forest covers resisted transition to roads or the built environment. Only about 0.45% of the landscape underwent a transition from trees to roads, and even less to the built environment (0.06%), both well within the expected ranges.

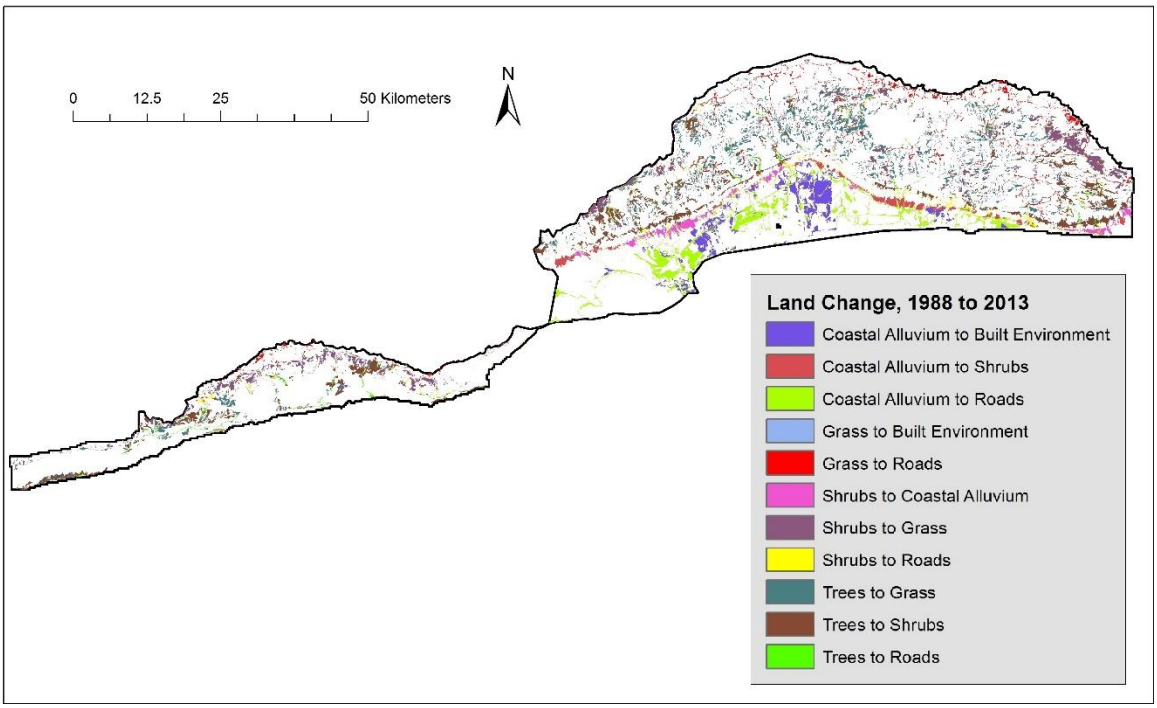

Figure 4.1: Land-cover change between 1988 and 2013.

Two land-cover transitions offered some support that infrastructure was driving at least moderate change. Coastal alluvium lost cover to roads or the built environment (about 4.5% of the total landscape), a result well beyond expectations (Table 4.3) and a product of peri-urban expansion. Grass cover also transitioned to road cover above expectations, occurring mainly in the cloud forest.

The structure of environmental change is registered in the transitions from trees to shrubs, shrubs to grass, and grass to roads (Tables 4.2 and 4.3). The transition of trees to shrubs and shrubs to grass hints at a gradual change in vegetation cover as opposed to the transition of grass to roads, a more abrupt type of change. Tree and shrub covers that converted to road covers between 1988 and 2013 comprised only about 1% of the

landscape (0.45% and 0.52%, respectively), which was below the expectations for trees and close to the expected transition for shrubs.

Table 4.2: Transition Matrix -rows represent land covers from 1988 and columns are 2013. Diagonal values show persistence. Off-diagonal cells show observed and expected transitions from row to column. The observed transitions are in bold, expected losses in italics, and expected gains are in normal font. Values are in terms of percent of landscape

		2013										
		DGP	W	CA	Ag	Gr	Tr	Shr	Rd	BE	Total	Gross Losses
1988	DGP	**0.33**	**0.00** *0.00* 0.00	**0.00** *0.02* 0.01	**0.00** *0.00* 0.00	**0.09** *0.05* 0.05	**0.01** *0.05* 0.00	**0.01** *0.02* 0.03	**0.06** *0.02* 0.03	**0.00** *0.01* 0.02	**0.50** *0.50* 0.47	**0.17** *0.17* 0.14
	W	**0.00** *0.00* 0.00	**0.53**	**0.06** *0.01* 0.01	**0.00** *0.00* 0.00	**0.00** *0.02* 0.06	**0.00** *0.02* 0.00	**0.00** *0.01* 0.03	**0.01** *0.01* 0.04	**0.01** *0.00* 0.02	**0.61** *0.61* 0.70	**0.08** *0.08* 0.17
	CA	**0.02** *0.03* 0.01	**0.11** *0.05* 0.02	**12.77**	**0.07** *0.06* 0.04	**0.01** *2.11* 1.87	**0.04** *1.95* 0.12	**0.84** *0.73* 0.92	**2.53** *0.62* 1.13	**1.93** *0.31* 0.69	**18.32** *18.32* 17.57	**5.56** *5.56* 4.80
	Ag	**0.00** *0.00* 0.00	**0.00** *0.00* 0.00	**0.02** *0.04* 0.01	**0.66**	**0.01** *0.08* 0.09	**0.00** *0.07* 0.01	**0.00** *0.03* 0.05	**0.13** *0.02* 0.06	**0.10** *0.01* 0.03	**0.92** *0.92* 0.91	**0.26** *0.26* 0.25
	Gr	**0.01** *0.01* 0.02	**0.00** *0.02* 0.03	**0.00** *0.40* 0.35	**0.00** *0.03* 0.06	**23.90**	**0.13** *0.82* 0.16	**0.08** *0.31* 1.30	**1.57** *0.26* 1.61	**0.33** *0.13* 0.98	**26.01** *26.01* 28.41	**2.12** *2.12* 4.51
	Tr	**0.02** *0.05* 0.02	**0.01** *0.08* 0.05	**0.05** *1.75* 0.49	**0.00** *0.11* 0.08	**3.93** *3.88* 3.69	**28.18**	**3.47** *1.35* 1.81	**0.45** *1.15* 2.24	**0.06** *0.57* 1.36	**36.17** *36.17* 37.92	**8.00** *8.00* 9.74
	Shr	**0.01** *0.02* 0.01	**0.00** *0.03* 0.01	**0.77** *0.69* 0.15	**0.01** *0.04* 0.02	**2.78** *1.54* 1.10	**0.24** *1.42* 0.07	**6.34**	**0.52** *0.46* 0.67	**0.11** *0.23* 0.40	**10.77** *10.77* 8.77	**4.44** *4.44* 2.43
	Rd	**0.00** *0.01* 0.00	**0.00** *0.01* 0.01	**0.20** *0.01* 0.07	**0.05** *0.01* 0.01	**0.16** *0.50* 0.52	**0.03** *0.46* 0.03	**0.04** *0.18* 0.25	**3.55**	**1.05** *0.07* 0.19	**5.08** *5.08* 4.63	**1.54** *1.54* 1.09
	BE	**0.00** *0.00* 0.00	**0.01** *0.00* 0.00	**0.07** *0.08* 0.02	**0.08** *0.01* 0.00	**0.06** *0.19* 0.16	**0.00** *0.17* 0.16	**0.02** *0.07* 0.08	**0.36** *0.06* 0.10	**1.00**	**1.60** *1.60* 1.38	**0.60** *0.60* 0.38
	Total	**0.40** *0.45* 0.40	**0.67** *0.73* 0.67	**13.94** *15.99* 13.88	**0.88** *0.92* 0.88	**30.95** *32.27* 30.95	**28.63** *33.15* 28.63	**10.79** *9.03* 10.79	**9.17** *6.14* 9.17	**4.58** *2.34* 4.58	**100.0**	**22.75**
	Gross gains	**0.07** *0.12* 0.07	**0.13** *0.20* 0.13	**1.17** *3.22* 1.17	**0.22** *0.26* 0.22	**7.05** *8.37* 7.55	**0.45** *4.97* 0.40	**4.46** *2.69* 4.46	**5.62** *2.59* 5.62	**3.58** *1.34* 3.70	**22.75**	

Table 4.3: Systematic gains and losses. Systematic losses are in bold, systematic gains in italics. Positive values indicate that the land cover for that row is prone to loss/gain to the land cover in the column. Negative values indicate resistance to loss or gain. Values are in percent of landscape. * indicates the highest systematic gains or losses

	DGP	W	CA	Ag	Gr	Tr	Shr	Rd	BE
DGP	**0.33**	**0.00** *0.00*	**-0.02** *0.00*	**0.00** *0.00*	**0.04** *0.04*	**-0.04** *0.00*	**-0.01** *-0.02*	**0.05** *0.03*	**-0.01** *-0.02*
W	**0.00** *0.00*	**0.53**	**0.05** *0.05*	**0.00** *0.00*	**-0.02** *-0.06*	**-0.02** *0.00*	**-0.01** *-0.03*	**0.00** *-0.03*	**0.00** *-0.02*
CA	**-0.01** *0.01*	**0.06** *0.08*	**12.77**	**0.01** *0.03*	**-2.09** *-1.86*	**-1.91** *-0.08*	**0.11** *-0.07*	**1.91*** *1.40**	**1.61*** *1.24**
Ag	**0.00** *0.00*	**0.00** *0.00*	**-0.02** *0.01*	**0.66**	**-0.07** *-0.09*	**-0.07** *-0.01*	**-0.03** *-0.05*	**0.11** *0.07*	**0.09** *0.07*
Gr	**0.00** *-0.01*	**-0.02** *-0.03*	**-0.40** *-0.35*	**-0.02** *-0.06*	**23.90**	**-0.69** *-0.03*	**-0.23** *-1.22*	**1.31*** *-0.04*	**0.19** *-0.65*
Tr	**-0.03** *0.00*	**-0.07** *-0.04*	**-1.70** *-0.44*	**-0.11** *-0.08*	**0.06** *0.24*	**28.18**	**2.12*** *1.66**	**-0.70** *-1.79*	**-0.51** *-1.30*
Shr	**-0.01** *0.00*	**-0.03** *-0.01*	**0.07** *0.62**	**-0.03** *-0.01*	**1.24*** *1.68**	**-1.18** *0.18*	**6.34**	**0.06** *-0.15*	**-0.12** *-0.29*
Rd	**0.00** *0.00*	**-0.01** *0.00*	**-0.03** *0.13*	**0.04** *0.04*	**-0.34** *-0.35*	**-0.44** *0.00*	**-0.14** *-0.22*	**3.55**	**0.98*** *0.86**
BE	**0.00** *0.00*	**0.01** *0.01*	**-0.01** *0.05*	**0.08** *0.08*	**-0.13** *-0.11*	**-0.17** *-0.01*	**-0.05** *-0.06*	**0.30** *0.26*	**1.00**

4.5.2 Subpixel (MESMA)

Figure 4.2 shows the vegetation fraction difference between 1988 and 2013. Visual interpretation reveals areas of decreasing vegetation fractions around the northern and eastern portions of the cloud forest, as well as areas to the east of Salalah. Some areas show increasing fraction, mainly in the forested areas of Jabal Qamar in the west and parts of Jabal Qamar in the central part of the cloud forest. There is also increasing vegetation fractions in eastern sections of the cloud forest.

Figure 4.3 displays the number of pixels that are increasing in vegetation fraction (> 10%), decreasing in fraction (< -10%), or constrained between 10% and -10% fraction.

More pixels are decreasing in vegetation fraction than those that are increasing or are constrained between -10% and 10%.

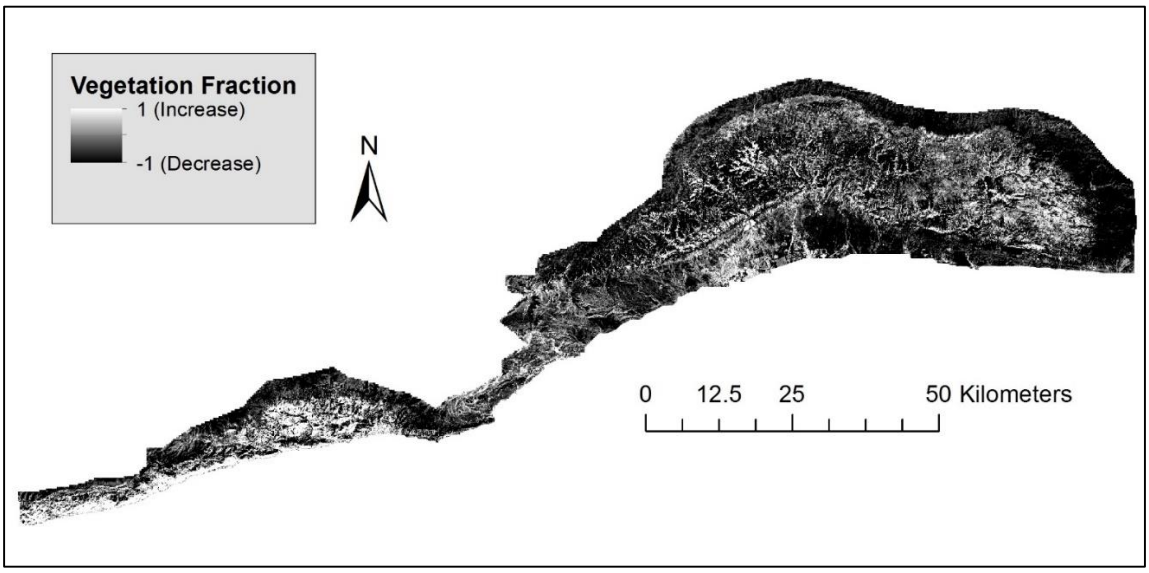

Figure 4.2: Vegetation Fractions derived from MESMA analysis.

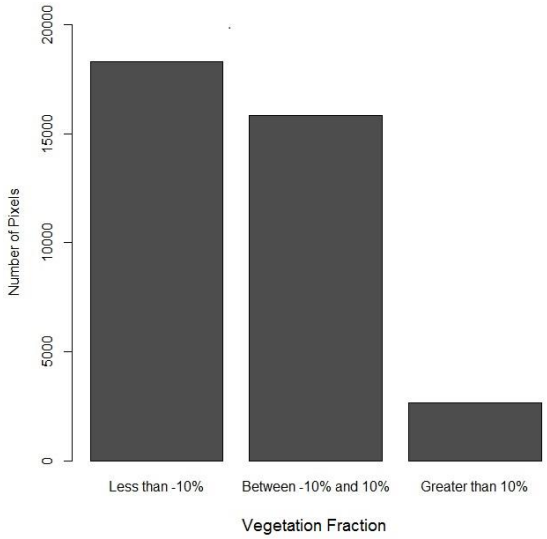

Figure 4.3: Vegetation fraction bar chart showing the number of pixels that went through a -10% or less decrease in fraction, pixels constrained between -10% and 10%, and greater than 10% increase in vegetation fraction.

Figure 4.4 illustrates the results of the LISA analysis. Two types of spatial clusters were highlighted: high-high and low-low. The high-high clusters are areas where pixels of increasing woody plant vegetation (i.e., vegetation fraction) are surrounded by other pixels of increasing woody plant vegetation. Low-low clusters are the opposite. The LISA analysis has the benefit of showing only statistically significant clusters, which helps to isolate areas where increasing or decreasing fractions are prevalent. Jabal Qamar, in the western part of the study area, has witnessed spatially consistent increases in fractions, while areas in the eastern portions of Jabal Qara show a number of pixels of decreasing vegetation fractions. Just west of this area, in the interior area of Jabal Qara's eastern half, the vegetation fractions appear to have increased. The western part of Salalah has increased vegetation fractions, while the eastern portion of the city has consistently decreased in this fraction.

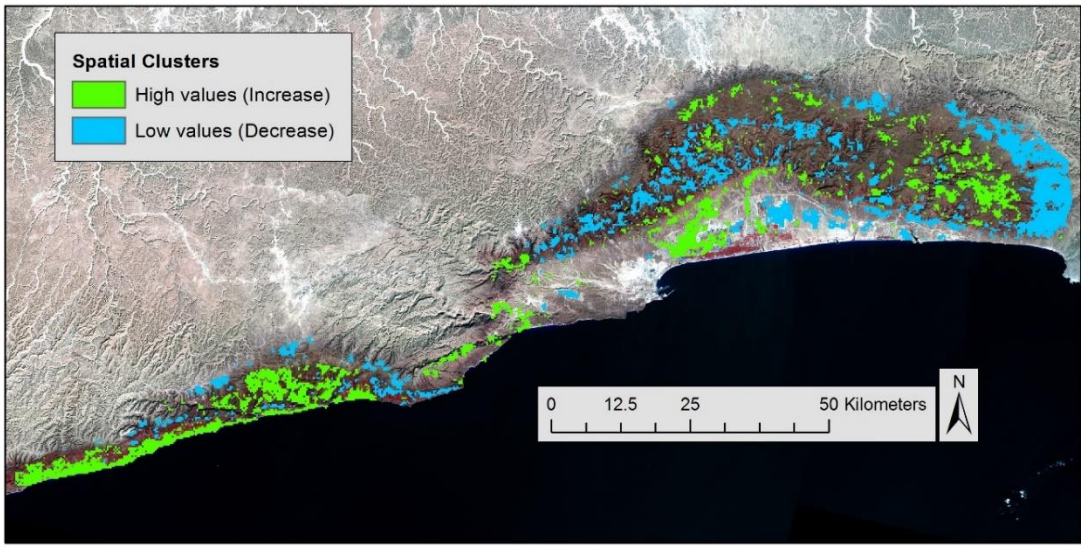

Figure 4.4: Spatial clusters of the vegetation fraction – only significant spatial clusters of high-high values and low-low values are presented. High-high clusters are pixels of increasing vegetation fraction located near other pixels of increasing vegetation fraction, while low-low clusters are decreasing in vegetation fraction.

4.5.3 Time Series Analysis

The results of the time series analysis are shown in Figures 4.5 and 4.6. Areas around Salalah and to the west of the city maintain large pockets of statistically significant decreasing trends in the mean annual NDVI (Amplitude 0, Figure 4.5), as well as some areas to the east of the city. There are only a few small pockets of pixels that show statistically significant increasing trends in Amplitude 0.

For Amplitude 1, that is, the difference between the minimum and maximum NDVI values (Figure 4.6), pockets of significantly increasing or decreasing trends were generally fewer than those found for Amplitude 0. The areas that showed decreasing Amplitude 1 trends seem to have occurred mainly around Salalah, while increasing trends appear to be occurring at several small areas in the cloud forest.

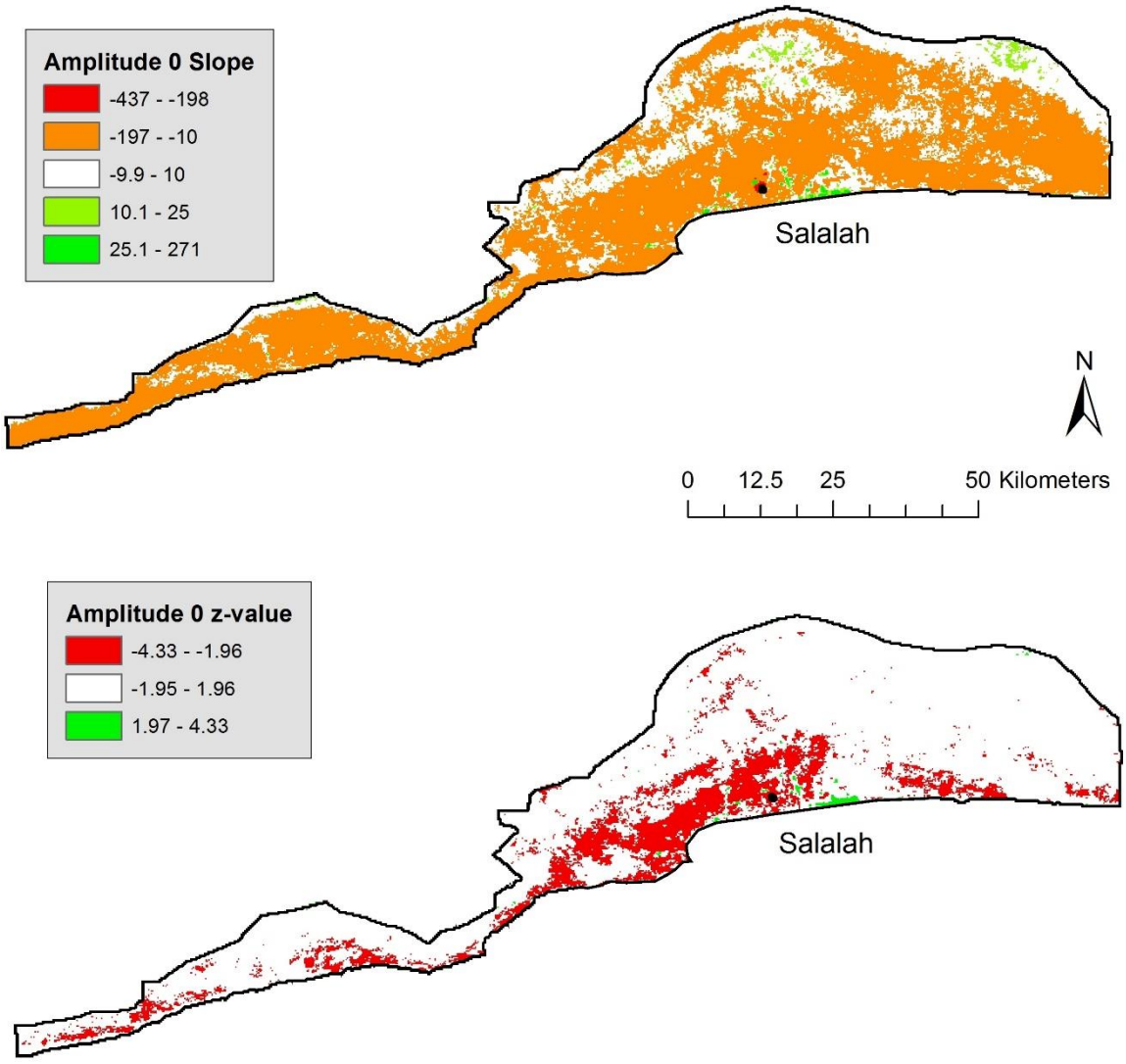

Figure 4.5: Amplitude 0 (annual mean NDVI) trend analysis results. The top map shows the slope of the trend as changes in average NDVI per year (MODIS NDVI = NDVI x 10000). The bottom map shows the z-values used to measure significance (greater than 1.96 or less than -1.96).

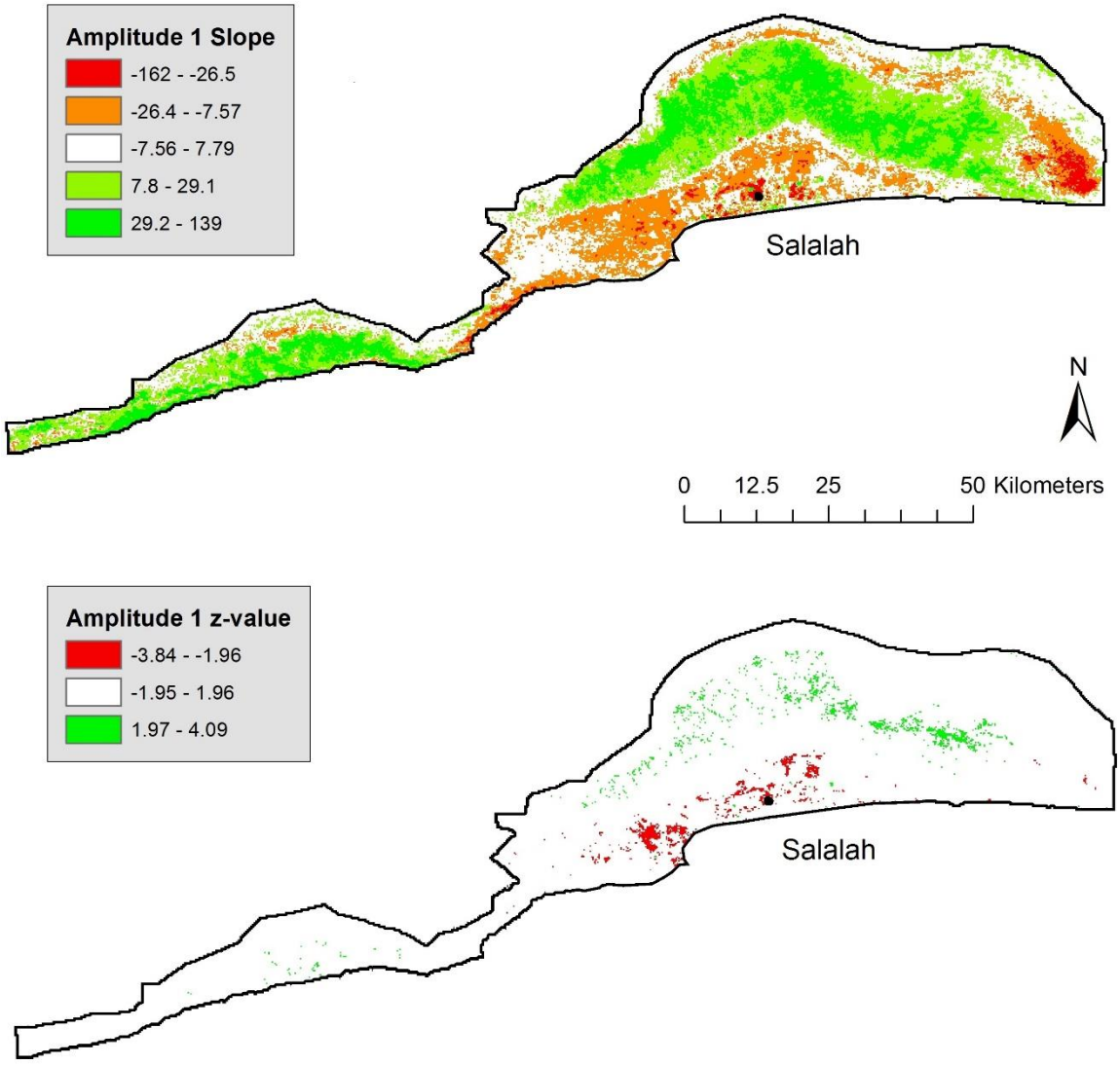

Figure 4.6: Amplitude 1 (difference between peak and minimum yearly NDVI) trend analysis results. The top map shows the slope of the trend as changes in peak NDVI per year (MODIS NDVI = NDVI x 10000). The bottom map shows the z-values used to measure significance (greater than 1.96 or less than -1.96).

4.6 Discussion

4.6.1 Land Changes

The analysis of vegetation fractions suggest there are complex changes occurring across the study area. Most of the cloud forest area examined witnessed a decrease in vegetation fraction or minimal change (Figure 4.3). Some areas of the cloud forest, however, actually increased in vegetation fractions, contradicting the local, prevalent notion of ubiquitous degradation or deforestation. Several explanations for this increase are plausible. Increased atmospheric CO_2 has been shown to lead to greening in warmer, arid environments (Donohue et al. 2013)—a phenomenon referred to as the CO_2 fertilization effect. Dhofar is one region thought to be experiencing this effect (Figure 2 in Donohue et al. 2013). Another possible reason is shrub encroachment, usually on grasslands (Asner et al. 2004) and associated with a disturbance to the ecosystem, such as fires or grazing (Anadón et al. 2014). In the case of Dhofar, shrub encroachment is generally associated with grazing, because the dominant and most abundant types of shrubs are those that are unpalatable to livestock (Miller and Morris 1988; Pickering and Patzelt 2008). Shrub encroachment can have different effects on an ecosystem - it may possibly lead to both increases and decreases in primary production (Eldridge et al. 2011). Since the transition matrix does not show any systematic transitions between grass and shrub covers, the shrub encroachment is likely occurring at a level where grasses are still the dominant land cover, and where shrub encroachment could lead to an increase in the woody plant fraction (i.e., an increase in the vegetation fraction).

Perhaps the most complex changes are those happening along the coast of Jabal Qamar. Here, there appears to be places that are increasing in vegetation fraction but

decreasing in the mean annual NDVI trend analysis (Amplitude 0). This counter-intuitive result may indicate a long-term increase in woody plant vegetation, but with decreasing health, which may be the result of a greening-browning process (de Jong et al. 2012; 2013). Additional research and more time series observations will be needed to understand this process.

A gross reduction in forest land covers comprising about 8% of the study area between 1988 and 2013, suggests that human activities, perhaps with minor climate changes (see below), have led to some deforestation. The widespread reductions in the vegetation fraction show that many parts of the cloud forest have undergone a greater than 10% reduction in woody plant fractions (Figure 4.2, 4.3, 4.4). The primary cause of deforestation and decrease in vegetation fraction is likely grazing. Grazing pressure has been noted in shrub distributions (Miller and Morris 1988, Pickering and Patzelt 2008), as we noted earlier, and previous research has shown that herd size has increased and grazing practices intensified since the 1970's (Janzen 1986, 2000).

The effects of over-grazing are known to cause desertification given the right climate conditions, such as decreasing or variable precipitation. Recent climate analyses of Dhofar have shown that temperatures are significantly increasing and precipitation is decreasing (not significant; Kwarteng et al. 2009; Alsarmi and Washington 2012). The IOM also appears to have changed, though the effects of this change are variable and only well understood over the Indian subcontinent (Kumar et al. 2011; Krishnan et al. 2013; Krishnaswamy et al. 2014). In Dhofar, the IOM manifests primarily as fog that blankets the southern facing watershed divide and coastal plain, a mist not registered adequately in the local records. We can surmise, however, that the margins of the cloud

forest adjacent to the desert may be vulnerable to any variability in the monsoon cloud cover. Based on the LISA analysis (Figure 4.4), distinct clusters of decreased vegetation fraction occurred along these margins. If continued warming of the atmosphere leads to increased variability or decreased stability of the monsoon, then increased pressure from grazing could lead to further degradation in the future. The clusters of low-low vegetation fractions (Figure 4.4) are hotspots of potential desertification, and will thus need to be monitored over the long term.

The time series analysis demonstrates that the most consistent decreases in the mean annual NDVI trend (Amplitude 0) occurred near Salalah, especially in the adjacent foothills of the Dhofar Mountains. The foothills benefit from the monsoon clouds and have a diverse collection of woody plants—a vital part of the cloud forest ecosystem. They are also home to a diverse array of trees and shrubs. One species in particular, *Boscia Arabica,* is threatened (Pickering and Patzelt 2008). The significant decreases in the mean annual NDVI trend (Amplitude 0) and the peak NDVI trend (Amplitude 1) around Salalah, apparently in its zones of expansion, suggests that pressure placed on foothills has resulted in significant decreases in vegetation health. This decrease in the NDVI trend coincides with the expansion of Salalah and neighboring suburbs and towns.

Three phenomena might help explain why the expansion of Salalah and the vegetation health of the foothills and surrounding areas are so intertwined. First, demand for respite during the hot Arabian summer has led to tourists flooding into the region during the monsoon season. These tourists come from all parts of the Arabian Peninsula and speculation suggests that Oman will continue to grow its tourism sector with even more tourists expected in the future (Lefebvre 2010). The foothills, with their close

proximity to Salalah, are popular tourist attractions, which leaves them vulnerable to increasing human presence and infrastructure development. Another possible factor is the relocation of summer herding camps. During the summer monsoon season, camel herds are brought from the mountains to live on the coastal plains around Salalah until the heavy fog and mud brought on by the monsoon clears (Janzen 1986). As Salalah expands, these temporary encampments are pushed further to the margins of the city and closer to the foothills, which increase vehicle traffic and grazing in these areas (Janzen 2000). Finally, increased demand for housing in and around Salalah has led to the development of new urban and suburban areas that perpetuate the pressures on the environment.

4.6.2 National Policies and Land Change in Dhofar

Since various proximate human activities, foremost changes in herding practices, seem to be the primary mechanism changing the land covers of the cloud forest, attention to factors that precipitated changes in the activities is warranted. The evidence points to policies generated by the Omani government as a response to the Dhofar War of 1970 to 1975, an uprising by Yemini backed rebels against the Sultan of Oman's armed forces and British Special Forces. These policies aimed to improve the livelihoods of the rural poor in the area, but had as an unforeseen consequence, in some cases, of increasing heard size and grazing intensity in Dhofar.

A policy designed to provide easier access to water for herds was, perhaps, the most proximate cause to changes herding practices and land cover. The government constructed 160 wells in the region, not only improving access to water but eliminating the need for lengthy excursions elsewhere to obtain it, thus concentrating herds for

intensive grazing. Another important policy created a paid militia system, or *firqat*, providing an important supplementary income used by herders to help maintain and grow their herds, especially regarding the purchase of fodder required during the winter vegetation senesce. Fodder has been at various times subsidized, but families usually pay a non-trivial amount of money each year for fodder. As herd sizes increase, more fodder must be purchased, which can put considerable pressure on a family's monthly budget (Janzen 2000). The *firqat* system is maintained today in part to help the local economy in general (Peterson 2004a), but it has also become an important part of herd maintenance. Finally, veterinary services were introduced during the Dhofar War and have subsequently been expanded. Before 1970, there were no such services available in Dhofar. Livestock diseases often led to fatalities or diminished animal lifespan, which served as an important check on livestock population. Begun by the British Special Forces (Hughes 2009; for a popular account see Higgins 2011) during the war and continued by the Omani government since, herders across the cloud forest today vaccinate their herds or have them medically treated when needed. By the 1980's, the population of cattle, camel, and goats had tripled since the end of the war, and are thought to have increased even more since then (Janzen 2000).

Changes to land tenure may also have played a role in land changes. Traditionally, pasture lands across Dhofar were grazed only in areas that were considered a part of a tribal boundary (Janzen 1986). New rules were developed for the entirety of the country that decreed all land under the ownership of the Omani national government (Janzen 2000 citing Omani Royal Decree 5/80, 3/83, and 81/84). According to Janzen (2000), there were two important outcomes of the nationalized land tenure decrees. First,

camel breeders, who formerly stayed on the fringes of the cloud forest, began to graze their herds on lands that traditionally belonged to cattle herders; they cited the nationalized land tenure policy as a rationale for this action. As part of these land tenure nationalization decrees, the government constructed buildings, schools, and mosques throughout the cloud forest. This development encouraged the formerly nomadic population to settle in one place in order to take advantage of the new benefits. As a result, grazing became more intensive and the traditional transhumance practice is undertaken mainly by camel herders.

Infrastructure development was a key factor of land change in Dhofar, particularly around the City of Salalah. The region received about 40% of government expenditures between 1988 and 2013, much of it for infrastructure development and related projects, despite only having about 10-25% of the population (Peterson 2004b). More than 4% of the total study area was converted to urban use around Salalah and other parts of the coastal plain, and a deep water port was built just outside of Salalah, as well as a paved road from Salalah to Jabal Qamar (Calvin and Rigsbee 2000). Road development in the cloud forest led to transitions from grass, shrub, and forest covers to road covers. Beginning in the 1990's, existing roads were improved and new roads were constructed between the coastal plain and the mountains. The new roads are intended to provide quicker access to the cloud forest or services in Salalah for those living in the mountains.

4.6.3 Land Change Mitigation Factors

While there have been notable changes to the environment of the cloud forest, common wisdom suggests there has been much more. Part of the reason may reside in

Oman's import of key food staples and the subsequent impact on local cultivation. In the past, cultivation was more widespread in the cloud forest, possibly as late as the 1970's (Janzen 1986). At some point after the 1970's, cultivation was reduced primarily to small frankincense plots, walled areas for hay production, or reforestation plots. With Oman's oil boom in the late 1960's, there has been little need to expand cultivation for staple crops and may have led to a reduction in cropped land as the country imported most of these foods. Our results suggest little change in cropped land. Dhofar has a strong tradition of herding rather than farming, and, the critical staples of the Omani diet, like rice, are increasingly imported rather than grown locally. Imports of rice into Oman during 2012 totaled about $174 million (OEC 2015).

4.7 Conclusion

The Dhofar cloud forest and coastal plains have witnessed land changes over the 25-year period of this study. These changes have been more complex than local, commonly expressed views of them entail. Systematic transitions have occurred between several types of land cover in the cloud forest, primarily tree cover to shrub cover, shrub cover to grass cover, and grass cover to road cover; while the coastal plains were systematically transitioning to road cover and the built environment. Vegetation fractions showed significant clusters of decreasing woody plant cover along the cloud forest margins and various parts of the coastal plain, and NDVI trend analysis indicates decreasing NDVI around the city of Salalah since 2001. These changes would appear to be linked primarily to changes in herding practices and road and peri-urban development, most of which are linked directly to changes in government policies directed to

developing the southern part of Oman. Whether these policies have led to a path dependent outcome—land-cover trends that are difficult to reverse or alter—remains an open question.

4.8 Acknowledgements

Support for this research was provided in part by a Fulbright grant to Oman funded by the U.S. Department of State and sponsored by the Office of the Advisor to His Majesty The Sultan for Economic Planning Affairs. Special thanks to Dr. Said Al-Saqri for support during the Fulbright grant period.

4.9 References

Alo, C. A., and R. G. Pontius Jr (2008), Identifying systematic land-cover transitions using remote sensing and GIS: the fate of forests inside and outside protected areas of Southwestern Ghana, *Environ. Plan. B Plan. Des.*, *35*(2), 280–295, doi:10.1068/b32091.

AlSarmi, S., and R. Washington (2011), Recent observed climate change over the Arabian Peninsula, *J. Geophys. Res.*, *116*(D11), D11109, doi:10.1029/2010JD015459.

Anadón, J. D., O. E. Sala, B. L. Turner II, and E. M. Bennett (2014), Effect of woody-plant encroachment on livestock production in North and South America, *Proc. Natl. Acad. Sci. U. S. A.*, *111*(35), 12948–12953, doi:10.1073/pnas.1320585111.

Anderson, D. M., J. T. Overpeck, and A. K. Gupta (2002), Increase in the Asian southwest monsoon during the past four centuries., *Science*, *297*(5581), 596–9, doi:10.1126/science.1072881.

Anselin, L. (1995), Local Indicators of Spatial Association, *Geogr. Anal.*, *27*(2), 93–115.

Asner, G. P., A. J. Elmore, L. P. Olander, R. E. Martin, and a. T. Harris (2004), Grazing Systems, Ecosystem Responses, and Global Change, *Annu. Rev. Environ. Resour.*, *29*(1), 261–299, doi:10.1146/annurev.energy.29.062403.102142.

Bai, Z. G., D. L. Dent, L. Olsson, and M. E. Schaepman (2008), Proxy global assessment of land degradation, *Soil Use Manag.*, *24*(3), 223–234, doi:10.1111/j.1475-2743.2008.00169.x.

Blaschke, T. (2010), Object based image analysis for remote sensing, *ISPRS J. Photogramm. Remote Sens.*, *65*(1), 2–16, doi:10.1016/j.isprsjprs.2009.06.004.

Boardman, J. W., F. A. Kruse, and R. O. Green (1995), Mapping target signatures via partial unmixing of AVIRIS data, in *Summaries of JPL Airborne Earth Science Workshop, JPL Publication 95-1*, pp. 23–26, Pasadena, CA.

Brannstrom, C., and J. M. Vadjunec (2014), *Land change science, political ecology and sustainability: synergies and divergences*, edited by C. Brannstrom and J. M. Vadjunec, Routledge.

Charabi, Y., and S. A. Abdul-Wahab (2009), Synoptic aspects of the summer monsoon of southern Oman and its global teleconnections, *J. Geophys. Res. Atmos.*, *114*(7), 1–9, doi:10.1029/2008JD010234.

Dawelbait, M., and F. Morari (2012), Monitoring desertification in a Savannah region in Sudan using Landsat images and spectral mixture analysis, *J. Arid Environ.*, *80*, 45–55, doi:10.1016/j.jaridenv.2011.12.011.

Defries, R. S., T. Rudel, M. Uriarte, and M. Hansen (2010), Deforestation driven by urban population growth and agricultural trade in the twenty-first century, *Nat. Geosci.*, *3*(3), 178–181, doi:10.1038/ngeo756.

Dennison, P. E., and D. A. Roberts (2003), Endmember selection for multiple endmember spectral mixture analysis using endmember average RMSE, *Remote Sens. Environ.*, *87*(2-3), 123–135, doi:10.1016/S0034-4257(03)00135-4.

Donohue, R. J., M. L. Roderick, T. R. McVicar, and G. D. Farquhar (2013), Impact of CO2 fertilization on maximum foliage cover across the globe's warm, arid environments, *Geophys. Res. Lett.*, *40*(12), 3031–3035, doi:10.1002/grl.50563.

Eastman, J. R., F. Sangermano, B. Ghimire, H. Zhu, H. Chen, N. Neeti, Y. Cai, E. a. Machado, and S. C. Crema (2009), Seasonal trend analysis of image time series, *Int. J. Remote Sens.*, *30*(10), 2721–2726, doi:10.1080/01431160902755338.

Eastman, J. R., F. Sangermano, E. a. Machado, J. Rogan, and A. Anyamba (2013), Global trends in seasonality of Normalized Difference Vegetation Index (NDVI), 1982-2011, *Remote Sens.*, *5*(10), 4799–4818, doi:10.3390/rs5104799.

Eldridge, D. J., M. a. Bowker, F. T. Maestre, E. Roger, J. F. Reynolds, and W. G. Whitford (2011), Impacts of shrub encroachment on ecosystem structure and

functioning: Towards a global synthesis, *Ecol. Lett.*, *14*(7), 709–722, doi:10.1111/j.1461-0248.2011.01630.x.

Geist, H. J., and E. F. Lambin (2002), Proximate Causes and Underlying Driving Forces of Tropical Deforestation, *Bioscience*, *52*(2), 143–150.

Ghazanfar, S. (1998), Status of the flora and plant conservation in the sultanate of Oman, *Biol. Conserv.*, *85*(5), 1167–1179.

Gupta, A. K., D. M. Anderson, and J. T. Overpeck (2003), Abrupt changes in the Asian southwest monsoon during the Holocene and their links to the North Atlantic Ocean, *Nature*, *421*(6921), 354–7, doi:10.1038/nature01340.

Higgins, A. (2011), *With the S.A.S and Other Animals: A Vet's Experiences During the Dhofar War 1974*, Pen and Sword Books Ltd, Barnsley, UK.

Higuera, D., B. Martín-López, and A. Sánchez-Jabba (2013), Social preferences towards ecosystem services provided by cloud forests in the neotropics: Implications for conservation strategies, *Reg. Environ. Chang.*, *13*(4), 861–872, doi:10.1007/s10113-012-0379-1.

Hildebrandt, A. (2005), Ecohydrology of a Seasonal Cloud Forest in Dhofar, PhD. Dissertation, Massachusetts Institute of Technology.

Hildebrandt, A., and E. A. B. Eltahir (2006), Forest on the edge: Seasonal cloud forest in Oman creates its own ecological niche, *Geophys. Res. Lett.*, *33*(11), 2–5, doi:10.1029/2006GL026022.

Hildebrandt, A., and E. a. B. Eltahir (2007), Ecohydrology of a seasonal cloud forest in Dhofar: 2. Role of clouds, soil type, and rooting depth in tree-grass competition, *Water Resour. Res.*, *43*(11), n/a–n/a, doi:10.1029/2006WR005262.

Hilker, T., E. Natsagdorj, R. H. Waring, A. Lyapustin, and Y. Wang (2014), Satellite observed widespread decline in Mongolian grasslands largely due to overgrazing, *Glob. Chang. Biol.*, *20*(2), 418–28.

Hughes, G. (2009), A "Model Campaign" Reappraised: The Counter-Insurgency War in Dhofar, Oman, 1965–1975, *J. Strateg. Stud.*, *32*(2), 271–305, doi:10.1080/01402390902743357.

Janzen, J. (1986), *Nomads in the sultanate of Oman: tradition and development in Dhofar*, Westview Press, Boulder.

Janzen, J. (2000), The destruction of resources among the mountain nomads of Dhofar, in *The Transformation of Nomadic Society in the Arab East*, edited by M. Mundy and B. Musallam, pp. 160–175, Cambridge University Press, Cambridge, UK.

De Jong, R., J. Verbesselt, M. E. Schaepman, and S. de Bruin (2012), Trend changes in global greening and browning: Contribution of short-term trends to longer-term change, *Glob. Chang. Biol.*, *18*(2), 642–655, doi:10.1111/j.1365-2486.2011.02578.x.

De Jong, R., J. Verbesselt, A. Zeileis, and M. E. Schaepman (2013), Shifts in global vegetation activity trends, *Remote Sens.*, *5*(3), 1117–1133, doi:10.3390/rs5031117.

Krishnan, R., T. P. Sabin, D. C. Ayantika, a. Kitoh, M. Sugi, H. Murakami, a. G. Turner, J. M. Slingo, and K. Rajendran (2013), Will the South Asian monsoon overturning circulation stabilize any further?, *Clim. Dyn.*, *40*(1-2), 187–211, doi:10.1007/s00382-012-1317-0.

Krishnaswamy, J., S. Vaidyanathan, B. Rajagopalan, M. Bonell, M. Sankaran, R. S. Bhalla, and S. Badiger (2014), Non-stationary and non-linear influence of ENSO and Indian Ocean Dipole on the variability of Indian monsoon rainfall and extreme rain events, *Clim. Dyn.*, doi:10.1007/s00382-014-2288-0.

Kumar, K. K., B. Rajagopalan, M. Hoerling, G. Bates, and M. Cane (2006), Unraveling the mystery of Indian monsoon failure during El Niño, *Science*, *314*(5796), 115–119.

Kumar, K. K., K. Kamala, B. Rajagopalan, M. P. Hoerling, J. K. Eischeid, S. K. Patwardhan, G. Srinivasan, B. N. Goswami, and R. Nemani (2011), The once and future pulse of Indian monsoonal climate, *Clim. Dyn.*, *36*(11-12), 2159–2170, doi:10.1007/s00382-010-0974-0.

Kwarteng, A. Y., S. Dorvlo, and G. T. V. Kumar (2009), Analysis of a 27-year rainfall data (1977 – 2003) in the Sultanate of Oman, *Int. J. Climatol.*, *617*(July 2008), 605–617, doi:10.1002/joc.

Lambin, E. F., B. L. Turner, H. J. Geist, S. B. Agbola, A. Angelsen, J. Bruce, O. Coomes, R. Dirzo, G. Fischer, and C. Folke (2001), The causes of land-use and land-cover change: moving beyond the myths, *Glob. Environ. Chang.*, *11*(4), 261–269, doi:10.1016/S0959-3780(01)00007-3.

Lambin, E. F., H. J. Geist, and E. Lepers (2003), Dynamics of Land-Use and Land-Cover Change in Tropical Regions, *Annu. Rev. Environ. Resour.*, *28*(1), 205–241.

Lefebvre, J. A. (2010), Oman's Foreign Policy in the Twenty-First Century, *Middle East Policy*, *17*(1), 99–114.

Li, S., P. H. Verburg, L. Shihai, J. Wu, and X. Li (2012), Spatial analysis of the driving factors of grassland degradation under conditions of climate change and intensive use in Inner Mongolia, China, *Reg. Environ. Chang.*, *12*(3), 461–474, doi:10.1007/s10113-011-0264-3.

Liu, J. et al. (2013), Framing Sustainability in a Telecoupled World, *Ecol. Soc.*, *18*(2), 26, doi:10.5751/ES-05873-180226.

Masek, J. G., E. F. Vermote, N. E. Saleous, R. Wolfe, F. G. Hall, K. F. Huemmrich, F. Gao, J. Kutler, and T. Lim (2006), A Landsat Surface Reflectance Dataset for North America, 1990-2000, *IEEE Geosci. Remote Sens. Lett.*, *3*(1), 68–72, doi:10.1109/LGRS.2005.857030.

Miller, A. G., and M. Morris (1988), *Plants of Dhofar, the southern region of Oman, traditional, economic and medicinal uses*, Office of the Adviser for Conservation of the Environment, Diwan of Royal Court, Sultanate of Oman.

O'Reilly, M. J. (1998), Omanibalancing: Oman Confronts an Uncertain Future, *Middle East J.*, *52*(1), 70–84.

OEC (2015), Observatory of Economic Complexity, Available from: https://atlas.media.mit.edu/en/ (Accessed 1 May 2015)

Patzelt, A. (2011), The Themeda Quadrivalvis Tall-Grass Savannah of Oman At the Crossroad Between Africa and Asia, *Edinburgh J. Bot.*, *68*(02), 301–319, doi:10.1017/S0960428611000217.

Peterson, J. E. (2004a), Oman: Three and a Half Decades Of Change and Development, *Middle East Policy*, *XI*(2), 125–137.

Peterson, J. E. (2004b), Oman's Diverse Society : Southern Oman, *Middle East J.*, *58*(1), 31–51.

Peterson, J. E. (2011), Oman Faces the Twenty-First Century, in *Political Change in the Arab Gulf States: Stuck in Transition*, edited by M. A. Tétreault, G. Okruhlik, and A. Kapiszewski, pp. 99–118, Lynne Rienner Publishers, Boulder.

Pickering, H. A., and A. Patzelt (2008), *Field Guide to the Wild Plants of Oman*, Kew Publishing, Richmond, UK.

Pontius, R. G., E. Shusas, and M. McEachern (2004), Detecting important categorical land changes while accounting for persistence, *Agric. Ecosyst. Environ.*, *101*(2-3), 251–268, doi:10.1016/j.agee.2003.09.008.

Powell, R. L., and D. A. Roberts (2010), Characterizing Urban Land-Cover Change in Rondônia, Brazil: 1985 to 2000, *J. Lat. Am. Geogr.*

Roberts, D., M. Gardner, R. Church, S. Ustin, G. Scheer, and R. Green (1998), Mapping Chaparral in the Santa Monica Mountains Using Multiple Endmember Spectral Mixture Models, *Remote Sens. Environ.*, *65*(3), 267–279, doi:10.1016/S0034-4257(98)00037-6.

Scholte, P., and P. De Geest (2010), The climate of Socotra Island (Yemen): A first-time assessment of the timing of the monsoon wind reversal and its influence on precipitation and vegetation patterns, *J. Arid Environ.*, *74*(11), 1507–1515, doi:10.1016/j.jaridenv.2010.05.017.

Sen, P. K. (1968), Estimates of the regression coefficient based on Kendall's tau, *J. Am. Stat. Assoc.*, *63*, 1379–1389.

Serneels, S., and E. F. Lambin (2001), Proximate causes of land-use change in Narok District, Kenya: a spatial statistical model, *Agric. Ecosyst. Environ.*, *85*(1-3), 65–81, doi:10.1016/S0167-8809(01)00188-8.

Seto, K. C., and A. Reenberg (2014), *Rethinking global land use in an urban era*, edited by K. C. Seto and A. Reenberg, MIT Press, Cambridge.

Settle, J. J., and N. A. Drake (1993), Linear mixing and the estimation of ground cover proportions, *Int. J. Remote Sens.*, *14*(6), 1159–1177.

Theil, H. (1950), A rank-invariant method of linear and polynomial regression analysis, I, II, III, *Proc. K. Ned. Acad. van Wet.*, *53*(386), 386–392, 512–525, 1397–1412.

Turner II, B. L., E. F. Lambin, and A. Reenberg (2007), Land Change Science Special Feature: The emergence of land change science for global environmental change and sustainability, *Proc. Natl. Acad. Sci. U. S. A.*, *104*(52), 20666–20671, doi:10.1073/pnas.0704119104.

UNEP (1994), *United Nations Convention to Combat Desertification in those Countries Experiencing Serious Drought and/or Desertification, Particularly in Africa*.

USGS (2015), *Product Guide: Landsat 4-7 Climate Data Record (CDR) Surface Reflectance v. 5.8*.

Vayda, A. P., and B. B. Walters (1999), Against political ecology, *Hum. Ecol.*, *27*(1), 167–179, doi:10.1023/A:1018713502547.

CHAPTER 5

CONCLUSIONS

5.1 Summary and Key Findings

Chapters 2, 3, and 4 provide the first systematic treatment of vegetation patterns and changes in the Dhofar cloud forest, linking various potential drivers to the changes observed. The results show that an answer to the question "what drives environmental change in Dhofar's cloud forest" is not easy to ascertain. It has long been thought that the environment in Dhofar is under stress from human and climatic influences. The studies presented in this dissertation attempt to unfurl the role of both influence and shed light on biodiversity across the cloud forest.

Chapter 2 was a study of ISM dynamics and its effects on NDVI time series for the cloud forest in Dhofar. The findings of this chapter provide compelling evidence that, while the timing and severity of the monsoon is variable, the cloud forest vegetation is rather robust to these variations, showing only weak to moderate correlations with June precipitation, and the area under the curve (AUC) of monsoon maximum daily temperatures. One factor proposed to maintain a strong influence, length of the monsoon, did not show any meaningful relationship to vegetation dynamics. The strongest driver of vegetation dynamics was SST in the Arabian Sea. Based on a linear time series model, SST is about six to nine months out of phase with NDVI measurements in the cloud forest. Previous research has shown that the presence of cloud cover is a key determinant in lowering evapotranspiration and providing precipitation that is not accurately measured by rain gauges or in climate station archives (Hildebrandt 2005; Hildebrandt

and Eltahir 2006; Hildebrandt et al. 2007; Hildebrandt and Eltahir 2007). Chapter 2 confirms the importance of cloud cover, both in determining the timing of the ISM and the importance it plays in shielding the vegetation from monsoon variation. While there is no evidence that climate changes have affected the cloud forest vegetation, a potential vulnerability exists: any destabilization of the upwelling that leads to cloud formation over southern Arabia could cause problems for the cloud forest.

Chapter 3 describes the vegetation diversity of the Dhofar cloud forest, and reconciles three possible mechanisms of biodiversity: (H1) neutral processes, (H2) biological interactions, and (H3) environmental gradients. Th biological interactions hypothesis has the most support in terms of explaining biodiversity. A cluster analysis showed two dominant groups of tree and shrub species in the cloud forest. A further analysis of species abundances shows that *A. dhofarica* and *Commiphora* spp. make-up almost 50% of the overall relative abundances in forested areas, and *C. procera*, *Commiphora* spp., and *S. incanum* make-up about 42% of relative species abundances in grassland areas. Species abundances (especially *A. dhofarica* and *Commiphora* spp.) suggest that the biogeographical history has played a role in today's biodiversity patterns in the forested areas. The cloud forest is a remnant of an ancient forest that developed during the Tertiary, and was thought to spread across the modern pan-Indian ocean region. Today, the endemic and non-endemic species that comprise the cloud forest show strong affinities with plant communities in Africa and India. The fact that these same species dominate the cloud forest's biodiversity patterns suggests that the Dhofar Mountains are an important refuge, and will be so for a long time to come. The grasslands show signs of human influence; the proliferation of *C. procera* and *S. incanum*

are a testament to the prevalence of livestock. These two species are known to be poisonous to livestock and thrive in areas where grazing is common, suggesting that human activities play a strong role in shaping biodiversity patterns as well.

Using a variety of methods to understand the extent of human influence on the environment, Chapter 4 shows that the Dhofar War has a strong legacy in transforming land use and thus land cover of the cloud forest and coastal region. The link between the Dhofar War and the environment is strongest in certain policies. Foremost among these are investments made in Dhofar's infrastructure and several policies put in place to improve the well-being of local inhabitants. The decision to invest heavily in Dhofar was a necessary compromise to end the war and cement the union between Dhofar and the rest of Oman. These policies helped to increase herd size, which eventually led to overgrazing and about 23,000 ha of deforestation. The infrastructure investments led to an additional 124 km^2 of buildings and roads added to the city of Salalah between 1988 and 2013. The impact of these new roads and urban development has been widespread and signs of stress to the coastal land cover are commonplace, particularly in the 21st century. Dhofar is now an example of the trade-off between human well-being and environmental degradation.

5.2 Reconciling the Role of Humans and Climate as Agents of Change

What role does climate and human impacts have on changing the cloud forest? The answer to this question appears clearer based on the finding from Chapters 2, 3, and 4. While the monsoon varies from year to year, the strongest evidence for the cause of environmental change points toward human activities. The evidence from a land change

model between 1988 and 2013, plus the MESMA and NDVI time series analyses point to one conclusion: humans are actively transforming the environment in Dhofar. While others have predicted the role of humans as an agent of change within Dhofar's cloud forest (Janzen 1986), the results in this dissertation provide the first quantitative evidence for this to date.

Understanding the role of humans in transforming the environment in Dhofar would not have been possible without a thorough examination of the climate. Global change research encompasses many different fields of inquiry. As researchers bring specialized knowledge to bear on environmental change problems, it is critical that the various threads of change be delineated and defined. Climate change has already transformed the Earth system, and will continue to do so for some time to come. Human activities have also transformed the Earth system through such activities as deforestation, land degradation, and urbanization. As this dissertation has demonstrated, claims about the cause of change require a thorough examination to decipher the actual role of climate and human modification.

Common wisdom in Dhofar suggests that the monsoon was changing and with it the environment. Common wisdom also suggests that grazing and development caused deforestation and land degradation. Before either of these claims could be examined in detail, it was necessary to reconcile each with a dedicated study. While Chapters 2, 3, and 4 show that human activity is largely responsible for the land cover changes identified. Perhaps over the longer-haul, global warming will affect the deep ocean layers of water and thus the circulation that drives the monsoon. For now, however, this change has a human imprint.

Framing questions of environmental change to incorporate the range of possible drivers and feedbacks requires both a global and local perspective (Harden 2012). Systemic changes to the Earth system can have local effects (i.e., climate changes), and local environmental changes (i.e., land use and covers) can accumulate and work as an aggregate force of change to the Earth system (Turner et al. 1990). This study sought to navigate between the systemic and cumulative attributes of environmental change, seeking which has had the most impact of the Dhofar cloud forest, within insights that may prove useful for other monsoon driven cloud forests in arid lands.

5.3 Contributions to Scientific Knowledge

This dissertation offers three broad contributions to research and outreach. First, it contributes to the efforts of land system science to monitor and understand land-cover changes, especially of sensitive ecosystems (Turner et al. 2007). In this case, this study demonstrates how to employ multiple platforms and sensors to detect and understand changes and the role of climate variability on vegetation dynamics. Second, it provides foundational data of interest to local decision makers and environmental-sustainability organizations interested in the preservation of the Dhofar cloud forest and the environmental services it provides. Lastly, this research offers perspectives on biodiversity and broader forces of land-cover change.

Most research on the ISM is studied through the lens of the Indian subcontinent. There have been few studies that address the ISM over southern Arabia, and fewer still that address the relationship between the monsoon and the cloud forest. Chapter 2 is the first study of its kind to attempt to develop a model of the timing of the monsoon over the

Arabian Peninsula. This chapter also develops a time series model of monsoon and vegetation dynamics. Cloud forests have been shown to be important centers of endemism and biodiversity. Chapter 2 contributes to knowledge about cloud forests by showing that they are robust to most climate fluctuations, with the exception of cloud cover and fog moisture. As such, the study of cloud forests and climate change should focus on how climate changes may affect the mechanisms of cloud formation and how this can be affected by future climate changes.

The analysis of cloud forest trees and shrubs in Chapter 3 offers interesting findings on how biological interactions can lead to dominance by a few species in cloud forest biodiversity. Perhaps what is most intriguing about this study is that both forests and grasslands show dominance by a small group of species, but possibly for different reasons. The study suggests that humans drive biodiversity patterns in the grasslands, while biogeographical history drives diversity in the forested areas. Few, if any studies, have suggested such when looking at a cohesive ecosystem.

Finally, the three models developed to study land change in Dhofar show how multiple methods can be combined to study how humans are altering landscapes. Commonly, land change is studied through the lens of a single model. But as Chapter 4 demonstrates, a subpixel analysis (MESMA), a land change model (the transition model), and time series analysis can be combined to study the way various aspects of an environment are changing. This study also details how national policies following the Dhofar War in the 1970's influence development patterns, and ultimately land change. Thus, it joins others in indicating how "distal" drivers operate on land use and thus land cover. Specifically, this study hints that there will be significant difficulties implementing

policies to mitigate overgrazing and deforestation in the Dhofar cloud forest because the very policies that increase human well-being have led to environmental degradation.

REFERENCES

Abdul-Wahab, S. A., H. Al-Hinai, K. A. Al-Najar, and M. S. Al-Kalbani (2007), Fog Water Harvesting: Quality of Fog Water Collected for Domestic and Agricultural Use, *Environ. Eng. Sci.*, *24*(4), 446–456, doi:10.1089/ees.2006.06-0066.

Allan, R., D. Chambers, W. Drosdowsky, H. Hendon, M. Latif, N. Nicholls, I. Smith, R. Stone, and Y. Tourre (2001), Is there an Indian Ocean dipole, and is it independent of the El Niño - Southern Oscillation?, *Clivar Exch.*, *6*(3), 18–22.

Alo, C. A., and R. G. Pontius Jr (2008), Identifying systematic land-cover transitions using remote sensing and GIS: the fate of forests inside and outside protected areas of Southwestern Ghana, *Environ. Plan. B Plan. Des.*, *35*(2), 280–295, doi:10.1068/b32091.

AlSarmi, S., and R. Washington (2011), Recent observed climate change over the Arabian Peninsula, *J. Geophys. Res.*, *116*(D11), D11109, doi:10.1029/2010JD015459.

Anadón, J. D., O. E. Sala, B. L. Turner II, and E. M. Bennett (2014), Effect of woody-plant encroachment on livestock production in North and South America, *Proc. Natl. Acad. Sci. U. S. A.*, *111*(35), 12948–12953, doi:10.1073/pnas.1320585111.

Anderson, D. M., J. T. Overpeck, and A. K. Gupta (2002), Increase in the Asian southwest monsoon during the past four centuries, *Science*, *297*(5581), 596–599.

Anselin, L. (1995), Local Indicators of Spatial Association, *Geogr. Anal.*, *27*(2), 93–115.

Anyamba, A., C. J. Tucker, and J. R. Eastman (2001), NDVI anomaly patterns over Africa during the 1997 / 98 ENSO warm event, *Intern. J. Remote Sens.*, *22*(10), 1847–1859.

Archer, E. (2004), Beyond the "climate versus grazing" impasse: using remote sensing to investigate the effects of grazing system choice on vegetation cover in the eastern Karoo, *J. Arid Environ.*, *57*(3), 381–408, doi:10.1016/S0140-1963(03)00107-1.

Ashok, K., Z. Guan, and T. Yamagata (2001), Impact of the Indian Ocean Dipole on the Relationship between the Indian Monsoon Rainfall and ENSO, *Geophys. Res. Lett.*, *28*(23), 4499–4502, doi:10.1029/2001GL013294.

Ashok, K., Z. Guan, N. H. Sagi, and T. Yagamata (2004), Individual and Combined influences of ENSO and the\rIndian Ocean Dipole on the Indian Summer Monsoon, *J. Clim.*, *17*(16), 3141–3155, doi:10.1175/1520-0442(2004)017<3141:IACIOE>2.0.CO;2.

Asner, G. P., A. J. Elmore, L. P. Olander, R. E. Martin, and a. T. Harris (2004), Grazing Systems, Ecosystem Responses, and Global Change, *Annu. Rev. Environ. Resour.*, *29*(1), 261–299, doi:10.1146/annurev.energy.29.062403.102142.

Bai, Z. G., D. L. Dent, L. Olsson, and M. E. Schaepman (2008), Proxy global assessment of land degradation, *Soil Use Manag.*, *24*(3), 223–234, doi:10.1111/j.1475-2743.2008.00169.x.

Berhane, A., Ø. Totland, M. Haile, and S. R. Moe (2015), Intense use of woody plants in a semiarid environment of Northern Ethiopia: Effects on species composition, richness and diversity, *J. Arid Environ.*, *114*, 14–21, doi:10.1016/j.jaridenv.2014.11.001.

De Beurs, K. M., and G. M. Henebry (2010), Spatio-Temporal Statistical Methods for Modelling Land Surface Phenology, in *Phenological Research*, edited by I. L. Hudson and M. R. Keatley, pp. 177–208, Springer Netherlands.

Blaschke, T. (2010), Object based image analysis for remote sensing, *ISPRS J. Photogramm. Remote Sens.*, *65*(1), 2–16, doi:10.1016/j.isprsjprs.2009.06.004.

Blechschmidt, I., A. Matter, F. Preusser, and D. Rieke-Zapp (2009), Monsoon triggered formation of Quaternary alluvial megafans in the interior of Oman, *Geomorphology*, *110*(3-4), 128–139, doi:10.1016/j.geomorph.2009.04.002.

Boardman, J. W., F. A. Kruse, and R. O. Green (1995), Mapping target signatures via partial unmixing of AVIRIS data, in *Summaries of JPL Airborne Earth Science Workshop, JPL Publication 95-1*, pp. 23–26, Pasadena, CA.

Borcard, D., and P. Legendre (2012), Is the Mantel correlogram powerful enough to be useful in ecological analysis? A simulation study, *Ecology*, *93*(6), 1473–1481, doi:10.1890/11-1737.1.

Borcard, D., F. Gillet, and P. Legendre (2011), *Numerical Ecology with R*, Springer, New York.

Brannstrom, C., and J. M. Vadjunec (2014), *Land change science, political ecology and sustainability: synergies and divergences*, edited by C. Brannstrom and J. M. Vadjunec, Routledge.

Burns, S. J., D. Fleitmann, A. Matter, U. Neff, and A. Mangini (2001), Speleothem evidence from Oman for continental pluvial events during interglacial periods, *Geology*, *29*(7), 623, doi:10.1130/0091-7613(2001)029<0623:SEFOFC>2.0.CO;2.

Charabi, Y. (2009), Arabian summer monsoon variability: Teleconexion to ENSO and IOD, *Atmos. Res.*, *91*(1), 105–117, doi:10.1016/j.atmosres.2008.07.006.

Charabi, Y., and S. A. Abdul-Wahab (2009), Synoptic aspects of the summer monsoon of southern Oman and its global teleconnections, *J. Geophys. Res. Atmos.*, *114*(7), 1–9, doi:10.1029/2008JD010234.

Chisholm, R. A., and S. W. Pacala (2010), Niche and neutral models predict asymptotically equivalent species abundance distributions in high-diversity ecological communities., *Proc. Natl. Acad. Sci. U. S. A.*, *107*(36), 15821–5, doi:10.1073/pnas.1009387107.

Condit, R. et al. (2002), Beta-diversity in tropical forest trees, *Science*, *295*(5555), 666–9, doi:10.1126/science.1066854.

Cook, B. I., R. L. Miller, and R. Seager (2009), Amplification of the North American "Dust Bowl" drought through human-induced land degradation, *Proc. Natl. Acad. Sci. U. S. A.*, *106*(13), 4997–5001, doi:10.1073/pnas.0810200106.

Cook, E. R., D. M. Meko, D. W. Stahle, and M. K. Cleaveland (1999), Drought Reconstructions for the Continental United States, *J. Clim.*, *12*, 1145–1163.

Cremaschi, M., and F. Negrino (2005), Evidence for an abrupt climatic change at 8700 14C yr B.P. in rockshelters and caves of Gebel Qara (Dhofar-Oman): Palaeoenvironmental implications, *Geoarchaeology*, *20*(6), 559–579, doi:10.1002/gea.20068.

Dauby, G., O. J. Hardy, M. Leal, F. Breteler, and T. Stévart (2014), Drivers of tree diversity in tropical rain forests: new insights from a comparison between littoral and hilly landscapes of Central Africa, edited by P. Linder, *J. Biogeogr.*, *41*(3), 574–586, doi:10.1111/jbi.12233.

Dawelbait, M., and F. Morari (2012), Monitoring desertification in a Savannah region in Sudan using Landsat images and spectral mixture analysis, *J. Arid Environ.*, *80*, 45–55, doi:10.1016/j.jaridenv.2011.12.011.

DeFries, R., and D. Pandey (2010), Urbanization, the energy ladder and forest transitions in India's emerging economy, *Land use policy*, *27*(2), 130–138, doi:10.1016/j.landusepol.2009.07.003.

Defries, R. S., T. Rudel, M. Uriarte, and M. Hansen (2010), Deforestation driven by urban population growth and agricultural trade in the twenty-first century, *Nat. Geosci.*, *3*(3), 178–181, doi:10.1038/ngeo756.

Dennison, P. E., and D. A. Roberts (2003), Endmember selection for multiple endmember spectral mixture analysis using endmember average RMSE, *Remote Sens. Environ.*, *87*(2-3), 123–135, doi:10.1016/S0034-4257(03)00135-4.

Donohue, R. J., M. L. Roderick, T. R. McVicar, and G. D. Farquhar (2013), Impact of CO2 fertilization on maximum foliage cover across the globe's warm, arid environments, *Geophys. Res. Lett.*, *40*(12), 3031–3035, doi:10.1002/grl.50563.

Eastman, J. R., F. Sangermano, B. Ghimire, H. Zhu, H. Chen, N. Neeti, Y. Cai, E. a. Machado, and S. C. Crema (2009), Seasonal trend analysis of image time series, *Int. J. Remote Sens.*, *30*(10), 2721–2726, doi:10.1080/01431160902755338.

Eastman, J. R., F. Sangermano, E. a. Machado, J. Rogan, and A. Anyamba (2013), Global trends in seasonality of Normalized Difference Vegetation Index (NDVI), 1982-2011, *Remote Sens.*, *5*(10), 4799–4818, doi:10.3390/rs5104799.

Eldridge, D. J., M. a. Bowker, F. T. Maestre, E. Roger, J. F. Reynolds, and W. G. Whitford (2011), Impacts of shrub encroachment on ecosystem structure and functioning: Towards a global synthesis, *Ecol. Lett.*, *14*(7), 709–722, doi:10.1111/j.1461-0248.2011.01630.x.

Fairhead, J., and M. Leach (1996), *Misreading the African landscape: Society and ecology in a forest-savanna mosaic*, Cambridge University Press.

Fasullo, J., and P. J. Webster (2003), A hydrological definition of Indian Monsoon onset and withdrawal, *J. Clim.*, *16*(19), 3200–3211, doi:10.1175/1520-0442(2003)016<3200a:AHDOIM>2.0.CO;2.

Fieux, M., and H. Stommel (1977), Onset of the Southwest Monsoon over the Arabian Sea from Marine Reports of Surface Winds: Structure and Variability, *Mon. Weather Rev.*, *105*(2), 231–236.

Flagg, C. N., and H. S. Kim (1998), Upper ocean currents in the northern Arabian Sea from shipboard ADCP measurements collected during the 1994-1996 U.S. JGOFS and ONR programs, *Deep. Res. Part II Top. Stud. Oceanogr.*, *45*(10-11), 1917–1959, doi:10.1016/S0967-0645(98)00059-9.

Fleitmann, D., and A. Matter (2009), The speleothem record of climate variability in Southern Arabia, *Comptes Rendus Geosci.*, *341*(8-9), 633–642, doi:10.1016/j.crte.2009.01.006.

Fleitmann, D., S. J. Burns, M. Mudelsee, U. Neff, J. Kramers, A. Mangini, and A. Matter (2003), Holocene forcing of the Indian monsoon recorded in a stalagmite from southern Oman, *Science (80-.).*, *300*(5626), 1737–1739, doi:10.1126/science.1083130.

Fleitmann, D., S. J. Burns, U. Neff, M. Mudelsee, A. Mangini, and A. Matter (2004), Palaeoclimatic interpretation of high-resolution oxygen isotope profiles derived

from annually laminated speleothems from Southern Oman, *Quat. Sci. Rev.*, *23*(7-8), 935–945, doi:10.1016/j.quascirev.2003.06.019.

Fleitmann, D., S. J. Burns, M. Pekala, A. Mangini, A. Al-Subbary, M. Al-Aowah, J. Kramers, and A. Matter (2011), Holocene and Pleistocene pluvial periods in Yemen, southern Arabia, *Quat. Sci. Rev.*, *30*(7-8), 783–787, doi:10.1016/j.quascirev.2011.01.004.

Geist, H. J., and E. F. Lambin (2002), Proximate Causes and Underlying Driving Forces of Tropical Deforestation, *Bioscience*, *52*(2), 143–150.

Ghazanfar, S. (1998), Status of the flora and plant conservation in the sultanate of Oman, *Biol. Conserv.*, *85*(3), 287–295, doi:10.1016/S0006-3207(97)00162-6.

Ghazanfar, S. A., and M. Fisher (eds) (1998), *Vegetation of the Arabian Peninsula*, edited by S. A. Ghazanfar and M. Fisher, Kluwer Academic Publishers, Dordrecht.

Goswami, B. N., and R. S. A. Mohan (2001), Intraseasonal oscillations and interannual variability of the Indian summer monsoon, *J. Clim.*, *14*(6), 1180–1198.

Grau, H. R., R. Torres, N. I. Gasparri, P. G. Blendinger, S. Marinaro, and L. Macchi (2014), Natural grasslands in the Chaco. A neglected ecosystem under threat by agriculture expansion and forest-oriented conservation policies, *J. Arid Environ., (in press)*, doi:10.1016/j.jaridenv.2014.12.006.

Gupta, A. K., D. M. Anderson, and J. T. Overpeck (2003), Abrupt changes in the Asian southwest monsoon during the Holocene and their links to the North Atlantic Ocean, *Nature*, *421*(6921), 354–7, doi:10.1038/nature01340.

Gutman, G., A. Janetos, C. Justice, E. F. Moran, J. F. Mustard, R. R. Rindfuss, D. Skole, B. L. Turner II, and M. A. Cochrane (2004), Land Change Science: Observing, Monitoring, and Understanding Trajectories of Change on the Earth's Surface, edited by F. D. Van Der Meer, *Remote Sens. Digit. Image Process.*, *6*, 482.

Harden, C. P. (2012), Framing and Reframing Questions of Human – Environment Interactions, *Ann. Assoc. Am. Geogr.*, *102*(4), 737–747.

Higgins, A. (2011), *With the S.A.S and Other Animals: A Vet's Experiences During the Dhofar War 1974*, Pen and Sword Books Ltd, Barnsley, UK.

Higuera, D., B. Martín-López, and A. Sánchez-Jabba (2013), Social preferences towards ecosystem services provided by cloud forests in the neotropics: Implications for conservation strategies, *Reg. Environ. Chang.*, *13*(4), 861–872, doi:10.1007/s10113-012-0379-1.

Hijmans, R. J., S. E. Cameron, J. L. Parra, P. G. Jones, and A. Jarvis (2005), Very high resolution interpolated climate surfaces for global land areas, *Int. J. Climatol.*, *25*(15), 1965–1978, doi:10.1002/joc.1276.

Hildebrandt, A. (2005), Ecohydrology of a Seasonal Cloud Forest in Dhofar, PhD. Dissertation, Massachusetts Institute of Technology.

Hildebrandt, A., and E. A. B. Eltahir (2006), Forest on the edge: Seasonal cloud forest in Oman creates its own ecological niche, *Geophys. Res. Lett.*, *33*(11), 2–5, doi:10.1029/2006GL026022.

Hildebrandt, A., and E. A. B. Eltahir (2007), Ecohydrology of a seasonal cloud forest in Dhofar: 2. Role of clouds, soil type, and rooting depth in tree-grass competition, *Water Resour. Res.*, *43*(11), 1–13, doi:10.1029/2006WR005262.

Hildebrandt, A., M. Al Aufi, M. Amerjeed, M. Shammas, and E. A. B. Eltahir (2007), Ecohydrology of a seasonal cloud forest in Dhofar: 1. Field experiment, *Water Resour. Res.*, *43*(10), 1–13, doi:10.1029/2006WR005261.

Hilker, T., E. Natsagdorj, R. H. Waring, A. Lyapustin, and Y. Wang (2014), Satellite observed widespread decline in Mongolian grasslands largely due to overgrazing, *Glob. Chang. Biol.*, *20*(2), 418–28.

Hubbell, S. P. (2006), Neutral theory and the evolution of ecological equivalence, *Ecology*, *87*(6), 1387–1398.

Hughes, G. (2009), A "Model Campaign" Reappraised: The Counter-Insurgency War in Dhofar, Oman, 1965–1975, *J. Strateg. Stud.*, *32*(2), 271–305, doi:10.1080/01402390902743357.

Hulme, M. (2001), Climatic perspectives on Sahelian desiccation: 1973 1998, *Glob. Environ. Chang.*, *11*(1), 19–29.

Hurrell, J. W. (1995), Decadal Trends in the North Atlantic Oscillation: regional temperatures and precipitation, *Science*, *269*(5224), 676–9, doi:10.1126/science.269.5224.676.

Ihara, C., Y. Kushnir, and M. a. Cane (2008), Warming trend of the Indian Ocean SST and Indian Ocean dipole from 1880 to 2004, *J. Clim.*, *21*(10), 2035–2046, doi:10.1175/2007JCLI1945.1.

IPCC (2014), *Synthesis Report. Contribution of Working Groups I, II and III to the Fifth Assessment Report of the Intergovernmental Panel on Climate Change*, edited by Core Writing Team, R. K. Pachauri, and L. A. Meyer, IPCC, Geneva, Switzerland.

Janzen, J. (1986), *Nomads in the sultanate of Oman: tradition and development in Dhofar*, Westview Press, Boulder.

Janzen, J. (2000), The destruction of resources among the mountain nomads of Dhofar, in *The Transformation of Nomadic Society in the Arab East*, edited by M. Mundy and B. Musallam, pp. 160–175, Cambridge University Press, Cambridge, UK.

De Jong, R., J. Verbesselt, M. E. Schaepman, and S. de Bruin (2012), Trend changes in global greening and browning: Contribution of short-term trends to longer-term change, *Glob. Chang. Biol.*, *18*(2), 642–655, doi:10.1111/j.1365-2486.2011.02578.x.

De Jong, R., J. Verbesselt, A. Zeileis, and M. E. Schaepman (2013), Shifts in global vegetation activity trends, *Remote Sens.*, *5*(3), 1117–1133, doi:10.3390/rs5031117.

Joseph, P. V., J. K. Eischeid, and R. J. Pyle (1994), Interannual Variability of the Onset of the Indian Summer Monsoon and Its Association with Atmospheric Features, El Niño, and Sea Surface Temperature Anomalies, *J. Clim.*, *7*(1), 81–105, doi:10.1175/1520-0442(1994)007<0081:IVOTOO>2.0.CO;2.

Joseph, P. V., K. P. Sooraj, and C. K. Rajan (2006), The Summer Monsoon Onset Process Over South Asia and an Objective Method for the Date of Monsoon Onset over Kerala, *Int. J. Climatol.*, *26*, 1871–1893, doi:10.1002/joc.1340.

Justice, C. O. et al. (1998), The Moderate Resolution Imaging Spectroradiometer (MODIS): land remote sensing for global change research, *IEEE Trans. Geosci. Remote Sens.*, *36*(4), 1228–1249, doi:10.1109/36.701075.

Kanamitsu, M., W. Ebisuzaki, J. Woollen, S.-K. Yang, J. J. Hnilo, M. Fiorino, and G. L. Potter (2002), NCEP–DOE AMIP-II Reanalysis (R-2), *Bull. Am. Meteorol. Soc.*, *83*(11), 1631–1643, doi:10.1175/BAMS-83-11-1631.

Krishnan, R., T. P. Sabin, D. C. Ayantika, a. Kitoh, M. Sugi, H. Murakami, a. G. Turner, J. M. Slingo, and K. Rajendran (2013), Will the South Asian monsoon overturning circulation stabilize any further?, *Clim. Dyn.*, *40*(1-2), 187–211, doi:10.1007/s00382-012-1317-0.

Krishnaswamy, J., S. Vaidyanathan, B. Rajagopalan, M. Bonell, M. Sankaran, R. S. Bhalla, and S. Badiger (2014), Non-stationary and non-linear influence of ENSO and Indian Ocean Dipole on the variability of Indian monsoon rainfall and extreme rain events, *Clim. Dyn.*, doi:10.1007/s00382-014-2288-0.

Kumar, K. K., B. Rajagopalan, and M. A. Cane (1999), On the Weakening Relationship Between the Indian Monsoon and ENSO, *Science (80-.).*, *284*(5423), 2156–2159, doi:10.1126/science.284.5423.2156.

Kumar, K. K., B. Rajagopalan, M. Hoerling, G. Bates, and M. Cane (2006), Unraveling the mystery of Indian monsoon failure during El Niño, *Science*, *314*(5796), 115–119.

Kumar, K. K., K. Kamala, B. Rajagopalan, M. P. Hoerling, J. K. Eischeid, S. K. Patwardhan, G. Srinivasan, B. N. Goswami, and R. Nemani (2011), The once and future pulse of Indian monsoonal climate, *Clim. Dyn.*, *36*(11-12), 2159–2170, doi:10.1007/s00382-010-0974-0.

Kürschner, H., P. Hein, N. Kilian, and M. A. Hubaishan (2004), The Hybantho durae-Anogeissetum dhofaricae ass. nova - phytosociology, structure and ecology of an endemic South Arabian forest community, *Phytocoenologia*, *34*, 569–612.

Kwarteng, A. Y., S. Dorvlo, and G. T. V. Kumar (2009), Analysis of a 27-year rainfall data (1977 – 2003) in the Sultanate of Oman, *Int. J. Climatol.*, *617*(July 2008), 605–617, doi:10.1002/joc.

Lambin, E. F., and M. Linderman (2006), Time series of remote sensing data for land change science, *Geosci. Remote Sens. IEEE Trans.*, *44*(7), 1926–1928, doi:10.1109/tgrs.2006.872932.

Lambin, E. F., B. L. Turner, H. J. Geist, S. B. Agbola, A. Angelsen, J. Bruce, O. Coomes, R. Dirzo, G. Fischer, and C. Folke (2001), The causes of land-use and land-cover change: moving beyond the myths, *Glob. Environ. Chang.*, *11*(4), 261–269, doi:10.1016/S0959-3780(01)00007-3.

Lambin, E. F., H. J. Geist, and E. Lepers (2003), Dynamics of Land-Use and Land-Cover Change in Tropical Regions, *Annu. Rev. Environ. Resour.*, *28*(1), 205–241.

Lefebvre, J. A. (2010), Oman's Foreign Policy in the Twenty-First Century, *Middle East Policy*, *17*(1), 99–114.

Legendre, P., and L. Legendre (1998), *Numerical ecology*, Developments in evironmental modelling, edited by S. E. Edition, Elsevier.

Legendre, P., D. Borcard, and P. R. Peres-Neto (2005), Analyzing beta diversity: Partitioning the spatial variation of community composition data, *Ecol. Monogr.*, *75*(4), 435–450.

Lenton, T. M., H. Held, E. Kriegler, J. W. Hall, W. Lucht, S. Rahmstorf, and H. J. Schellnhuber (2008), Tipping elements in the Earth's climate system, *Proc. Natl. Acad. Sci. U. S. A.*, *105*(6), 1786–1793.

Li, S., P. H. Verburg, L. Shihai, J. Wu, and X. Li (2012), Spatial analysis of the driving factors of grassland degradation under conditions of climate change and intensive

use in Inner Mongolia, China, *Reg. Environ. Chang.*, *12*(3), 461–474, doi:10.1007/s10113-011-0264-3.

Liu, J. et al. (2013), Framing Sustainability in a Telecoupled World, *Ecol. Soc.*, *18*(2), 26, doi:10.5751/ES-05873-180226.

Mann, H. (1945), Nonparametric tests against trend, *Econometrica*, *13*, 245–259.

Manson, S. M., and T. Evans (2007), Agent-based modeling of deforestation in southern Yucatan, Mexico, and reforestation in the Midwest United States, *Proc. Natl. Acad. Sci. U. S. A.*, *104*(52), 20678–20683.

Masek, J. G., E. F. Vermote, N. E. Saleous, R. Wolfe, F. G. Hall, K. F. Huemmrich, F. Gao, J. Kutler, and T. Lim (2006), A Landsat Surface Reflectance Dataset for North America, 1990-2000, *IEEE Geosci. Remote Sens. Lett.*, *3*(1), 68–72, doi:10.1109/LGRS.2005.857030.

Mekonnen, Y. (1994), A survey of plants (potentially) toxic to livestock in the Ethiopian flora, *Sinet, an Ethiop. J. Sci.*, *17*(1), 9–32.

Meyfroidt, P., and E. F. Lambin (2009), Forest transition in Vietnam and displacement of deforestation abroad, *Proc. Natl. Acad. Sci. U. S. A.*, *106*(38), 16139–16144.

Miller, A. G., and M. Morris (1988a), *Plants of Dhofar, the southern region of Oman, traditional, economic and medicinal uses*, Office of the Adviser for Conservation of the Environment, Diwan of Royal Court, Sultanate of Oman.

Miller, A. G., and M. Morris (1988b), *Plants of Dhofar, The Southern Region of Oman: Traditional, Economic, and Medicinal Uses*, Office of the Adviser for Conservation of the Environment, Diwan of Royal Court, Sultanate of Oman.

Mitchell, K. (2007), *Quantitative analysis by the point-centered quarter method*, Geneva, NY.

Mac Nally, R. (2007), Use of the abundance spectrum and relative-abundance distributions to analyze assemblage change in massively altered landscapes, *Am. Nat.*, *170*(3), 319–30, doi:10.1086/519859.

Neeti, N., and J. R. Eastman (2011), A Contextual Mann-Kendall approach for the assessment of trend significance in image time series, *Trans. GIS*, *15*(5), 599–611, doi:10.1111/j.1467-9671.2011.01280.x.

Nicholson, S. E. (2009), A revised picture of the structure of the "monsoon" and land ITCZ over West Africa, *Clim. Dyn.*, *32*(7-8), 1155–1171, doi:10.1007/s00382-008-0514-3.

Nicholson, S. E., C. J. Tucker, and M. B. Ba (1998), Surface Vegetation : An Example from the West African Sahel, *Bull. Am. Meteorol. Soc.*, *79*(5), 815–829.

Nieves, V., J. K. Willis, and W. C. Patzert (2015), Recent hiatus caused by decadal shift in Indo-Pacific heating, *Science*, *349*(6247), 532–535.

NRC (2013), *Advancing Land Change Modeling: Opportunities and Research Requirements*, Washington D.C.

O'Reilly, M. J. (1998), Omanibalancing: Oman Confronts an Uncertain Future, *Middle East J.*, *52*(1), 70–84.

OEC (2015), Observatory of Economic Complexity, Available from: https://atlas.media.mit.edu/en/ (Accessed 1 May 2015)

Overpeck, J. T., D. Anderson, S. Trumbore, and W. Prell (1996), The southwest Indian Monsoon over the last 18,000 years, *Clim. Dyn.*, *12*, 213–225.

Panday, P. K., and B. Ghimire (2012), Time-series analysis of NDVI from AVHRR data over the Hindu Kush–Himalayan region for the period 1982–2006, *Int. J. Remote Sens.*, *33*(21), 6710–6721, doi:10.1080/01431161.2012.692836.

Parker, A. G., and J. I. Rose (2008), Climate change and human origins in southern Arabia, *Proc. Semin. Arab. Stud.*, *38*, 25–42.

Patzelt, A. (2011), The Themeda Quadrivalvis Tall-Grass Savannah of Oman At the Crossroad Between Africa and Asia, *Edinburgh J. Bot.*, *68*(02), 301–319, doi:10.1017/S0960428611000217.

Peterson, J. E. (2004a), Oman: Three and a Half Decades Of Change and Development, *Middle East Policy*, *XI*(2), 125–137.

Peterson, J. E. (2004b), Oman's Diverse Society : Southern Oman, *Middle East J.*, *58*(1), 31–51.

Peterson, J. E. (2011), Oman Faces the Twenty-First Century, in *Political Change in the Arab Gulf States: Stuck in Transition*, edited by M. A. Tétreault, G. Okruhlik, and A. Kapiszewski, pp. 99–118, Lynne Rienner Publishers, Boulder.

Pickering, H., and A. Patzelt (2008a), *Field Guide to the Wild Plants of Oman*, Royal Botanical Gardens, Kew, Kew, United Kingdom.

Pickering, H. A., and A. Patzelt (2008b), *Field Guide to the Wild Plants of Oman*, Kew Publishing, Richmond, UK.

Pielke, R. A. (2005), Land use and climate change, *Science*, *310*(5754), 1625–1626.

Pitman, N. C. A., J. Terborgh, M. R. Silman, and P. Nunez V. (1999), Tree Species Distributions in an Upper Amazonian Forest, *Ecology*, *80*(8), 2651–2661.

Pitman, N. C. A., J. W. Terborgh, M. R. Silman, P. N. V, A. David, C. E. Cerón, W. A. Palacios, and M. Aulestia (2001), Dominance and Distribution of Tree Species in Upper Amazonian Terra Firme Forests, *Ecology*, *82*(8), 2101–2117.

Pontius, R. G., E. Shusas, and M. McEachern (2004), Detecting important categorical land changes while accounting for persistence, *Agric. Ecosyst. Environ.*, *101*(2-3), 251–268, doi:10.1016/j.agee.2003.09.008.

Population Reference Bureau (2012), *2012 World Population Data Sheet*, Washington D.C.

Powell, R. L., and D. A. Roberts (2010), Characterizing Urban Land-Cover Change in Rondônia, Brazil: 1985 to 2000, *J. Lat. Am. Geogr.*

Pozo-Vazquez, D., M. J. Esteban-Parra, F. S. Rodrigo, and Y. Castro-Diez (2001), A study of NAO variability and its possible non-linear influences on European surface temperature, *Clim. Dyn.*, *17*, 701–715.

Radcliffe Smith A (1980), The vegetation of Dhofar, in *The scientific results of the Oman Flora and Fauna Survey, 1977, (Dhofar)*, edited by N. Shaw-Reade, S, B. Sale, J, D. Gallagher, M, and H. Daly, R, pp. 59–86.

Rayner, N. A., D. E. Parker, E. B. Horton, C. K. Folland, L. V. Alexander, D. P. Rowell, E. C. Kent, and A. Kaplan (2003), Global analyses of sea surface temperature, sea ice, and night marine air temperature since the late Nineteenth Century, *J. Geophys. Res.*, *108*, doi:10.1029/2002JD002670.

Reich, P. B., and R. Borchert (1984), Water Stress and Tree Phenology in a Tropical Dry Forest in the Lowlands of Costa Rica, *J. Ecol.*, *72*(1), 61–74.

Reynolds, J. F., and D. M. Stafford-Smith (2002), *Global Desertification: Do Humans Cause Deserts?*, Dahlem University Press, Berlin.

Reynolds, J. F. et al. (2007), Global desertification: building a science for dryland development, *Science*, *316*(5826), 847–851.

Reynolds, R. W., N. a. Rayner, T. M. Smith, D. C. Stokes, and W. Wang (2002), An improved in situ and satellite SST analysis for climate, *J. Clim.*, *15*(13), 1609–1625, doi:10.1175/1520-0442(2002)015<1609:AIISAS>2.0.CO;2.

Rickbeil, G. J. M., N. C. Coops, M. E. Andrew, D. K. Bolton, N. Mahony, and T. A. Nelson (2014), Assessing conservation regionalization schemes: employing a beta diversity metric to test the environmental surrogacy approach, edited by S. Ferrier, *Divers. Distrib.*, *20*(5), 503–514, doi:10.1111/ddi.12146.

Roberts, D., M. Gardner, R. Church, S. Ustin, G. Scheer, and R. Green (1998), Mapping Chaparral in the Santa Monica Mountains Using Multiple Endmember Spectral Mixture Models, *Remote Sens. Environ.*, *65*(3), 267–279, doi:10.1016/S0034-4257(98)00037-6.

Rosindell, J., S. P. Hubbell, and R. S. Etienne (2011), The unified neutral theory of biodiversity and biogeography at age ten., *Trends Ecol. Evol.*, *26*(7), 340–8, doi:10.1016/j.tree.2011.03.024.

Rousseeuw, P. J. (1987), Silhouettes: A graphical aid to the interpretation and validation of cluster analysis, *J. Comput. Appl. Math.*, *20*, 53–65, doi:10.1016/0377-0427(87)90125-7.

Saji, N. H., B. N. Goswami, P. N. Vinayachandran, and T. Yamagata (1999), A dipole mode in the tropical Indian Ocean, *Nature*, *401*, 360–363.

Schlecht, E., L. G. H. Zaballos, D. Quiroz, P. Scholte, and A. Buerkert (2014), Traditional land use and reconsideration of environmental zoning in the Hawf Protected Area, south-eastern Yemen, *J. Arid Environ.*, *109*, 92–102, doi:10.1016/j.jaridenv.2014.05.016.

Scholte, P., and P. De Geest (2010), The climate of Socotra Island (Yemen): A first-time assessment of the timing of the monsoon wind reversal and its influence on precipitation and vegetation patterns, *J. Arid Environ.*, *74*(11), 1507–1515, doi:10.1016/j.jaridenv.2010.05.017.

Schott, F. A., and J. P. McCreary (2001), The monsoon circulation of the Indian Ocean, *Prog. Oceanogr.*, *51*(1), 1–123, doi:10.1016/S0079-6611(01)00083-0.

Sen, P. K. (1968), Estimates of the regression coefficient based on Kendall's tau, *J. Am. Stat. Assoc.*, *63*, 1379–1389.

Serneels, S., and E. F. Lambin (2001), Proximate causes of land-use change in Narok District, Kenya: a spatial statistical model, *Agric. Ecosyst. Environ.*, *85*(1-3), 65–81, doi:10.1016/S0167-8809(01)00188-8.

Seto, K. C., and A. Reenberg (2014a), *Rethinking Global Land Use in an Urban Era*, edited by K. C. Seto and A. Reenberg, MIT Press, Cambridge, Mass.

Seto, K. C., and A. Reenberg (2014b), *Rethinking global land use in an urban era*, edited by K. C. Seto and A. Reenberg, MIT Press, Cambridge.

Seto, K. C., R. Sánchez-Rodríguez, and M. Fragkias (2010), The New Geography of Contemporary Urbanization and the Environment, *Annu. Rev. Environ. Resour.*, *35*(1), 167–194.

Seto, K. C., A. Reenberg, C. G. Boone, M. Fragkias, D. Haase, T. Langanke, P. Marcotullio, D. K. Munroe, B. Olah, and D. Simon (2012), Urban land teleconnections and sustainability, *Proc. Natl. Acad. Sci. U. S. A.*, *109*(20), 7687–92, doi:10.1073/pnas.1117622109.

Settle, J. J., and N. A. Drake (1993), Linear mixing and the estimation of ground cover proportions, *Int. J. Remote Sens.*, *14*(6), 1159–1177.

Shi, W., J. M. Morrison, E. Böhm, and V. Manghnani (2000), The Oman upwelling zone during 1993, 1994 and 1995, *Deep. Res. Part II Top. Stud. Oceanogr.*, *47*(7-8), 1227–1247, doi:10.1016/S0967-0645(99)00142-3.

Shmida, A., and M. V. Wilson (1985), Biological determinants of species diversity, *J. Biogeogr.*, *12*(1), 1–20.

Southgate, D., T. Haab, J. Lundine, and F. Rodríguez (2009), Payments for environmental services and rural livelihood strategies in Ecuador and Guatemala, *Environ. Dev. Econ.*, *15*(01), 21, doi:10.1017/S1355770X09005361.

Stafford Smith, D. M., G. M. McKeon, I. W. Watson, B. K. Henry, G. S. Stone, W. B. Hall, and S. M. Howden (2007), Learning from episodes of degradation and recovery in variable Australian rangelands, *Proc. Natl. Acad. Sci.*, *104*(52), 20690–20695.

Sun, J., H. Wang, and W. Yuan (2008), Decadal variations of the relationship between the summer North Atlantic Oscillation and middle East Asian air temperature, *J. Geophys. Res.*, *113*(D15), D15107, doi:10.1029/2007JD009626.

Theil, H. (1950), A rank-invariant method of linear and polynomial regression analysis, I, II, III, *Proc. K. Ned. Acad. van Wet.*, *53*(386), 386–392, 512–525, 1397–1412.

Trenberth, K. E. (1984), Signal Versus Noise in the Southern Oscillation, *Mon. Weather Rev.*, *112*(2), 326–332, doi:10.1175/1520-0493(1984)112<0326:SVNITS>2.0.CO;2.

Tuomisto, H., and K. Ruokolainen (2006), Analyzing or explaining beta diversity? Understanding the targets of different methods of analysis, *Ecology*, *87*(11), 2697–2708.

Turner II, B. L., and P. Robbins (2008), Land-Change Science and Political Ecology: Similarities, Differences, and Implications for Sustainability Science, *Annu. Rev. Environ. Resour.*, *33*(1), 295–316, doi:10.1146/annurev.environ.33.022207.104943.

Turner II, B. L., R. E. Kasperson, W. B. Meyer, K. M. Dow, D. Golding, J. X. Kasperson, R. C. Mitchell, and S. J. Ratick (1990), Two types of global environmental change: definitional and spatial-scale issues in their human dimensions, *Glob. Environ. Chang.*, *1*(1), 14–22, doi:10.1016/0959-3780(90)90004-S.

Turner II, B. L., E. F. Lambin, and A. Reenberg (2007), Land Change Science Special Feature: The emergence of land change science for global environmental change and sustainability, *Proc. Natl. Acad. Sci. U. S. A.*, *104*(52), 20666–20671, doi:10.1073/pnas.0704119104.

Turner, M. G. (1989), Landscape Ecology: The Effect of Pattern on Process, *Annu. Rev. Ecol. Syst.*, *20*(1), 171–197, doi:10.1146/annurev.es.20.110189.001131.

UNEP (1994), *United Nations Convention to Combat Desertification in those Countries Experiencing Serious Drought and/or Desertification, Particularly in Africa*.

USGS (2015), *Product Guide: Landsat 4-7 Climate Data Record (CDR) Surface Reflectance v. 5.8*.

Vayda, A. P., and B. B. Walters (1999), Against political ecology, *Hum. Ecol.*, *27*(1), 167–179, doi:10.1023/A:1018713502547.

Vuorio, V., A. Muchiru, R. S. Reid, and J. O. Ogutu (2014), How pastoralism changes savanna vegetation : impact of old pastoral settlements on plant diversity and abundance in south-western Kenya, *Biodivers. Conserv.*, *23*, 3219–3240, doi:10.1007/s10531-014-0777-4.

Walsh, S., A. Mccleary, C. Mena, Y. Shao, J. Tuttle, A. Gonzalez, and R. Atkinson (2008a), QuickBird and Hyperion data analysis of an invasive plant species in the Galapagos Islands of Ecuador: Implications for control and land use management, *Remote Sens. Environ.*, *112*(5), 1927–1941, doi:10.1016/j.rse.2007.06.028.

Walsh, S. J., Y. Shao, C. F. Mena, and A. L. McCleary (2008b), Integration of hyperion satellite data and a household social survey to characterize the causes and consequences of reforestation patterns in the northern Ecuadorian Amazon, *Photogramm. Eng. Remote Sensing*, *74*(6), 725–735.

Wessels, K., S. Prince, J. Malherbe, J. Small, P. Frost, and D. Vanzyl (2007), Can human-induced land degradation be distinguished from the effects of rainfall

variability? A case study in South Africa, *J. Arid Environ.*, *68*(2), 271–297, doi:10.1016/j.jaridenv.2006.05.015.

Wessels, K. J., F. van den Bergh, and R. J. Scholes (2012), Limits to detectability of land degradation by trend analysis of vegetation index data, *Remote Sens. Environ.*, *125*, 10–22, doi:10.1016/j.rse.2012.06.022.

Williams-Linera, G. (2002), Tree species richness complementarity , disturbance and fragmentation in a Mexican tropical montane cloud forest, *Biodivers. Conserv.*, *11*, 1825–1943.

Zhang, X., F. W. Zwiers, G. C. Hegerl, F. H. Lambert, N. P. Gillett, S. Solomon, P. a Stott, and T. Nozawa (2007), Detection of human influence on twentieth-century precipitation trends, *Nature*, *448*(7152), 461–5, doi:10.1038/nature06025.

APPENDIX A

DETAILS OF THE CANONICAL CORRESPONDENCE ANALYSIS CONDUCTED IN CHAPTER 3

Table A.1: Variables used in the CCA analysis to determine the relationship between species abundances, sample points, and environmental/climatic variables

Variable	Short Name	Source
Mean temperature of the driest month	T_dry_9	Worldclim (Hijmans et al. 2006)
Mean temperature of the wettest month	T_wet_8	Worldclim
Maximum temperature of the warmest month	MaxTwar5	Worldclim
Minimum temperature of the coldest month	MinTcol6	Worldclim
Average yearly temperature	AvgT_yr1	Worldclim
Precipitation seasonality	Prc_season	
Isothermality		Worldclim
Preciptiation of the driest month	Prc_dry	Worldclim
Precipitation of the wettest month	Prc_wet	Worldclim
Precipitation of the wettest quarter	Prc_wetq	Worldclim
Precipitation of the driest quarter	Prc_dryq	Worldclim
Precipitation of the warmest quarter	Prc_warmq	Worldclim
Precipitation of the coldest quarter	Prc_coldq	Worldclim
Annual precipitation	Ann_prcp	Worldclim
Slope	Slope	SRTM DEM (90 m)
Northness (Aspect)	Northness	SRTM DEM (90 m)
Eastness (Aspect)	Eastness	SRTM DEM (90 m)
Hydrology	Hydro1k	SRTM DEM (90 m)

Table A.2: *Study area* - Variable scores and their significances used in the CCA analysis of all 102 sample points. Significance is estimated using 9999 permutations of an ANOVA test. The leading variable for each axis is in bold

Variable	**CCA1**	**CCA2**	**CCA3**	**CCA4**	**CCA5**
Slope	0.1288	0.343	**-0.736**	0.1184	**0.55722**
T_dry_9	0.7262	0.2867	-0.3349	0.02698	-0.52703
T_wet_8	-0.2287	**0.6252**	-0.343	**-0.64644**	-0.14578
Prc_wetq	0.5418	0.397	0.6932	-0.24323	0.09399
MaxTwar5	**-0.8219**	0.4146	-0.2195	0.32261	0.01056
Significance	**0.0001**	**0.0001**	**0.0017**	**0.0028**	**0.7627**

Table A.3: *Forest* - Variable scores and their significances used in the CCA analysis of all forest sample points (n=36). Significance is estimated using 9999 permutations of an ANOVA test. The leading variable for each axis is in bold

Variable	**CCA1**	**CCA2**	**CCA3**
Prc_wetq	0.007851	-0.101	**0.9949**
MaxTwar5	**-0.93075**	-0.2033	-0.304
Prc_warmq	-0.53835	**0.5811**	0.6102
Significance	**0.0001**	**0.0121**	**0.1553**

Table A.4: *Grassland* - Variable scores and their significances used in the CCA analysis of the all grassland sample points (n=59). Significance is estimated using 9999 permutations of an ANOVA test. The leading variable for each axis is in bold

Variable	**CCA1**	**CCA2**	**CCA3**	**CCA4**	**CCA5**
Slope	-0.1453	0.01666	-0.06292	**-0.8638**	-0.47847
T_dry_9	0.5668	0.19338	0.08538	-0.3537	**0.71424**
Prc_wetq	0.8328	0.16872	-0.41794	0.3079	0.0897
MinTcol6	-0.4414	-0.06332	**-0.65738**	-0.4787	0.37364
Prc_dryq	**0.9186**	**-0.35742**	0.11836	0.1199	0.01416
Significance	**0.0001**	**0.0001**	**0.0195**	**0.1208**	**0.7843**

APPENDIX B

DETAILS OF THE CLUSTER ANALYSIS CONDUCTED IN CHAPTER 3

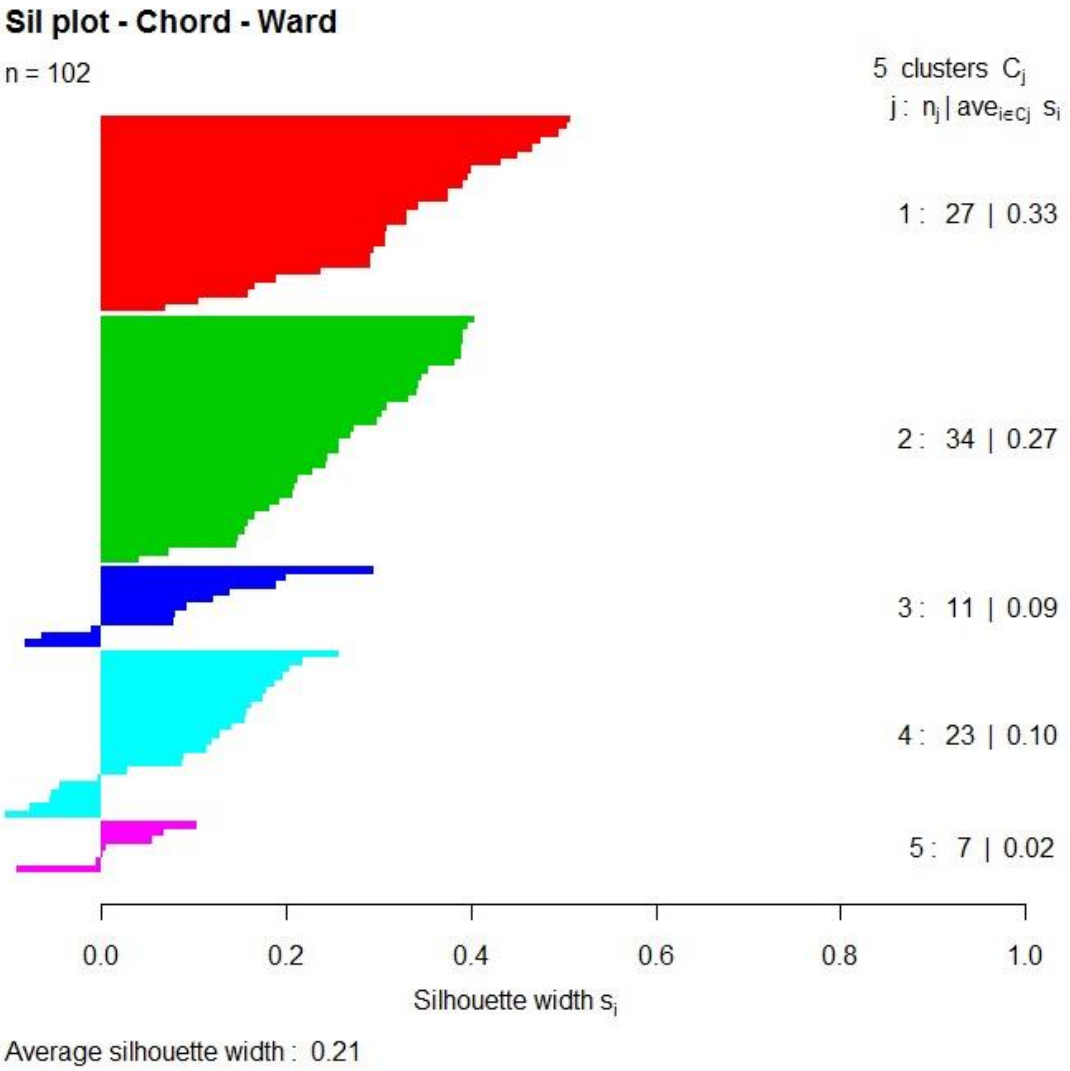

Figure B.1: Silhouette plot showing outliers and relative strength of the clusters identified in the cluster analysis. The far right column contains the number of sample points in a cluster (n_j) and the silhouette width (s_i). s_i is interpreted similarly to a correlation coefficient. Anything to the left of 0.0 is considered an outlier. The R package 'vegan' was used to determine the clusters and produce the figure.

Table B.1: Breakdown of each cluster group and the number of sample points from the grassland, forest, and foothills that are represented in each cluster group.

	Number of sites per cluster			
	Grassland	**Forest**	**Foothills**	
Cluster 1	25	1	1	
Cluster 2	11	23	0	
Cluster 3	2	7	2	
Cluster 4	18	5	0	
Cluster 5	3	0	4	
Total	**59**	**36**	**7**	**102**